Title
Identification of new RNA substrates for the NMD and exosome RNA surveillance pathways in Saccharomyces cerevisiae

Author
Sayani, Shakir

Publication Date
2012

Peer reviewed|Thesis/dissertation

UNIVERSITY OF CALIFORNIA

Los Angeles

Identification of new RNA substrates for the NMD and exosome RNA surveillance pathways in *Saccharomyces cerevisiae*

A dissertation submitted in partial satisfaction of the

requirements for the Degree Doctor of Philosophy

in Biochemistry and Molecular Biology

by

Shakir Sayani

2012

ABSTRACT OF THE DISSERTATION

Functional redundancy between nuclear and cytoplasmic RNA degradation pathways limits the accumulation of unspliced transcripts

by

Shakir Sayani

Doctor of Philosophy in Biochemistry and Molecular Biology

University of California, Los Angeles, 2012

Professor Guillaume Chanfreau, Chair

Using the yeast, *Saccharomyces cerevisiae*, as a model system, we utilized Affymetrix tiling arrays to globally investigate novel targets of the nonsense mediated decay pathway. The research that has been presented in the first chapter of this dissertation is centered around the investigation of extended transcripts and the degradation pathways that contribute to its rapid turnover in yeast cells. This work was published in the online version of the journal, *PLoS Genetics*. The work that is presented in the second chapter is based on our findings that intron-retained or unspliced RNAs are markedly stabilized in NMD mutant strains which led us to conclude the widespread impact of the nonsense mediated decay pathway in the degradation of

unspliced RNAs. We further expanded our work and showed that introns emanating from NMD-sensitive loci can elicit an NMD-sensitive phenotype in trans, which led us to conclude that the intron (intronic sequences) are necessary for proper NMD-targeting. We further discovered that sequences located within the 5'SS as well as the branchpoint (BP) are responsible in part for the generation of unspliced/inefficiently spliced transcripts. Lastly, we showed that amino acid starvation results in a transient inhibition of nuclear splicing resulting in hyperaccumulation of unspliced transcripts. Under this condition, we elucidated a stress-specific role for the NMD pathway in rapidly targeting and degrading these unspliced transcripts. The results that have been presented in the second chapter of this dissertation have been published in the Molecular Cell journal (August 8th, 2008 issue). The third chapter (part) of this dissertation explores themes that have directly evolved from the first part. Specifically, the second part has shown that there are more complex routes for the degradation for unspliced transcripts besides the NMD pathway. In particular, synergistic modes of degradation involving components of the nuclear exosome and factors involved in NMD function to limit and hence degrade these unspliced transcripts. Decay measurements were undertaken to show that there are unspliced RNAs whose degradation mode depends on a synergistic mode of degradation requiring both the nuclear exosome component, Rrp6p and the NMD factor, Upf1p. Conversely, we found a class of unspliced transcripts whose turnover relies largely on the action of the NMD pathway and not on synergistic degradation. We further expanded our research and showed that inactivation of an essential, conserved, yeast RNA export factor, Mex67p, results in the nuclear sequestration and degradation of normally cytoplasmically degraded unspliced transcripts. This result highlighted the generic features of RNA degradation and has shown that temporal changes (such as malfunction of proper nuclear-to-cytoplasmic RNA trafficking) cause spatial redistribution and degradation of the unspliced

RNA. We have also shown that the nuclear periphery factor, Mlp1p, could have a potential role in the retention of nuclear-degraded unspliced RNA. Deletion of this factor led to an increase in the cytoplasmic concentration of the unspliced RNA which was then degraded by the NMD pathway.

The dissertation of Shakir Sayani is approved

Douglas L. Black

Albert J. Courey

Guillaume F. Chanfreau, Committee Chair

University of California, Los Angeles

2012

TABLE OF CONTENTS PAGE

LIST OF FIGURES PAGE

LIST OF FIGURES PAGE

ACKNOWLEDGEMENTS

Professional

Chapter 1

Chapter 1 is a reprint of the article entitled "Cryptic Transcription Mediates Repression of Subtelomeric Metal Homeostasis Genes." My contribution to this publication was performing decay analysis for the *ZRT1* CD-CUT in Figure 2. This article was published online at *PLoS Genetics*. The article was originally published online on June 30, 2011. **Citation:** Toesca I, Nery CR, Fernandez CF, Sayani S, Chanfreau GF (2011) Cryptic Transcription Mediates Repression of Subtelomeric Metal Homeostasis Genes. PLoS Genet 7(6): e1002163. doi:10.1371/journal.pgen.1002163. I thank the Public Library of Science (PLoS) for giving me an opportunity to use the reprint.

Chapter 2

I would like to thank Elsevier for granting me permission to reproduce the article in electronic format originally published in the August 8th, 2008 issue of the journal, *Molecular Cell* titled: "Widespread Impact of Nonsense-Mediated mRNA decay on the Yeast Intronome." The license number given from Copyright Clearance Center/Rights Link is: 2878520607511. I performed all of the experiments that are in the paper with the following exceptions: All of the bioinformatics analysis was done by Michael Janis and Guillaume Chanfreau; the microscopy was performed by Chrissie Young Lee; and the *xrn1*Δ tiling array was done by Isabelle Toesca. Guillaume Chanfreau helped design, direct, plan, interpret the outcome of the experiments and wrote the paper with input from all of the authors.

Chapter 3

The contents within the third chapter are unpublished results. Guillaume Chanfreau and I designed the experiments and I performed all of the experiments that are within this chapter.

Personal

First, I would like to thank my mentor, Dr. Guillaume Chanfreau, for taking a chance and accepting me into the group and for the intellectual support that he has provided over the years. I am also tremendously indebted to Guillaume for his ideas that have brought about the work presented in this dissertation. I would also like to thank Ana Mariscal, who is probably the most helpful and responsible lab helper in our lab. Ana's continuous commitment to making plates, media, buffers, and washing and autoclaving glassware for the lab is immeasurable! I would also like to thank the past and the present members of the Chanfreau Lab for help and advice with experiments and their friendship. Lastly, I would like to thank my wonderful committee members: Drs. Doug Black, Al Courey, Steve Clarke, and David Campbell for their help and support.

VITA

1981	Born, Ahmedabad, India
2001	Associate in Arts, Santa Monica College
2003	B.S., Molecular, Cellular, Developmental Biology, UCLA
2004	Graduate Program in Biochemistry and Molecular Biology, UCLA
2012	Ph.D., Biochemistry and Molecular Biology, UCLA

Chapter 1—Cryptic Transcription Mediates Repression of Subtelomeric Metal Homeostasis Genes

OPEN ACCESS Freely available online PLoS GENETICS

Cryptic Transcription Mediates Repression of Subtelomeric Metal Homeostasis Genes

Isabelle Toesca[◔¤], Camille R. Nery[◔], Cesar F. Fernandez, Shakir Sayani, Guillaume F. Chanfreau*

Department of Chemistry and Biochemistry and the Molecular Biology Institute, University of California Los Angeles, Los Angeles, California, United States of America

Abstract

Nonsense-mediated mRNA decay (NMD) prevents the accumulation of transcripts bearing premature termination codons. Here we show that *Saccharomyces cerevisiae* NMD mutants accumulate 5′–extended RNAs (CD-CUTs) of many subtelomeric genes. Using the subtelomeric *ZRT1* and *FIT3* genes activated in response to zinc and iron deficiency, respectively, we show that transcription of these CD-CUTs mediates repression at the *bona fide* promoters, by preventing premature binding of RNA polymerase II in conditions of metal repletion. Expression of the main *ZRT1* CD-CUT is controlled by the histone deacetylase Rpd3p, showing that histone deacetylases can regulate expression of genes through modulation of the level of CD-CUTs. Analysis of binding of the transcriptional activator Zap1p and insertion of transcriptional terminators upstream from the Zap1p binding sites show that CD-CUT transcription or accumulation also interferes with binding of the transcriptional activator Zap1p. Consistent with this model, overexpressing Zap1p or using a constitutively active version of the Aft1p transcriptional activator rescues the induction defect of *ZRT1* and *FIT3* in NMD mutants. These results show that cryptic upstream sense transcription resulting in unstable transcripts degraded by NMD controls repression of a large number of genes located in subtelomeric regions, and in particular of many metal homeostasis genes.

Citation: Toesca I, Nery CR, Fernandez CF, Sayani S, Chanfreau GF (2011) Cryptic Transcription Mediates Repression of Subtelomeric Metal Homeostasis Genes. PLoS Genet 7(6): e1002163. doi:10.1371/journal.pgen.1002163

Editor: Hiten D. Madhani, University of California San Francisco, United States of America

Received April 12, 2011; **Accepted** May 14, 2011; **Published** June 30, 2011

Funding: This work is supported by grants GM61518 from NIH and RSG 06-040 from the American Cancer Society to GFC and by NRSA F31 GM084678 from the National Institute from General Medical Sciences to CRN. The funders had no role in study design, data collection and analysis, decision to publish, or preparation of the manuscript.

Competing Interests: The authors have declared that no competing interests exist.

* E-mail: guillom@chem.ucla.edu

◔ These authors contributed equally to this work.

¤ Current address: Department of Microbiology, Immunology, and Molecular Genetics, University of California Los Angeles, Los Angeles, California, United States of America

Introduction

A large fraction of eukaryotic genomes is transcribed, even in the non-coding regions (reviewed in [1]). One of the major questions that arise from these observations is to understand whether the RNAs expressed from these regions serve any functional purpose or whether they correspond to genomic noise that is ultimately routed for degradation. Transcription of non-coding (nc) RNAs nearby protein-coding genes has emerged as a means of transcriptional control (reviewed in [1,2]). In the yeast *S.cerevisiae*, the first and best-documented example is the *SRG1* ncRNA, which regulates transcription of the *SER3* gene involved in serine metabolism through transcriptional interference [3]. While the *SRG1* ncRNA is transcribed in the sense direction upstream of its target gene, most ncRNAs found to regulate *S.cerevisiae* transcription are antisense transcripts, such as the ones described for the *PHO84*, *Ty-1* and *GAL10* loci [4–7], which control chromatin modification marks at these genes. However, upstream sense transcription resulting in the *ICR1* ncRNA has been found to regulate the *FLO11* gene [8].

Cryptic transcripts can also be generated through the transcription of elements that control the expression of *bona fide* protein coding genes. There is ample evidence that promoter regions are associated with bidirectional transcription in *S.cerevisiae* [2,9]. In addition, it has been shown that enhancers are transcribed by RNA polymerase II [10]. In *S.cerevisiae*, many transcripts associated with intergenic or promoter transcription are unstable under normal conditions. They are hardly detectable in wild-type strains because of their rapid degradation by nuclear RNA turnover. Indeed, many transcripts associated with cryptic transcription are detectable only when the activity of the nuclear exosome, or that of the TRAMP-complex, which stimulates exosome activity, is inhibited [2,11,12]. Therefore, these transcripts have been labeled "CUTs" for Cryptic Unstable Transcripts. Most of the degradative activities targeting CUTs seem to be concentrated in the nucleus. However, the cytoplasmic exonuclease Xrn1p can degrade the antisense RNAs that regulate the *Ty-1* gene [5]. In addition, several CUTs can be degraded by the cytoplasmic degradation machinery [12–13], showing that the degradation of RNAs arising from transcription in non-coding regions can result from both nuclear and cytoplasmic RNA degradation pathways.

Nonsense mediated decay is an RNA surveillance mechanism that recognizes transcripts containing premature translation termination codons (PTCs; [14,15]). This degradation system is used to prevent accumulation of aberrant mRNAs that would encode potentially toxic proteins [16,17], but is also used for gene expression control. For example, NMD degrades alternatively or inefficiently spliced mRNAs that contain PTCs [18–21], and transcripts containing long 3′-UTRs [22]. In *S.cerevisiae*, NMD also controls Mg^{++} uptake by degrading the transcript encoding the

Author Summary

Precise expression of genes relies on their accurate and timely transcription and on turning off these genes when production of the proteins is not required. Our study describes that in the baker's yeast, *S. cerevisiae*, repression of many genes relies on transcription of long extended RNAs upstream from where transcription normally initiates. These long extended RNAs are degraded by a machinery that recognizes that these RNAs do not encode any functional proteins. Using genes involved in controlling the uptake of the essential elements zinc and iron, we find that transcription of these long extended non-coding RNAs represses transcription by preventing the binding of the transcriptional machinery to the normal transcriptional control elements. Our findings show that repression of transcription of many genes relies on the transcription of unstable long RNAs and that this mechanism of control is particularly prevalent for genes involved in controlling the level of metals inside cells.

major Mg^{++} transporter [23]. Previous studies using microarray analysis of *S.cerevisiae* NMD mutants have shown that NMD influences directly or indirectly the expression of many genes, including some that do not exhibit PTCs [24–26]. The identification of RNAs that associate with the NMD factor Upf1p by RNA pull-down has proved to be an efficient way to discriminate direct and indirect NMD targets [27]. However, many NMD targets do not accumulate to high levels in the presence of a functional NMD system, which renders this approach difficult for low expression transcripts. In this study, using tiling microarrays, we show that NMD degrades 5′-extended transcripts generated by cryptic transcription upstream from *bona fide* promoters, and that upstream transcription is responsible for the repression of metals homeostasis genes in conditions of metal repletion. These results show that NMD controls the expression of a large number of genes by modulating the expression of 5′-extended RNAs that control transcription.

Results

Accumulation of 5′-extended unstable RNAs of subtelomeric genes in NMD mutants

We previously used tiling microarrays to show that NMD controls the degradation of inefficiently spliced *S.cerevisiae* pre-mRNAs [21]. Further analysis of these microarrays in intergenic areas revealed that many subtelomeric regions accumulated RNA signal outside and upstream from the open-reading frames (ORF) in the *upf1Δ* and *xrn1Δ* mutants. Examples shown in Figure 1 include the subtelomeric *ZRT1* gene encoding the primary zinc transporter [28], the *FIT3* gene involved in siderophore-iron transport facilitation [29], and the *FLO5* gene encoding a cell wall protein (Figure 1). Many genes located in subtelomeric regions are involved in the response to adverse growth conditions [30]. In the case of the *FIT3* and *FLO5* genes, the array profiles suggested that these species originate 5′-to the normal transcriptional start site and extend in the open-reading frame (which was confirmed by northern analysis, see below). In the case of *ADH4* and *ZRT1*, increase of signal in the upstream regions correlated with a decrease of signal in the downstream regions (Figure 1). Northern blot analysis using antisense riboprobes confirmed that these species correspond to 5′-extended transcripts originating upstream from the *bona fide* promoters and partially or completely overlapping the open-reading frame (Figure 2 and see below). Based on the array profiles, some of these species were very long, containing 5′-extensions up to several kb for *ZRT1* (Figure 1, Figure S2). In the case of *FIT3*, a previous study had mapped in detail the 5′-extended species that extends into the ORF [31]. Thus, these species are different from the short antisense CUTs transcribed divergently from the promoters [2,9]. Accumulation of 5′-extended transcripts in NMD mutants has been reported for a few transcripts, but was interpreted as the result of transcriptional noise [27]. We hypothesized that some of these 5′-extended unstable transcripts might be used for regulatory purposes, as shown in other systems [3,32,33]. Because the accumulation of 5′-extended transcripts relied on the inactivation of cytoplasmic degradation pathways, we named these 5′-extended species CD-CUTs (Cytoplasmically Degraded Cryptic Unstable Transcripts).

NMD mutants show a delay in the induction of subtelomeric metal homeostasis genes

In the case of subtelomeric genes involved in zinc metabolism (*ZRT1*, *ADH4*, *VEL1*, *YOR387C*, Figure 1; ZPS1, Figure S1), the accumulation of CD-CUTs was correlated with a decreased signal in the ORF regions, suggesting that they might play a negative role in the expression of the *bona fide* mRNAs. Interestingly, zinc regulon genes not located in subtelomeric areas, such as the one encoding the low affinity zinc transporter *ZRT2* [34] did not exhibit CD-CUTs (data not shown). We found that the growth conditions used for the microarrays (synthetic complete minimal medium) corresponded to mild zinc deficiency conditions, in which some of the zinc regulon genes were partially induced (data not shown). Therefore the decrease of signal observed in the ORF regions for *ZRT1* and *ADH4* (Figure 1) might be due to a defect in the partial induction of these genes in minimal medium. We further analyzed the expression of zinc responsive mRNAs and their corresponding CD-CUTs in wild-type and *upf1Δ* strains grown in the presence or absence of zinc, using northern blots and antisense riboprobes covering the open-reading frames (ORFs) or the upstream (UP) regions (Figure 2A). This analysis confirmed the accumulation of CD-CUTs of *ZRT1*, *ADH4* and *ZPS1* in the *upf1Δ* mutant strain. For *ZPS1*, CD-CUTs were readily detectable in the wild-type as well as in the *upf1Δ* strain, explaining why only a modest increase in upstream signal was observed for this gene on the arrays, which compare the transcripts levels of the *upf1Δ* mutant to the wild-type (Figure S1). Some CD-CUTs were detected only with the upstream riboprobes, demonstrating that they are independent from the ORFs (Figure 2A). However, most CD-CUTs were also detected using the ORF riboprobes (Figure 2A and see below), indicating that they extend through the ORFs. A detailed characterization of the *ZRT1* and *ADH4* CD-CUTs using various upstream probes and ORF probes is shown in Figure S2 and described below. ORF riboprobes detected the induction of the normal *ZPS1*, *ADH4*, and *ZRT1* mRNAs in wild-type cells grown in a medium lacking zinc (Figure 2A). However, these mRNAs were less abundant in the *upf1Δ* mutant (Figure 2A). This observation suggested that the accumulation of CD-CUTs due to NMD inactivation was deleterious to the expression of the *bona fide* mRNAs. We further characterized the expression of these genes in the *upf1Δ* mutant by monitoring their kinetics of induction (Figure 2B). This experiment showed that the *upf1Δ* mutant exhibited a delay in the induction of the subtelomeric *ZPS1*, *ZRT1*, *ADH4* (Figure 2B) and *VEL1/YOR387C* genes (Figure S3A). The induction defect was also observed in the *upf2Δ* and *upf3Δ* strains (Figure S3A), indicating that it is a general feature of NMD mutants. In contrast, the induction of other zinc regulon genes such as *ZRT2*, *GPG1* (*YGL121C*) and *PHM7* (*YOL084W*), which are not localized in subtelomeric regions and do not exhibit CD-CUTs (data not shown) was unaffected by

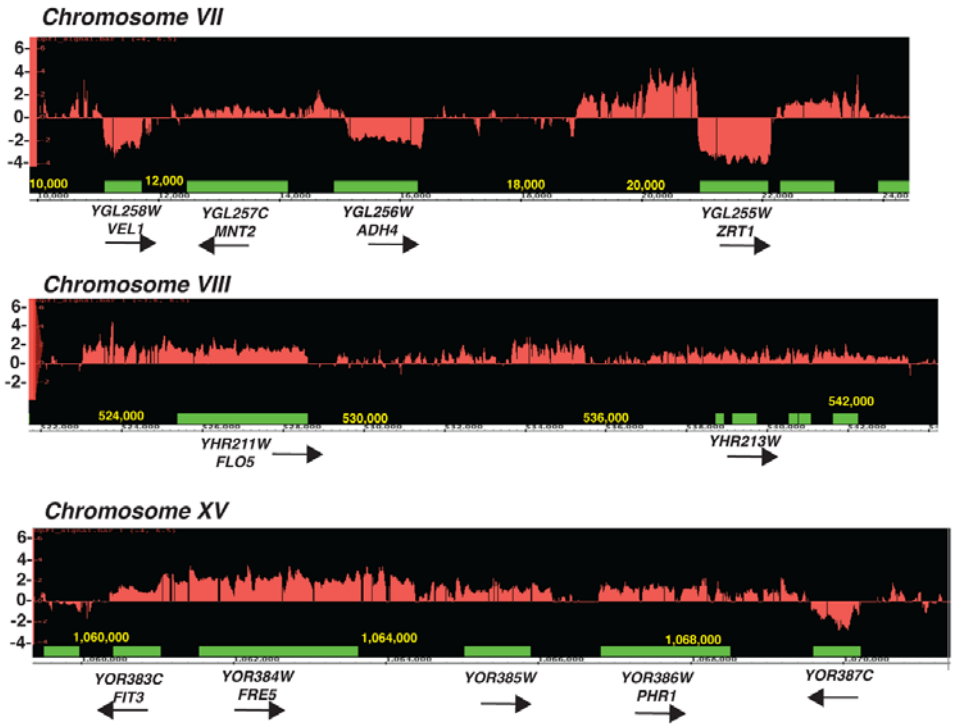

Figure 1. Tiling arrays profiles of the *upf1Δ* mutant relative to the wild-type strain. Green boxes represent the boundaries of open-reading frames, red the $\log_2$ ratio of the RNA signals detected in the *upf1Δ* mutant relative to wild-type. Arrows indicate the direction of transcription of the ORFs. Shown are three segments of three chromosomes.
doi:10.1371/journal.pgen.1002163.g001

Upf1p absence (Figure 2B). A previous study found that NMD can influence gene expression by controlling the level of transcriptional activators [35]. We found that the mRNA levels of the Zap1p activator (which activates zinc regulon genes) were similar in wild-type and *upf1Δ* mutants (Figure S3B), suggesting that the delay of induction in the absence of Upf1p was not due to reduced Zap1p levels. Overall these results show that the defective induction of subtelomeric zinc-responsive genes in the *upf1Δ* mutant is not due to a global deficiency in zinc sensing in this mutant, but is specific to genes that exhibit CD-CUTs. Defective induction was also observed for the *FIT3* iron depletion-responsive gene in a strain lacking Xrn1p or Upf1p activity (Figure S4). Overall these observations suggest that the presence or transcription of CD-CUTs represses the expression of many subtelomeric genes, some of which are involved in zinc or iron homeostasis.

Long 5′-extended transcripts of subtelomeric genes are primarily targeted by NMD, while short 5′-extended transcripts are degraded by NMD and nuclear RNA degradation pathways

To further investigate the mechanisms of turnover of CD-CUTs by the different RNA degradation machineries, we analyzed the accumulation of CD-CUTs of *ZRT1* and *ADH4* in strains lacking Upf1p, the nuclear exosome component Rrp6p, or both. These two genes were chosen because the 5′-extensions found in the CD-CUTs of *ZRT1* and *ADH4* are very different in size (extension of 2 kb for *ZRT1* vs. a few hundred nucleotides for *ADH4*). This analysis showed that the major *ZRT1* CD-CUT (CD-CUT1, Figure 2C) accumulated dramatically in the *upf1Δ* strain, and to a much lesser extent in the *rrp6Δ* mutant. Accumulation of the *ZRT1* main CD-CUT-1 was not increased in the *upf1Δrrp6Δ* double mutant compared to the *upf1Δ* single mutant (Figure 2C). These observations suggest that the degradation of the longer CD-CUT of *ZRT1* relies mostly on NMD, consistent with the long upstream region lacking any extended ORF. In contrast, the short *ADH4* CD-CUT accumulated to similar levels in the *upf1Δ* and *rrp6Δ* strains (Figure 2D). Strikingly, the accumulation of this CD-CUT was dramatically increased in the *upf1Δrrp6Δ* double mutant (Figure 2D, time zero), suggesting that this CD-CUT is degraded by the cooperative action of the nuclear exosome and of NMD. Interestingly the induction of the *bona fide ADH4* mRNA was completely defective in this double mutant strain, while the single mutants were only partially delayed. The correlation between the strong accumulation of the *ADH4* CD-CUT in the *upf1Δrrp6Δ* double mutant and the severe induction defect of the *bona fide ADH4* mRNA provides further evidence for the repression of this subtelomeric gene by its CD-CUT.

The CD-CUT of the subtelomeric iron responsive gene *FIT3* was previously shown to accumulate in the *xrn1Δrat1-1* double mutant [31], raising the question of which exonuclease was primarily responsible for its degradation. We analyzed the

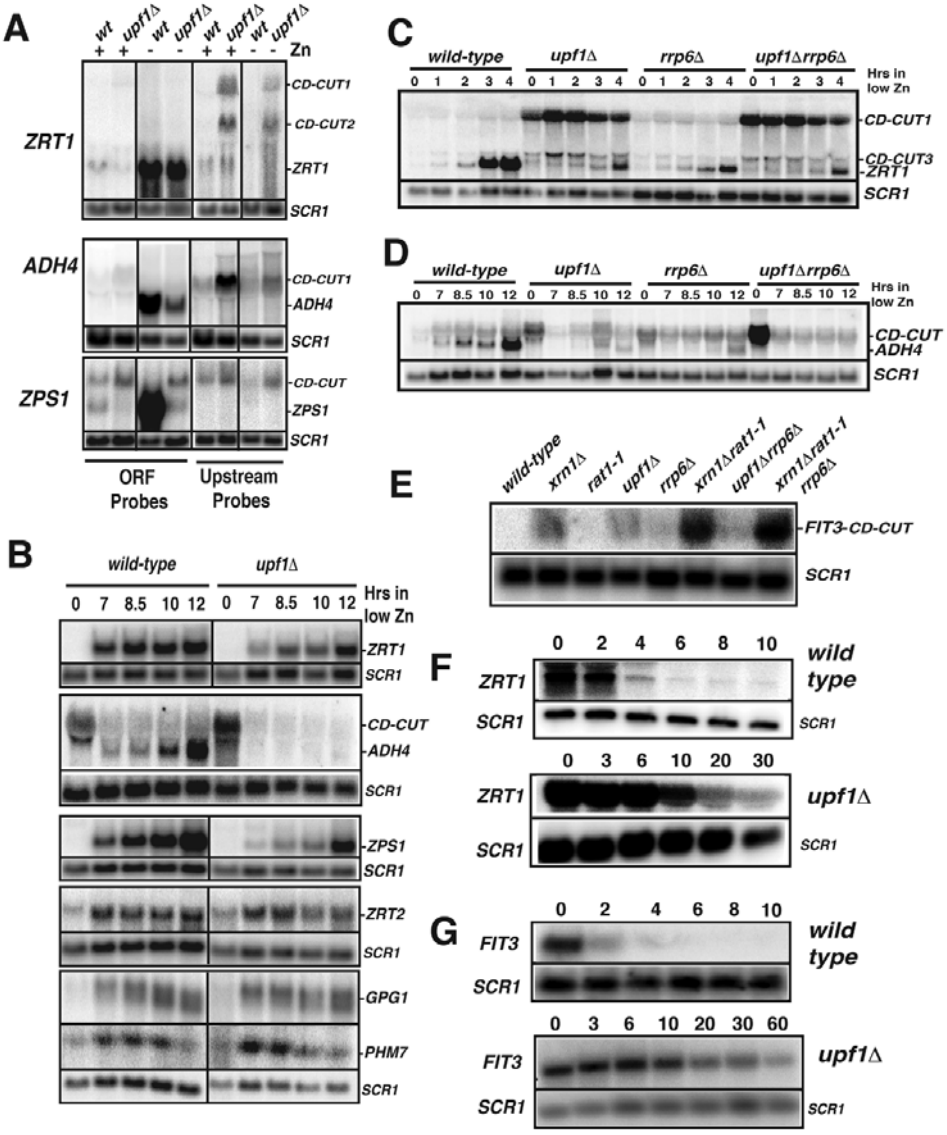

Figure 2. Characterization of CD-CUT of zinc and iron responsive genes. A. Northern blots of indicated genes in wild-type and *upf1Δ* strains grown in the presence (+) or absence (−) of zinc. Extended species are marked as CD-CUT1 and 2. *SCR1* was used as a loading control. B. Kinetics of induction of zinc regulon genes in wild-type and *upf1Δ* strains after a shift to a medium lacking zinc. C–E. Analysis of *ZRT1*, *ADH4* and *FIT3* CD-CUT and mRNA expression in ribonuclease mutants. C. Northern analysis of *ZRT1* induction in wild-type, *upf1Δ*, *rrp6Δ* and *upf1Δrrp6Δ* prior to and after a shift into low zinc medium. D, as in A for *ADH4*. E, northern analysis of the *FIT3* CD-CUT in iron-replete conditions in the indicated strains. F–G. Analysis of *ZRT1* (F) and *FIT3* (G) CD-CUT turnover in wild-type and *upf1Δ* strains. The GAL promoter was inserted upstream from the major site of transcription initiation of the *ZRT1* or *FIT3* CD-CUTs. After growth in galactose containing medium, cells were switched to glucose-containing medium and cell aliquots were harvested at the indicated times after the switch. CD-CUT levels were analyzed by northern blots using upstream riboprobes.
doi:10.1371/journal.pgen.1002163.g002

expression of this CD-CUT in strains lacking Xrn1p, Upf1p, Rrp6p, in the *xrn1Δrat1-1* mutant strain and in other double mutant strains. This analysis revealed that the long CD-CUT of *FIT3* accumulated to the highest level in the strain lacking Xrn1p and to a lesser extent Upf1p (Figure 2E), and its accumulation was not dramatically increased by Rrp6p inactivation, in contrast to

what was found for *ADH4*. Thus, based on this steady-state analysis, the long CD-CUT of *FIT3* is also primarily targeted by cytoplasmic turnover pathways that include Xrn1p and Upf1p.

The turnover of the *ZRT1* and *FIT3* CD-CUTs is dependent on NMD

Because CD-CUTs exhibit a lack of extended ORFs, we interpreted their accumulation in the *upf1Δ* and *xrn1Δ* mutant strains as the result of a lack of degradation by NMD. Alternatively, we could not rule out that transcription of these upstream regions might be indirectly up-regulated in these mutants. To test this hypothesis, *GFP-HIS3* cassettes [36] were inserted upstream from the normal *ZRT1* or *ADH4* promoters in wild-type and *upf1Δ* strains, such that the expression of the *GFP* mRNA was under the control of the upstream regions (Figure S5A). Northern blot analysis of *GFP* inserted upstream from *ZRT1* or *ADH4* showed that this reporter transcript was expressed at similar levels in the wild-type and *upf1Δ* strains (Figure S5B). These results suggested that the accumulation of CD-CUTs in NMD mutants is not due to an increased transcription of these upstream regions, but to the absence of ORF in the 5′- extension of the CD-CUTs.

To gain further evidence that the turnover of CD-CUTs is directly dependent on NMD, we replaced the region upstream from the site of transcription initiation of the *ZRT1* and *FIT3* CD-CUTs with a galactose inducible promoter. This allowed us to measure the rate of decay of these CD-CUTs in the presence or absence of functional NMD. The kinetics of turnover of the *ZRT1* CD-CUT (Figure 2F) or of the *FIT3* CD-CUT (Figure 2G) showed that these species are much more unstable in the presence of functional NMD ($t_{1/2}$ = 2–3 min.) than in the absence of Upf1p ($t_{1/2}$ = 20–30 min.). Because the turnover rate of these species is strongly decreased when NMD is inactivated, we conclude that these CD-CUTs are directly targeted by NMD for their degradation.

The main CD-CUT of *ZRT1* is activated by the histone deacetylase Rpd3p

Previous microarray analysis of a strain inactivated for the histone deacetylase Rpd3p showed that *ZRT1* is derepressed in the *rpd3Δ* strain and that Sir2p played a role antagonistic to Rpd3p in *ZRT1* expression [37]. To investigate whether Rpd3p or Sir2p control *ZRT1* by modulating the expression of its CD-CUT, we inactivated Upf1p in *rpd3Δ* or *sir2Δ* backgrounds and studied the induction of *ZRT1* in these strains. *ZRT1* was strongly derepressed in the *rpd3Δ* strain (Figure 3A, time zero), in agreement with previous data [37]. Strikingly, inactivation of Rpd3p in the *upf1Δ* strain completely rescued the induction defect of this NMD mutant, and resulted in a strong derepression of *ZRT1* in normal zinc conditions (Figure 3A). Inactivation of Rpd3p also resulted in the almost complete disappearance of the *ZRT1* CD-CUT observed in the *upf1Δ* strain. These results show that Rpd3p positively controls the expression of CD-CUT of *ZRT1*, and suggest that the derepression of *ZRT1* in the *rpd3Δ* mutant [37] is due to the absence of the CD-CUT. In contrast, Sir2p inactivation reduced *ZRT1* levels (Figure 3A), in agreement with the previous results [37]. Combining the *sir2Δ* deletion to the *upf1Δ* deletion exacerbated the *ZRT1* induction delay when compared to the *upf1Δ* mutant (Figure 4A), but the *sir2Δupf1Δ* mutant did not exhibit higher levels of CD-CUT than the *upf1Δ* single mutant (Figure 4A). Therefore, the negative effects of Sir2p inactivation on *ZRT1* expression are unlikely to be directly linked to its effect on the *ZRT1* CD-CUT.

To investigate the specificity of the effect observed with Rpd3p on the *ZRT1* CD-CUT levels, we performed the same genetic analysis with the Hos1p, Hda1p, Hda2p and Hda3p deacetylases. The *hos1Δ* strain showed a slight delay in the induction of *ZRT1*, correlated with an increase of CD-CUT levels, but the *hos1Δupf1Δ* double mutant showed no additive effect when combined with the *upf1Δ* deletion (Figure 3B). Neither Hda1p (Figure 3C), nor Hda2p or Hda3p (Figure S6) were found to affect *ZRT1* induction or repression. These results show that the major effect observed with Rpd3p on the *ZRT1* CD-CUT is specific to this deacetylase. We tried to corroborate these results by monitoring the presence of Rpd3p in the region 5′ to *ZRT1* but could not obtain reproducible evidence for enrichment by ChIP (data not shown). However the genetic data shown above strongly suggest that Rpd3p mediates the repression of *ZRT1* through the modulation of the transcription of the CD-CUT.

Inactivation of the transcription of the CD-CUTs by deletion or transcriptional termination relieves *ZRT1* and *FIT3* repression and can rescue the induction defect of the *upf1Δ* mutant

If CD-CUTs are involved in the repression of the *ZRT1* gene, we predicted that the replacement of its upstream region by the *GFP-HIS3* coding cassette (Figure S5A) might alleviate its repression. Northern blot analysis of the strain carrying one of the insertions upstream from *ZRT1* (*zrt1-up1*; inserted 1978 to 578 nucleotides upstream from the *ZRT1* ATG; Figure S5A) showed a four-fold derepression of *ZRT1* in zinc repletion conditions, both in the wild-type and *upf1Δ* backgrounds (Figure 4A). Insertion of this cassette eliminated the detection of the main CD-CUT of *ZRT1*, with the exception of the short CD-CUT3 (Figure 4A). This insertion also partially suppressed the induction defect of the *upf1Δ* strain during zinc deficiency (Figure S5C). The kinetics of disappearance of *ZRT1* upon shifting back to zinc-containing medium was also monitored in these strains after 4 hours of induction, but we found no difference in the rate of *ZRT1* shutoff in the presence or absence of its main CD-CUT (Figure S5C). A similar derepression was observed for *FIT3* in a strain carrying a 3 Kb deletion of the region upstream of the *FIT3* gene (from −4 kb to −1 kb upstream *FIT3*; *fit3-upΔ*, Figure 4B). Analysis of the *fit3-upΔxrn1Δ* double mutant strain showed that the CD-CUTs of *FIT3* were eliminated in this double mutant, which confirmed that the derepression was due to the absence of the CD-CUT. Thus, deleting the regions encoding the CD-CUTs is sufficient to trigger derepression of the *bona fide* mRNAs, even in a wild-type context.

To provide more direct evidence that transcription of CD-CUTs is responsible for repression of the downstream promoters, we inserted the *ADH1* transcription terminator (*ADH1t*) at 3 positions upstream from *ZRT1* (*tA*: −1839, *tB*: −771 and *tC*: −184 bp; Figure 4C, 4D). If CD-CUT transcription or accumulation prevents the binding of RNA polymerase or of the transcriptional activator Zap1p, we hypothesized that terminating transcription of the CD-CUTs prior to the *ZRT1* transcriptional control elements could derepress *ZRT1* and/or rescue of the induction defect of NMD mutants. We first assessed *ZRT1* mRNA and CD-CUTs levels in these strains in normal zinc conditions (Figure 4C). A sample from a strain grown in low zinc conditions was included as a control for the *ZRT1* mRNA. Insertion of *ADH1t* at position A did not result in major *ZRT1* derepression, probably because terminating transcription at this site results in activation of an alternative CD-CUT downstream from that site (labeled CD-CUT1′. Figure 4C). However insertion of this terminator resulted in a much shorter transcript that was now insensitive to a *upf1* deletion, further showing that the sensitivity of

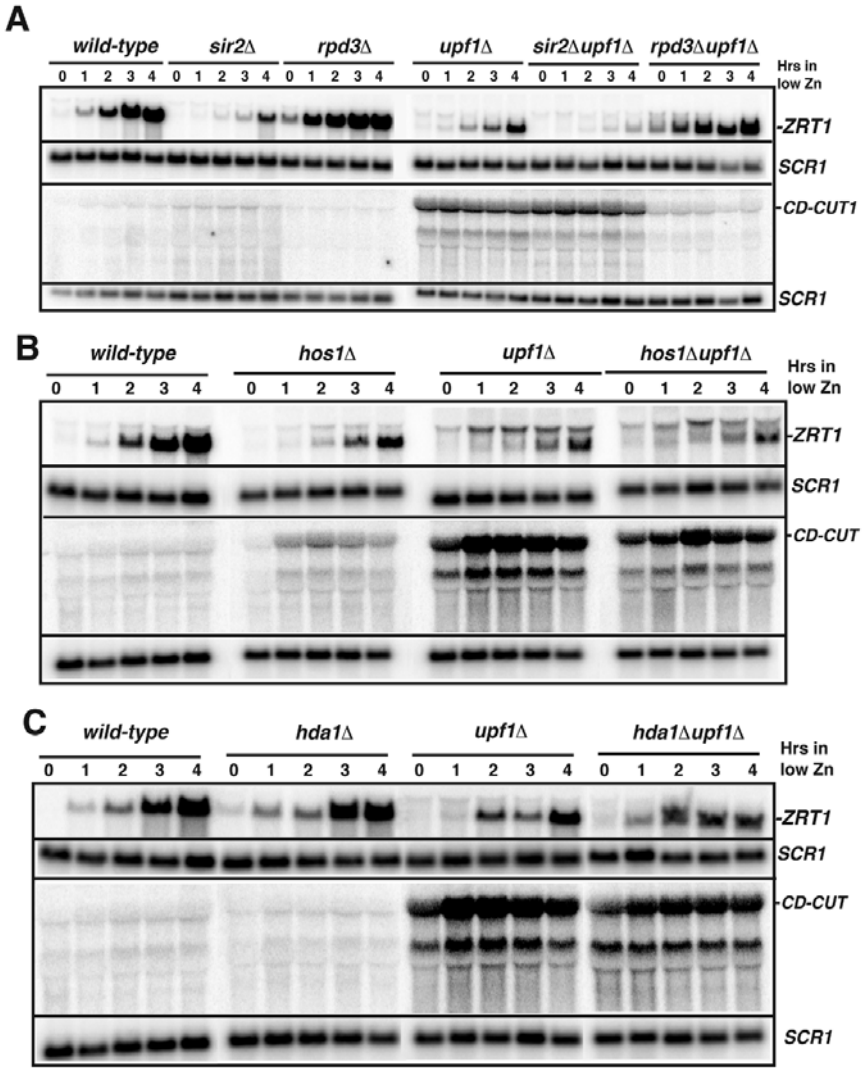

Figure 3. The main *ZRT1* CD-CUT is controlled by the histone deacetylase Rpd3p. A. Northern blot analysis of *ZRT1* mRNA and CD-CUTs in wild-type, *sir2Δ*, *rpd3Δ*, *upf1Δ* and *sir2Δupf1Δ* and *rpd3Δupf1Δ* deletion strains. B. Northern blot analysis of *ZRT1* mRNA and CD-CUTs in wild-type, *hos1Δ*, *upf1Δ* and *hos1Δupf1Δ* strains. C. Northern blot analysis of *ZRT1* mRNA and CD-CUTs in wild-type, *hda1Δ*, *upf1Δ* and *hda1Δupf1Δ* strains.
doi:10.1371/journal.pgen.1002163.g003

CD-CUTs to NMD is dependent on their long size, and potentially on the lack of extended ORF in the 5′-extension. Strikingly, insertion of the *ADH1t* at positions −771 (B) or −184 (C) resulted in a derepression of *ZRT1* (Figure 4C). The strongest effect was observed for *ADH1t-C*, possibly because this terminator stops all CD-CUT transcription immediately before the *ZRT1* TATA box. In the *ADH1t-B* strain, an increased accumulation of the CD-CUT3 is observed, while this species disappears in the *ADH1t-C* strain. These results show that terminating transcription of the CD-CUTs upstream from the *ZRT1* promoter is sufficient to derepress *ZRT1* in conditions of non-induction. Additionally, insertion of these terminators allowed us to map in further detail the CD-CUTs upstream from *ZRT1*. Based on the hybridization pattern with the different probes (Figure S2A), the effect of the various terminators on their mobility in northern blots (Figure 4C), the approximate architecture of these CD-CUTs is shown in Figure 4D.

Transcription of the zinc regulon genes is activated by binding of the transcriptional activator Zap1p to their promoters during zinc deficiency [28,38]. The terminator sequence inserted at position 771 is located upstream from the three major Zap1 binding sites (ZRE; [38]), while the terminator sequence inserted

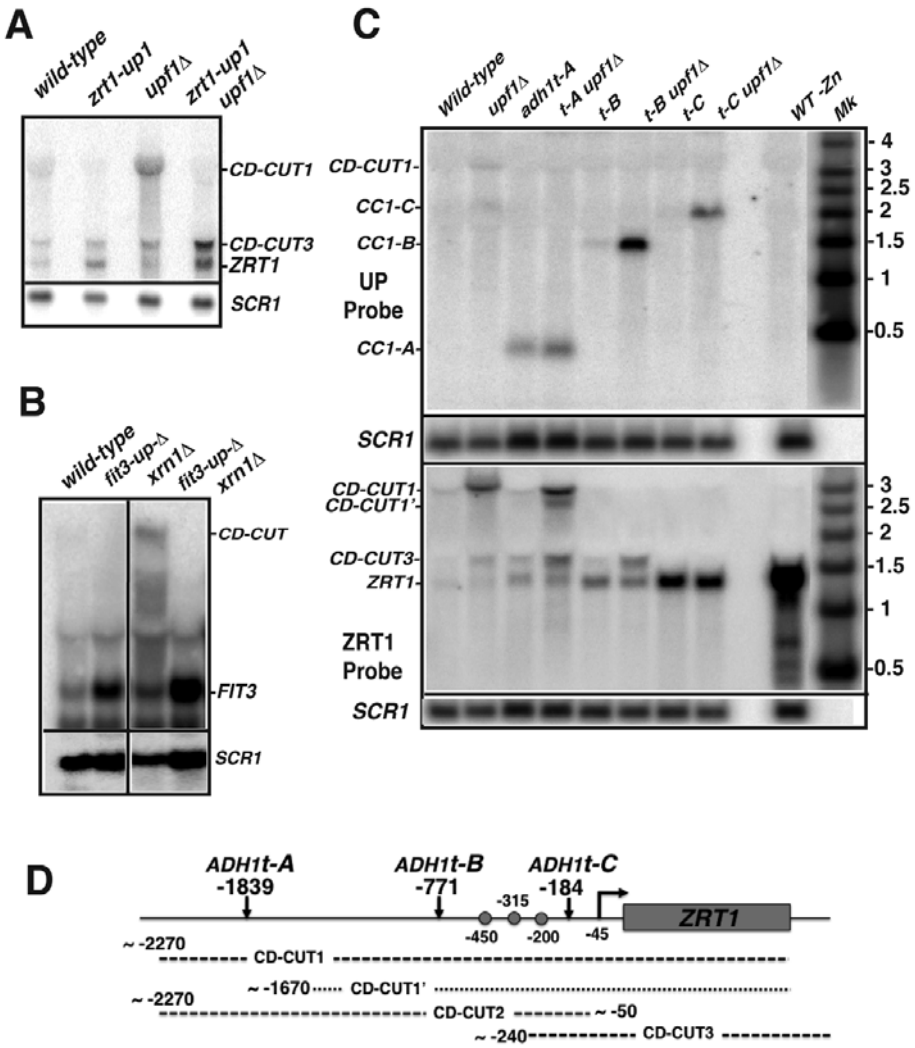

Figure 4. Mutations of the upstream regions and insertion of transcription terminators result in a derepression of *ZRT1* and *FIT3*. A. Effects of the insertion of a *GFP-HIS3* cassette upstream *ZRT1* (*zrt1-up1*) on *ZRT1* mRNA levels in zinc repletion conditions in wild-type and *upf1Δ* strains. *ZRT1* RNAs were assessed by northern blot using an ORF probe. B. Effects of the deletion of the region upstream *FIT3* (*fit3-upΔ*) on *FIT3* levels in iron repletion conditions in wild-type and *xrn1Δ* strains. *FIT3* RNAs were assessed by northern blot using an ORF probe. C. Effects of the insertion of *ADH1t* transcriptional terminators at various sites upstream *ZRT1* on *ZRT1* mRNA and CD-CUT levels in zinc repletion conditions in wild-type and *upf1Δ* strains. Mk is a size marker. The upper membrane was hybridized with a probe upstream from the *ZRT1* ORF, while the lower membrane was hybridized with a probe corresponding to the *ZRT1* ORF. D. *ADH1t* terminator insertion sites and schematic maps of *ZRT1* CD-CUT species. Dots represent the three major Zap1p binding sites.
doi:10.1371/journal.pgen.1002163.g004

at position 184 is inserted downstream from them (Figure 4D). Based on this, we hypothesized that if transcription of the CD-CUTs prevents binding of Zap1p, the two strains containing terminators at the two positions might behave differently during a shift into low zinc conditions. Indeed, insertion of the *ADH1t* at position B derepressed *ZRT1*, and also fully rescued the induction defect of the *upf1Δ* strain (Figure 5A). However strains carrying an insertion of the *ADH1t* at position C failed to induce *ZRT1* in conditions of induction, even in a context of active NMD. This result suggests that the region located between positions B and C, which contains most of the Zap1p binding sites must be accessible for *ZRT1* induction. It is unclear why the strain containing the *ADH1t* at position C failed to induce *ZRT1*, even when NMD is active. It is possible that the higher levels of expression of the

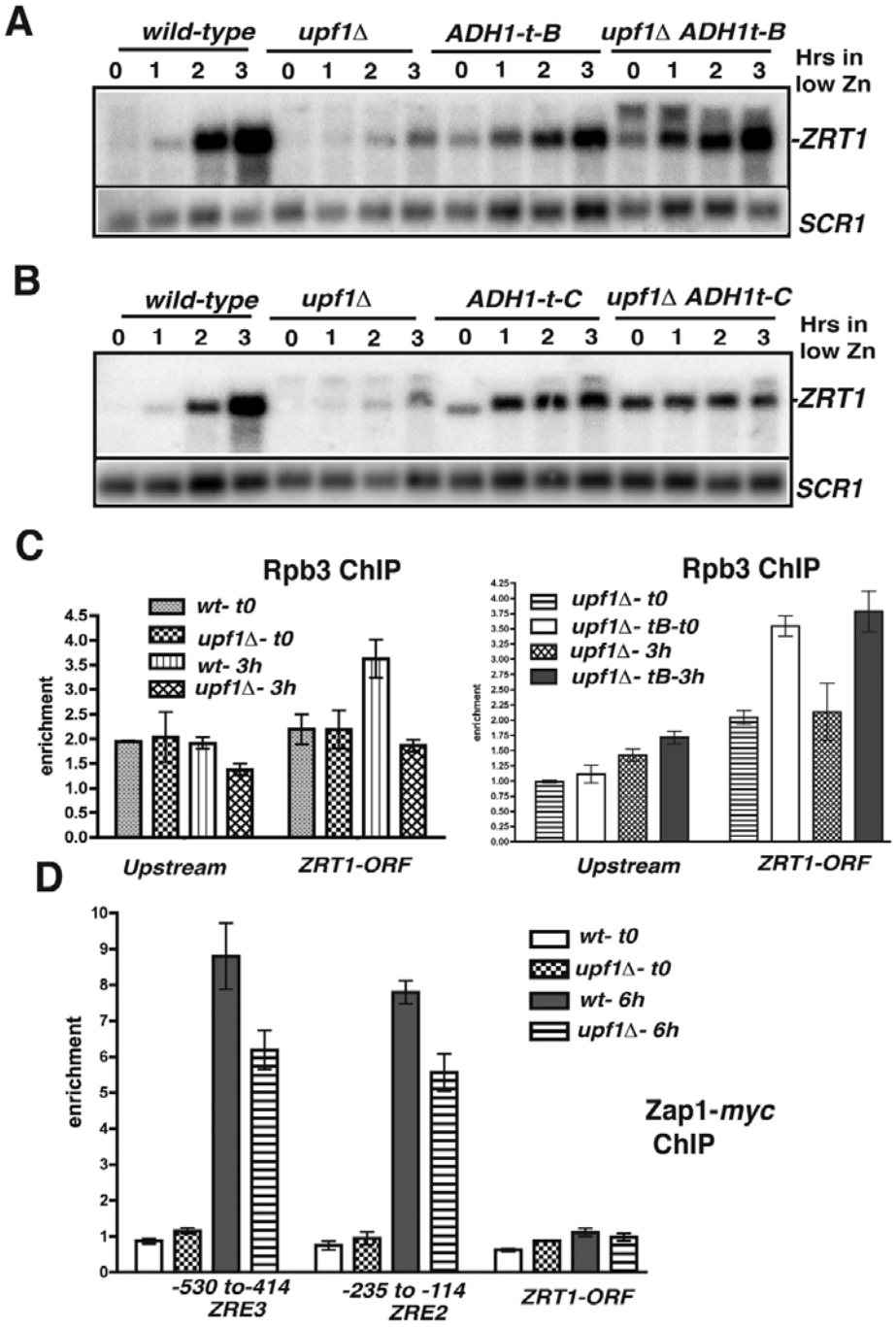
A
wild-type
upf1Δ
ADH1-t-B
upf1Δ ADH1t-B
0 1 2 3 0 1 2 3 0 1 2 3 0 1 2 3
Hrs in low Zn
-ZRT1
SCR1
B
wild-type
upf1Δ
ADH1-t-C
upf1Δ ADH1t-C
0 1 2 3 0 1 2 3 0 1 2 3 0 1 2 3
Hrs in low Zn
-ZRT1
SCR1
C
Rpb3 ChIP
wt- t0
upf1Δ- t0
wt- 3h
upf1Δ- 3h
enrichment
Upstream
ZRT1-ORF
Rpb3 ChIP
upf1Δ- t0
upf1Δ- tB-t0
upf1Δ- 3h
upf1Δ- tB-3h
enrichment
Upstream
ZRT1-ORF
D
wt- t0
upf1Δ- t0
wt- 6h
upf1Δ- 6h
enrichment
Zap1-myc ChIP
-530 to-414 ZRE3
-235 to -114 ZRE2
ZRT1-ORF

Figure 5. Effects of transcription terminators upstream *ZRT1* on *ZRT1* induction and analysis of RNA Polymerase II and Zap1p occupancies by ChIP. A and B. Effects of the insertion of ADH1 transcriptional terminators at various sites upstream *ZRT1* on *ZRT1* mRNA during zinc depletion in wild-type and *upf1Δ* strains. C. Analysis of RNA polymerase II occupancy in wild-type, *upf1Δ* and *upf1Δ ADH1t*-B strains grown in normal zinc medium (t0) or after a 3 hours shift in low zinc. Shown are normalized qPCR analysis of the different regions from ChIP samples obtained using anti-Rpb3p antibodies normalized to input DNA and to a qPCR product for a control non-transcribed region. D. Analysis of Zap1p occupancy at different sites of the *ZRT1* gene. Legends as in 5C except that a myc-tagged version of Zap1p was used.
doi:10.1371/journal.pgen.1002163.g005

ZRT1 transporter in non-induction conditions resulted in higher cellular zinc levels prior to induction, thus delaying the response. Additionally we cannot rule out that inserting the *ADH1t* at site C might have changed the chromatin structure, and thus perturbed the induction of *ZRT1*.

Binding of RNA Polymerase II and of the transcriptional activator Zap1p is defective in the NMD mutant *upf1Δ*

To corroborate these results, we studied RNA Polymerase II occupancy in two regions, upstream from *ZRT1* (−1223 to −1123), and within the *ZRT1* ORF (+905 to +1021), using chromatin immunoprecipitation (ChIP) of the Rpb3p subunit. We found slightly above background levels of occupancy of the polymerase in conditions of zinc repletion in both regions in wild-type and *upf1Δ* strains (Figure 5C). Interestingly, Rpb3p occupancy was similar for both strains in the upstream region, indicative of a similar level of transcription of the CD-CUTs. This result further indicates that accumulation of the CD-CUTs in the *upf1Δ* strain is due to a lack of degradation rather than increased transcription. Upon a shift to low zinc medium, Rpb3p occupancy increased for the wild-type strain in the *ZRT1* ORF, but not in the upstream region, reflecting the induction of the *ZRT1* gene. However this increase was not observed in the *upf1Δ* strain, corroborating the results observed by northern analysis. To show that the insertion of the terminator upstream from *ZRT1* rescues the induction defect of the *upf1Δ* strain by allowing polymerase binding, we performed the same analysis by comparing Rpb3p occupancy in the *upf1Δ* and *upf1Δ-ADH1t-B* strains. Strikingly, Rpb3p levels were increased upon insertion of *ADH1t* at position B in the *upf1Δ* strain, both in normal zinc medium and after 3 hrs of induction, showing that the derepression of *ZRT1* and the rescue of the induction defects are due to increased RNA Polymerase occupancy.

We also analyzed binding of the transcriptional activator Zap1p by ChIP in wild-type and *upf1Δ* strains using a *myc*-tagged version of Zap1p inserted at the chromosomal locus. We found background levels of Zap1p occupancy to its binding sites (ZREs) in conditions of repression in both strains (Figure 5D). However increased occupancy was observed in the wild-type strain upon a shift to low zinc (Figure 5D). Binding was reduced in the *upf1Δ* mutant, further showing that the accumulation of CD-CUTs perturbs Zap1p binding during *ZRT1* induction. Zap1p enrichment was highly specific, as it was not observed in the *ZRT1* coding region (Figure 5D). Overall the differences in RNA polymerase II and Zap1p occupancies in the *ZRT1* gene are consistent with the results described above by Northern blot, showing that the effects observed in NMD mutants upon accumulation of CD-CUTs are indicative of transcriptional defects of the *ZRT1* gene.

Overexpression or constitutive activation of transcriptional activators of subtelomeric genes suppresses their induction defect in the *upf1Δ* and *xrn1Δ* strains

The previous result showed that binding of the Zap1p activator is deficient in the NMD mutant *upf1Δ* during the low zinc response. If so, we predicted that overexpressing Zap1p might suppress the induction delay in this strain. Indeed, overexpressing Zap1p in the *upf1Δ* mutant was sufficient to rescue *ZRT1* induction to levels comparable to those observed in the wild-type strain (Figure 6A). This result shows that defective binding of Zap1p to the ZREs in the *upf1Δ* mutant can be overcome by overexpressing this activator. To extend these results to another gene induced in different conditions and controlled by a different activator, we monitored the expression of *FIT3* in wild-type and *xrn1Δ* strains expressing *aft1-up*, a constitutively active version of Aft1p (kindly provided by J.Kaplan; [39,40]. Aft1p is one of the two major transcriptional activators involved in the low iron response [39]. As expected, expression of the *aft1-up* allele resulted in derepression of the *FIT3* mRNA in normal iron conditions in the wild-type strain (Figure 6B). However, similar levels of the mature *FIT3* transcript were observed in an *xrn1Δ* background when the *aft1-up* allele was expressed, showing that the presence of a constitutively activated form of Aft1p can overcome CD-CUT-mediated repression. The accumulation of the *FIT3* CD-CUT was not affected by expression of the *aft1-up* construct (Figure 6B), showing that this effect was not due to a decrease of expression of CD-CUT. We also monitored *FIT3* induction in these strains upon a shift to low iron conditions (Figure 6C). Interestingly, *FIT3* levels did not increase in the *aft1-up* strain upon a shift to low iron conditions (Figure 6C). However *FIT3* accumulation was higher in the *xrn1Δ aft1-up* double mutant, possibly because of a reduced degradation of the *FIT3* mRNA in the absence of Xrn1p.

Accumulation of CD-CUTs abolishes the derepression of *FIT3* induced by a Mediator component mutation

To investigate the specificity of the effects described above, we searched for conditions in which the induction of *ZRT1* or *FIT3* was uncoupled from activation by their transcriptional activators. Mutation of the Med2p tail component of the Mediator complex into a non-phosphorylated isoform (*med2-S208A*) was shown to result in a constitutive expression of *FIT3* [41]. This observation led us to investigate the effect of the accumulation of the *FIT3* CD-CUT on the derepression of *FIT3* induced by this Mediator component mutation. We inactivated Xrn1p in a strain carrying the *med2-S208A* mutation (kind gift of F.Holstege) and analyzed the expression of *FIT3*. *FIT3* derepression was observed in the *med2-S208A* mutant grown in normal medium (Figure 6D; time zero), in agreement with previous findings [41], but this mutant did not exhibit any further induction in low iron until 3 hours after the shift. Strikingly, inactivating Xrn1p in the *med2-S208A* strain abolished the derepression of *FIT3* observed in the *med2-S208A* strain (Figure 6D). However the *xrn1Δmed2-S208A* mutant strain was not as defective for induction as the *xrn1Δ* strain, since the double mutant showed kinetics of *FIT3* induction comparable to the wild-type strain. The result obtained in normal iron conditions (time zero, Figure 6D) shows that the accumulation of the *FIT3* CD-CUT can inhibit the activation of *FIT3* that results from a mediator component mutation. These results contrast with the result observed previously with the *aft1-up* mutation, which can activate expression of *FIT3* even when CD-CUTs accumulate due to the inactivation of Xrn1p. Taken together, these results suggest

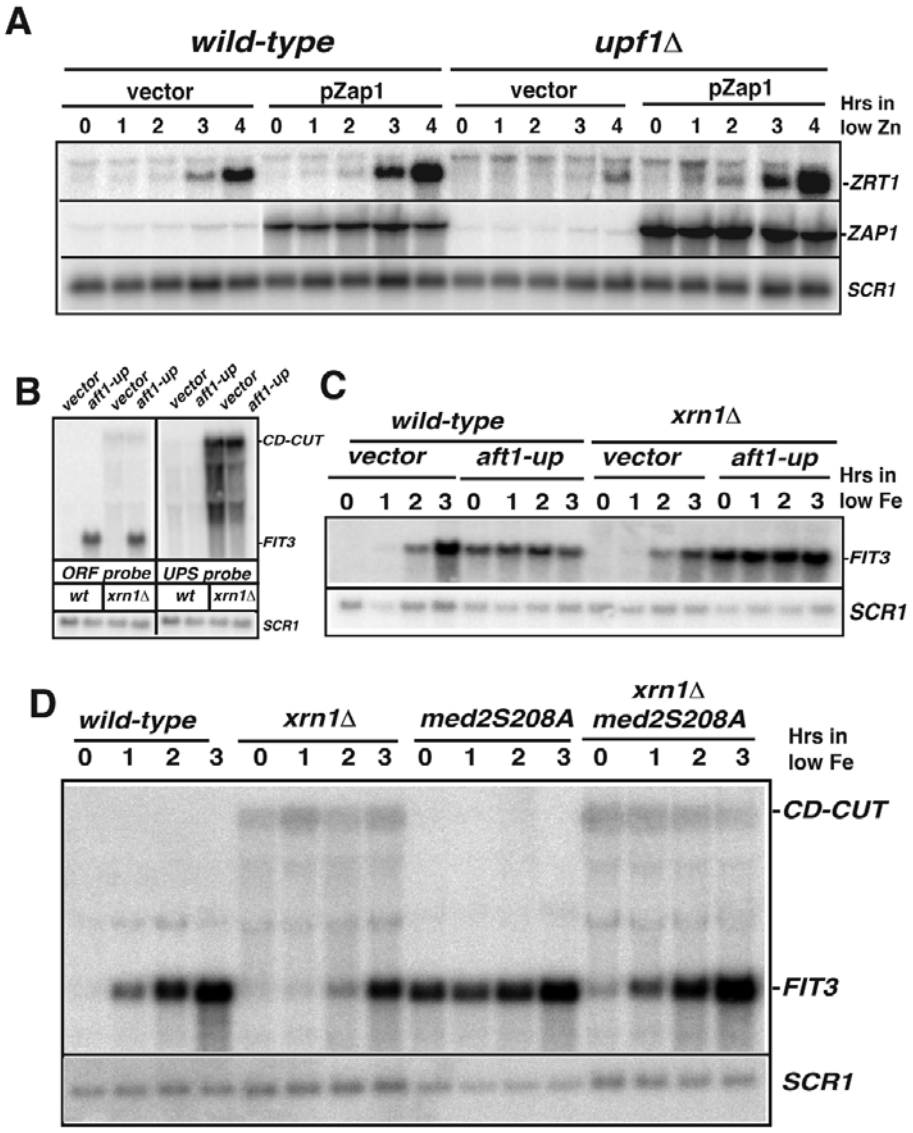

Figure 6. CD-CUT mediated transcriptional repression can be rescued by overexpression or constitutive activation of transcriptional activators. A. Overexpression of Zap1 rescues the *ZRT1* induction defect observed in the *upf1Δ* mutant. Induction of *ZRT1* in wild-type and *upf1Δ* mutant containing an empty vector or a vector overexpressing Zap1p (pZap1) under the control of a *MET25* promoter. The WT or *upf1Δ* stains containing the vector pUG35 or pIT31 were grown in normal zinc conditions (time zero) or after overexpression of Zap1 and shift into low zinc medium. B and C. Expression of the *aft1-up* allele induces *FIT3* expression even in the presence of the *FIT3* CD-CUT. A plasmid expressing the *aft1-up* allele or a control vector were transformed into wild-type and *xrn1Δ* strain, and the levels of *FIT3* mature mRNA or those of the CD-CUT were assessed by northern analysis using an ORF or an upstream (UP) probe, respectively. In panel C, the level of the *FIT3* mRNA was assessed in these strains prior to and after a shift to low iron conditions. D. Analysis of *FIT3* induction in wild-type, *xrn1Δ*, *med2S208A* and double mutant strains.
doi:10.1371/journal.pgen.1002163.g006

that the function of the *FIT3* and *ZRT1* CD-CUTs is to prevent the premature binding of the RNA polymerase or of transcriptional activators such as Zap1 and Aft1p when these genes are transcriptionally repressed.

Discussion

Stable non-coding RNAs that can be detected without perturbations of the RNA degradation machinery have been shown to accumulate near many genes [42–44]. Here we show that strains defective for NMD accumulate 5′-extended forms (CD-CUTs) of many subtelomeric genes, some of which are involved in zinc and iron uptake and homeostasis. The accumulation of CD-CUTs is observed for a large number of genes located in subtelomeric regions in NMD mutants (Figure 1; Table S1). NMD also degrades the upstream sense ncRNA *ICR1* that regulates the *FLO11* gene ([8]; Figure S1B). Therefore CD-CUTs degraded by NMD are not exclusively involved in regulating metal homeostasis genes. Given the number of transcripts for which we detected a potential accumulation of CD-CUTs in NMD mutants by tiling arrays (Table S1), and the fact that extended forms of *SRG1*, which regulate *SER3* transcription can be degraded by NMD [13], we speculate that cryptic upstream sense transcription might be used more widely than previously thought. However most of these transcripts are normally undetectable or present at very low levels because of active NMD.

CD-CUTs are clearly degraded by NMD, as shown by their extended half-life in the absence of Upf1p (Figure 2F, 2G) and because they are no longer stabilized by a *upf1* deletion when a long ORF is inserted in their place (Figure S5B). CD-CUTs are likely recognized as NMD substrates because of the lack of extended ORFs in the 5′-regions upstream from the natural ORF. This might result in random translation initiation in the 5′-region, followed shortly by a stop codon, resulting in recognition of a *faux*/extended 3′-UTR [45], thus targeting them to NMD. In support of this model, terminating transcription of the main *ZRT1* CD-CUT in a manner that results in a shorter transcript renders it insensitive to a *upf1* deletion (Figure 4C, *adh1t-A* strain). CD-CUTs accumulating in NMD-deficient strains are different from the CUTs accumulating in nuclear exosome or TRAMP complex mutants [11,46,47]. CD-CUTs are much larger than CUTs, and most of them extend within the open-reading frames to terminate at or near the site of normal 3′ processing of the ORF mRNAs (Figure 1 and Figure 2, Figure S2, Figure 4D). Thus, both the nuclear exosome and cytoplasmic NMD degradation machineries are used to regulate gene expression but act on different sets of promoter-associated unstable RNAs. However, the two pathways can sometimes intersect, for example, in the case of the *ADH4* CD-CUT, which is efficiently degraded only when both NMD and the nuclear exosome is inactivated (Figure 2; Figure 7).

How do CD-CUTs mediate transcriptional repression?

The precise mechanism by which CD-CUTs mediate transcriptional repression is not fully understood. Accumulation of CD-CUTs in NMD mutants negatively interferes with production of the normal transcripts and with RNA polymerase II and transcriptional activator binding (Figure 5, Figure 6, Figure 7). We do not know whether acting in *cis* is strictly required, which would be consistent with an *SRG1*-like transcriptional interference model [3]. We tried to express the *ZRT1* CD-CUTs from a plasmid to test for the possibility of a *trans* effect, but could not detect any reproducible effect on *ZRT1* induction (data not shown). A recent study showed that transcription of the sense upstream ncRNA *ICR1* mediates transcriptional control of the subtelomeric *FLO11* gene [8]. We found that the region upstream from the *FLO11* gene encoding *ICR1* shows elevated RNA levels in the *upf1Δ* strain (Figure S6). Like *ICR1*, expression of the *ZRT1* CD-CUT is under the control of the histone deacetylase Rpd3p (Figure 4 and [8]). Based on these similarities, it is possible that the mechanisms of transcriptional control of the *FLO11* gene mediated by *ICR1* described in [8] may be applicable to the action of the CD-CUTs that control other subtelomeric regions.

The experiments in which we inserted transcription terminators upstream from *ZRT1* do not allow us to differentiate between the *cis* and *trans*-acting models for CD-CUTs. Insertion of the terminator at position B relieves repression and allows the *upf1Δ* strain to induce *ZRT1* in low zinc conditions (Figure 5). However in this strain, the CD-CUTs terminate before the Zap1 binding sites, so the results could be interpreted either way (transcriptional interference or *trans*-acting). Insertion of the terminator at position C relieves repression, but also inhibits *ZRT1* induction even when NMD is active (Figure 5). Thus, we cannot conclude whether the CD-CUTs act in *trans* or are only the product of transcription that generates transcriptional interference. Because NMD mutants show higher CD-CUTs levels without a higher level of RNA Polymerase in the CD-CUT transcribed region (Figure 5C) and also result in stronger repression, we favor the hypothesis that these RNAs act in *trans*. However, further work is required to fully prove this point. Another unanswered question is to understand how the transcriptional machinery overcomes CD-CUT mediated repression in conditions of induction. It is possible that CD-CUT transcription is decreased in these conditions, but neither northern analysis nor the ChIP data seem to indicate that this is the case. Another alternative is that activation of the transcriptional activators is so potent during induction that it can overcome CD-CUTs mediated repression, even if the level of transcription of CD-CUTs does not change. The results obtained with the Zap1p overexpression or the constitutive Aft1p allele strains (Figure 6) are consistent with this model.

How does a cytoplasmic degradation pathway influence nuclear transcription?

One of the paradoxes raised by our observations is that 5′-extended species of subtelomeric genes are degraded by NMD, which is a cytoplasmic degradation pathway (Figure 7), yet, these CD-CUTs mediate transcriptional repression, and must therefore be localized to the nucleus if they mediate repression. Interestingly, many subtelomeric genes exhibit a perinuclear localization in *S.cerevisiae* [48]. In addition, connections have been made between nuclear activation of genes and localization at the periphery of the nuclear envelope near the nuclear pores (reviewed in [49]). Finally, Upf1p has been shown to interact with two nucleoporins localized on the outer side of the nuclear envelope, Nup100p and Nup116p ([50]; Figure 7), suggesting that at least part of the NMD process might occur at the vicinity of the nuclear envelope (Figure 7). Therefore if both subtelomeric genes and NMD components are localized close to the nuclear envelope but on opposite sides of the nuclear pores, the physical distance between the sites of transcription and action of CD-CUTs, and their site of degradation might be closer than thought from just considering the nuclear/cytoplasmic distribution (Figure 7). This would possibly allow retrograde transport of these CD-CUTs from their site of degradation to their site of action, and would allow a regulation of transcription by ncRNAs primarily degraded in the cytoplasm (Figure 7). It is also possible that CD-CUTs might be

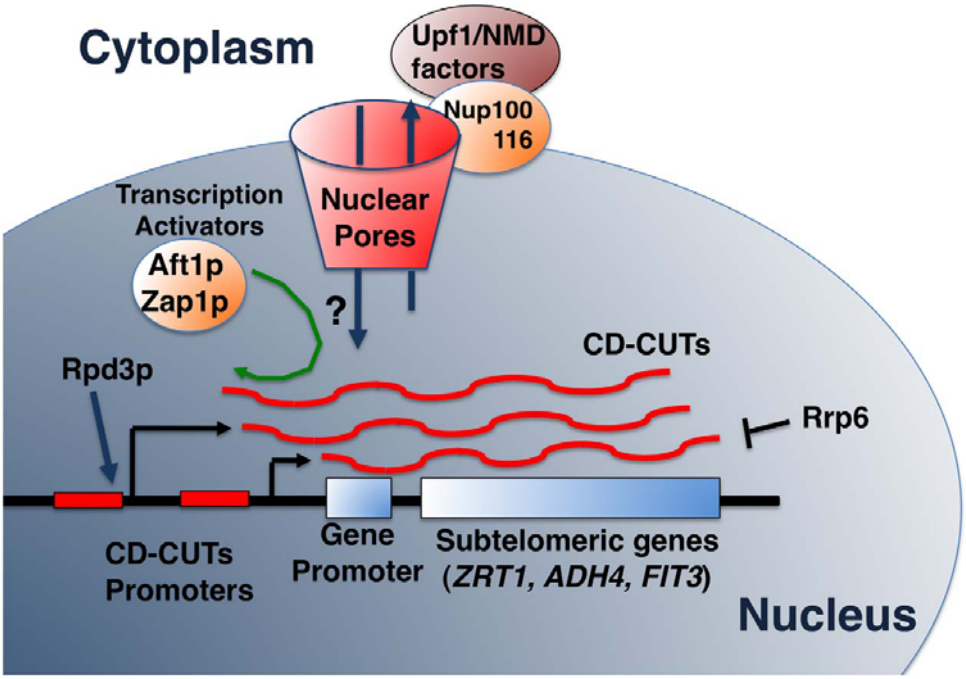

Figure 7. Model of biogenesis, action, and degradation of CD-CUTs. The model shows the degradation of CD-CUTs by the NMD pathway, potentially localized at the vicinity of the nuclear pore due to the anchoring by the Nup100/116 nucleoporins [50]. Hypothetical retrograde transport of CD-CUTs is shown by a question mark but would explain the increased repression of subtelomeric genes in the absence of cytoplasmic degradation in NMD mutants.
doi:10.1371/journal.pgen.1002163.g007

degraded when they emerge out of the nuclear pore complex, and that failure to degrade induces an increase of their nuclear localization, explaining a higher level of repression in NMD mutants. A better analysis of the mechanisms of nuclear/cytoplasmic trafficking of these CD-CUTs will ultimately allow a full understanding of their mechanisms of action.

Conserved functions for ncRNAs and NMD in the control of the expression of metal homeostasis genes

Despite these unanswered questions, our results have uncovered a novel function for NMD in controlling the accumulation of transcripts that negatively interfere with transcription of genes involved in zinc and iron homeostasis. Previous work has shown that upstream ncRNAs are involved in controlling gene expression related to metals homeostasis. It was shown that Zap1p activates the transcription of ncRNAs which mediate the repression of zinc-dependent alcohol dehydrogenases by transcriptional interference during zinc deficiency [51]. However it is unclear whether or not these ncRNAs are targeted by NMD, in a manner similar to CD-CUTs that regulate *ZRT1*, *ADH4* and *FIT3*. A potential transcriptional interference mechanism involving long unstable upstream sense ncRNA has also been described in *Chlamydomonas* during copper deficiency [52], suggesting that this mechanism has been conserved during evolution to contribute generally to metal homeostasis genes regulation. Thus, there seems to be prevalent use of ncRNA transcription to control gene expression during metals homeostasis in different organisms.

In addition to the potential crosstalk with transcription described here, NMD was also recently shown to regulate Mg^{++} cellular levels [23] by degrading the transcript encoding the main Mg^{++} transporter. The fact that this RNA surveillance system is so intimately implicated in the regulation of metals homeostasis in general might be linked to the prevalence of these metals in the ribosome and in their function of translation and in its fidelity [23], possibly revealing another layer of co-evolution between NMD and translation.

Materials and Methods

Yeast strains and media

Most strains were derived from BY4741 or 4742 (Open Biosystems). Strains in which the *GFP-HIS* cassette in the upstream region of *ZRT1* or *ADH4* gene were obtained by homologous recombination [36]. The strain carrying the deletion of the region upstream *FIT3* and the strains containing the terminator insertions were obtained by *delitto perfetto* [53]. Double mutants in which the *UPF1* or *XRN1* genes were knocked out were obtained by direct disruption of these genes in other mutant strains, as described [21]. Insertion of the myc-tag for Zap1p was performed as described [36].

Strains were grown in conditions of non-induction in either YPD or Synthetic Complete medium (SC) supplemented with 2 mM $ZnCl_2$. Growth in condition of low zinc gene induction was performed in either a Chelex-treated synthetic complete medium (CSC) or a SC medium containing 1 mM EDTA, pH adjusted to

4.4 with 20 mM citrate. CSC was prepared as described [28] except that all amino acid required were added and pH adjusted to 4.4. Growth in conditions of low iron gene induction was performed by adding BPS chelator as described [31]. Strains were grown in YPD (pre-low iron shifts) or SC+2 mM Zn (pre-low zinc shifts) until $OD_{600} = 0.5$, washed twice in sterile water, and shifted into YPD medium with BPS (low iron shift) or SC+EDTA medium (low zinc shift) for the indicated times. For the experiments including overexpression of Zap1p, WT or *upf1Δ* strains containing the vector pUG35 or pIT31 (see below) were grown in SC medium without Uracil (SC-URA) supplemented with 2 mM Zn. At $OD_{600} = 0.45$, cells were washed twice in sterile water and shifted in SC-URA without methionine (SC-URA-MET) supplemented with 2 mM Zn for 2 hours to overexpress Zap1p prior to zinc starvation. After 2 h, cells were washed twice in sterile water and maintained in log phase in SC-URA-MET medium containing 1 mM EDTA. Kinetics of induction were performed as described above.

Plasmids

A PCR product corresponding to the *ZAP1* gene was generated from genomic DNA with primers containing the restriction sites *ClaI* and *SalI* and inserted in the vector pUG35 digested by the same restriction enzymes. After transformation and amplification in *E. coli*, the plasmid (pIT31) was confirmed by sequencing. The *aft1-up* expression plasmid was obtained from J.Kaplan (U.of Utah).

RNA analysis

Tiling Arrays used in this study were described previously [21,31] and are accessible in the GEO database (accession number GSE11621). Northern blot hybridization analysis was performed as previously described [21,31]. All riboprobes were synthesized with the T3 MAXIscript kit (Ambion). Riboprobes were hybridized at 67°C except for the *ADH4* ORF probe (65°C).

Chromatin Immunoprecipitation (ChIP)

ChIPs using anti-Rpb3 RNA polymerase II subunit and a myc-tagged version of Zap1p inserted at the chromosomal locus were performed as described [54,55].

Supporting Information

Figure S1 Tiling array profiles of *ZPS1* and *FLO11*. A. Tiling array profile in the region of the *ZPS1* gene. Shown is the $\log_2$ ratio of signal detected for the *upf1Δ* strain divided by the signal for the wild-type strain. B. Tiling Array profile of the *upf1Δ* mutant compared to the wild-type strain in the right subtelomeric region of Chr IX containing the *FLO11* gene. The *FLO11* gene is localized on the Crick strand (transcribed right to left) from positions 393,672 to 389,569. The increase of signal in the *upf1Δ* mutant upstream from the *FLO11* gene is indicative of higher levels of the *ICR1* ncRNA controlling *FLO11*. Note that the neighbor genes *MRS1* and *SEC11* located in region 397,000–399,000 are not affected by the *upf1Δ* deletion.
(TIF)

Figure S2 Mapping of the CD-CUTs of *ZRT1* (A) and *ADH4* (B) genes by northern blot analysis. The *ZRT1* probes cover the following nucleotides: Probe 1: −2410 to −2089; Probe 2: −800 to −211; Probe 3: −257 to −84; Probe 4: +931 to +1131; Probe 5: +1141 to +1341 (downstream from the ORF).
(TIF)

Figure S3 Analysis of zinc regulon genes induction in NMD mutants. A. Kinetics of induction of zinc regulon genes in wild-type, *upf2Δ* and *upf3Δ* strains after a shift to a medium lacking zinc. Gene induction was monitored by northern blot using probes hybridizing to the corresponding genes. *SCR1* was used as a loading control. B. Analysis of *ZAP1* mRNAs levels in wild-type and *upf1Δ* strains. *ZAP1* mRNA levels were analyzed by northern blot from cells grown in SC+2 mM Zn (time zero), or after a shift to SC+EDTA (low Zn). An RNA sample from a *zap1Δ* strain was included as a negative control for the detection of the ZAP1 mRNA.
(TIF)

Figure S4 Kinetics of *FIT3* induction in strains lacking Xrn1p, Upf1p or in the double mutant *xrn1Δrat1-1*. Shown is a northern blot analysis of *FIT3* expression in the indicated strains using a probe complementary to *FIT3*.
(TIF)

Figure S5 Insertion of GFP cassettes upstream from *ZRT1* and *ADH4*. A. Schematic representation of the *ZRT1* and *ADH4* genes and location of the *GFP-HIS3* cassettes deletions/insertions (UP1 and UP2, UP). The dashed lines represent the regions replaced by the cassettes. B. GFP mRNA levels analyzed by northern blot in the different insertion strains. Levels were normalized to *SCR1*. A strain without GFP insertion was included as negative control. C. Effects of the deletion of the upstream region and of the insertion of a *GFP-HIS3* cassette on the kinetics of induction and shutoff of *ZRT1*. Insertion of the *GFP-HIS3* cassette upstream from *ZRT1* (*zrt1-up1*) results in a three-fold increase in the *ZRT1* mRNA peak in the *upf1Δ* strain during zinc deficiency. *ZRT1* induction was faster in the strain carrying this insertion compared to the wild-type, as shown by the amount of the *ZRT1* mRNA expressed after 30 to 120 minutes. After 4 hours of induction, the kinetics of disappearance of *ZRT1* upon shifting back to zinc-containing medium was also monitored in these strains (+zinc), and samples were harvested at the indicated times after addition of zinc to the medium. RNAs extracted from all four strains were loaded on the same gel and analyzed on the same membranes exposed to the same times, but each strain is shown as a separate panel for clarity and space purposes.
(TIF)

Figure S6 Kinetics of *ZRT1* induction in wild-type, *hda2Δ hda3Δ*, *upf1Δ*, *hda2Δupf1Δ* and *hda3Δupf1Δ* strains.
(TIF)

Table S1 List of *S.cerevisiae* ORFs for which 5′ extended species were observed by tiling microarrays in the *upf1Δ* and/or *xrn1Δ*strains.
(XLS)

Acknowledgments

We thank Cynthia Lee, Sabeeha Merchant, Michael Grunstein, and Siavash Kurdistani for helpful discussions; F. Holstege and S. Kurdistani for yeast strains; J.Kaplan for the *aft1-up* plasmid; Kevin Roy for critical reading of the manuscript; and one anonymous reviewer of a grant proposal for helpful suggestions.

Author Contributions

Conceived and designed the experiments: IT CRN GFC. Performed the experiments: IT CRN CFF SS. Analyzed the data: IT CRN CFF SS GFC. Wrote the paper: GFC.

References

1. Jacquier A (2009) The complex eukaryotic transcriptome: unexpected pervasive transcription and novel small RNAs. Nat Rev Genet 10: 833–844.
2. Neil H, Malabat C, d'Aubenton-Carafa Y, Xu Z, Steinmetz LM, et al. (2009) Widespread bidirectional promoters are the major source of cryptic transcripts in yeast. Nature 457: 1038–1042.
3. Martens JA, Laprade L, Winston F (2004) Intergenic transcription is required to repress the Saccharomyces cerevisiae SER3 gene. Nature 429: 571–574.
4. Camblong J, Iglesias N, Fickentscher C, Dieppois G, Stutz F (2007) Antisense RNA stabilization induces transcriptional gene silencing via histone deacetylation in S. cerevisiae. Cell 131: 706–717.
5. Berretta J, Pinskaya M, Morillon A (2008) A cryptic unstable transcript mediates transcriptional trans-silencing of the Ty1 retrotransposon in S. cerevisiae. Genes Dev 22: 615–626.
6. Houseley J, Rubbi L, Grunstein M, Tollervey D, Vogelauer M (2008) A ncRNA modulates histone modification and mRNA induction in the yeast GAL gene cluster. Mol Cell 32: 685–695.
7. Camblong J, Beyrouthy N, Guffanti E, Schlaepfer G, Steinmetz LM, et al. (2009) Trans-acting antisense RNAs mediate transcriptional gene cosuppression in S. cerevisiae. Genes Dev 23: 1534–1545.
8. Bumgarner SL, Dowell RD, Grisafi P, Gifford DK, Fink GR (2009) Toggle involving cis-interfering noncoding RNAs controls variegated gene expression in yeast. Proc Natl Acad Sci U S A 106: 18321–18326.
9. Xu Z, Wei W, Gagneur J, Perocchi F, Clauder-Munster S, et al. (2009) Bidirectional promoters generate pervasive transcription in yeast. Nature 457: 1033–1037.
10. Kim TK, Hemberg M, Gray JM, Costa AM, Bear DM, et al. (2010) Widespread transcription at neuronal activity-regulated enhancers. Nature 465: 182–187.
11. Wyers F, Rougemaille M, Badis G, Rousselle JC, Dufour ME, et al. (2005) Cryptic pol II transcripts are degraded by a nuclear quality control pathway involving a new poly(A) polymerase. Cell 121: 725–737.
12. Lee A, Hansen KD, Bullard J, Dudoit S, Sherlock G (2008) Novel low abundance and transient RNAs in yeast revealed by tiling microarrays and ultra high-throughput sequencing are not conserved across closely related yeast species. PLoS Genet 4: e1000299. doi:10.1371/journal.pgen.1000299.
13. Thompson DM, Parker R (2007) Cytoplasmic decay of intergenic transcripts in Saccharomyces cerevisiae. Mol Cell Biol 27: 92–101.
14. Chang YF, Imam JS, Wilkinson MF (2007) The Nonsense-Mediated Decay RNA Surveillance Pathway. Annu Rev Biochem 76: 51–74.
15. Isken O, Maquat LE (2007) Quality control of eukaryotic mRNA: safeguarding cells from abnormal mRNA function. Genes Dev 21: 1833–1856.
16. Frischmeyer PA, Dietz HC (1999) Nonsense-mediated mRNA decay in health and disease. Hum Mol Genet 8: 1893–1900.
17. Kuzmiak HA, Maquat LE (2006) Applying nonsense-mediated mRNA decay research to the clinic: progress and challenges. Trends Mol Med 12: 306–316.
18. Mitrovich QM, Anderson P (2000) Unproductively spliced ribosomal protein mRNAs are natural targets of mRNA surveillance in C. elegans. Genes Dev 14: 2173–2184.
19. Lareau LF, Inada M, Green RE, Wengrod JC, Brenner SE (2007) Unproductive splicing of SR genes associated with highly conserved and ultraconserved DNA elements. Nature 446: 926–929.
20. Ni JZ, Grate L, Donohue JP, Preston C, Nobida N, et al. (2007) Ultraconserved elements are associated with homeostatic control of splicing regulators by alternative splicing and nonsense-mediated decay. Genes Dev 21: 708–718.
21. Sayani S, Janis M, Lee CY, Toesca I, Chanfreau GF (2008) Widespread impact of nonsense-mediated mRNA decay on the yeast intronome. Mol Cell 31: 360–370.
22. Kebaara BW, Atkin AL (2009) Long 3′-UTRs target wild-type mRNAs for nonsense-mediated mRNA decay in Saccharomyces cerevisiae. Nucleic Acids Res 37: 2771–2778.
23. Johansson MJ, Jacobson A (2010) Nonsense-mediated mRNA decay maintains translational fidelity by limiting magnesium uptake. Genes Dev 24: 1491–1495.
24. Lelivelt MJ, Culbertson MR (1999) Yeast Upf proteins required for RNA surveillance affect global expression of the yeast transcriptome. Mol Cell Biol 19: 6710–6719.
25. He F, Li X, Spatrick P, Casillo R, Dong S, et al. (2003) Genome-wide analysis of mRNAs regulated by the nonsense-mediated and 5′ to 3′ mRNA decay pathways in yeast. Mol Cell 12: 1439–1452.
26. Guan Q, Zheng W, Tang S, Liu X, Zinkel RA, et al. (2006) Impact of nonsense-mediated mRNA decay on the global expression profile of budding yeast. PLoS Genet 2: e203. doi:10.1371/journal.pgen.0020203.
27. Johansson MJ, He F, Spatrick P, Li C, Jacobson A (2007) Association of yeast Upf1p with direct substrates of the NMD pathway. Proc Natl Acad Sci U S A 104: 20872–20877.
28. Lyons TJ, Gasch AP, Gaither LA, Botstein D, Brown PO, et al. (2000) Genome-wide characterization of the Zap1p zinc-responsive regulon in yeast. Proc Natl Acad Sci U S A 97: 7957–7962.
29. Protchenko O, Ferea T, Rashford J, Tiedeman J, Brown PO, et al. (2001) Three cell wall mannoproteins facilitate the uptake of iron in Saccharomyces cerevisiae. J Biol Chem 276: 49244–49250.
30. Robyr D, Suka Y, Xenarios I, Kurdistani SK, Wang A, et al. (2002) Microarray deacetylation maps determine genome-wide functions for yeast histone deacetylases. Cell 109: 437–446.
31. Lee A, Henras AK, Chanfreau G (2005) Multiple RNA surveillance pathways limit aberrant expression of iron uptake mRNAs and prevent iron toxicity in S. cerevisiae. Mol Cell 19: 39–51.
32. Martianov I, Ramadass A, Serra Barros A, Chow N, Akoulitchev A (2007) Repression of the human dihydrofolate reductase gene by a non-coding interfering transcript. Nature 445: 666–670.
33. Wang X, Arai S, Song X, Reichart D, Du K, et al. (2008) Induced ncRNAs allosterically modify RNA-binding proteins in cis to inhibit transcription. Nature.
34. Zhao H, Eide D (1996) The ZRT2 gene encodes the low affinity zinc transporter in Saccharomyces cerevisiae. J Biol Chem 271: 23203–23210.
35. Taylor R, Kebaara BW, Nazarenus T, Jones A, Yamanaka R, et al. (2005) Gene set coregulated by the Saccharomyces cerevisiae nonsense-mediated mRNA decay pathway. Eukaryot Cell 4: 2066–2077.
36. Longtine MS, McKenzie A, 3rd, Demarini DJ, Shah NG, Wach A, et al. (1998) Additional modules for versatile and economical PCR-based gene deletion and modification in Saccharomyces cerevisiae. Yeast 14: 953–961.
37. Bernstein BE, Tong JK, Schreiber SL (2000) Genomewide studies of histone deacetylase function in yeast. Proc Natl Acad Sci U S A 97: 13708–13713.
38. Zhao H, Butler E, Rodgers J, Spizzo T, Duesterhoeft S, et al. (1998) Regulation of zinc homeostasis in yeast by binding of the ZAP1 transcriptional activator to zinc-responsive promoter elements. J Biol Chem 273: 28713–28720.
39. Yamaguchi-Iwai Y, Dancis A, Klausner RD (1995) AFT1: a mediator of iron regulated transcriptional control in Saccharomyces cerevisiae. EMBO J 14: 1231–1239.
40. Philpott CC, Rashford J, Yamaguchi-Iwai Y, Rouault TA, Dancis A, et al. (1998) Cell-cycle arrest and inhibition of G1 cyclin translation by iron in AFT1-1(up) yeast. EMBO J 17: 5026–5036.
41. van de Peppel J, Kettelarij N, van Bakel H, Kockelkorn TT, van Leenen D, et al. (2005) Mediator expression profiling epistasis reveals a signal transduction pathway with antagonistic submodules and highly specific downstream targets. Mol Cell 19: 511–522.
42. Bertone P, Stolc V, Royce TE, Rozowsky JS, Urban AE, et al. (2004) Global identification of human transcribed sequences with genome tiling arrays. Science 306: 2242–2246.
43. Kapranov P, Cheng J, Dike S, Nix DA, Duttagupta R, et al. (2007) RNA maps reveal new RNA classes and a possible function for pervasive transcription. Science 316: 1484–1488.
44. Nagalakshmi U, Wang Z, Waern K, Shou C, Raha D, et al. (2008) The transcriptional landscape of the yeast genome defined by RNA sequencing. Science 320: 1344–1349.
45. Amrani N, Dong S, He F, Ganesan R, Ghosh S, et al. (2006) Aberrant termination triggers nonsense-mediated mRNA decay. Biochem Soc Trans 34: 39–42.
46. Davis CA, Ares M, Jr. (2006) Accumulation of unstable promoter-associated transcripts upon loss of the nuclear exosome subunit Rrp6p in Saccharomyces cerevisiae. Proc Natl Acad Sci U S A 103: 3262–3267.
47. Chekanova JA, Gregory BD, Reverdatto SV, Chen H, Kumar R, et al. (2007) Genome-wide high-resolution mapping of exosome substrates reveals hidden features in the Arabidopsis transcriptome. Cell 131: 1340–1353.
48. Grund SE, Fischer T, Cabal GG, Antunez O, Perez-Ortin JE, et al. (2008) The inner nuclear membrane protein Src1 associates with subtelomeric genes and alters their regulated gene expression. J Cell Biol 182: 897–910.
49. Dieppois G, Stutz F (2010) Connecting the transcription site to the nuclear pore: a multi-tether process that regulates gene expression. J Cell Sci 123: 1989–1999.
50. Nazarenus T, Cedarberg R, Bell R, Cheatle J, Forch A, et al. (2005) Upf1p, a highly conserved protein required for nonsense-mediated mRNA decay, interacts with the nuclear pore proteins Nup100p and Nup116p. Gene 345: 199–212.
51. Bird AJ, Gordon M, Eide DJ, Winge DR (2006) Repression of ADH1 and ADH3 during zinc deficiency by Zap1-induced intergenic RNA transcripts. EMBO J 25: 5726–5734.
52. Moseley JL, Page MD, Alder NP, Eriksson M, Quinn J, et al. (2002) Reciprocal expression of two candidate di-iron enzymes affecting photosystem I and light-harvesting complex accumulation. Plant Cell 14: 673–688.
53. Storici F, Lewis LK, Resnick MA (2001) In vivo site-directed mutagenesis using oligonucleotides. Nat Biotechnol 19: 773–776.
54. Yang PK, Hoareau C, Froment C, Monsarrat B, Henry Y, et al. (2005) Cotranscriptional recruitment of the pseudouridylsynthetase Cbf5p and of the RNA binding protein Naf1p during H/ACA snoRNP assembly. Mol Cell Biol 25: 3295–3304.
55. Steinmetz EJ, Warren CL, Kuehner JN, Panbehi B, Ansari AZ, et al. (2006) Genome-wide distribution of yeast RNA polymerase II and its control by Sen1 helicase. Mol Cell 24: 735–746.

Chapter 2—The Nonsense Mediated Decay Pathway

Nonsense mediated decay (NMD) is an intracellular quality control mechanism that removes and degrades RNA messages containing premature translation termination codons (PTC) [Chang et al., 2007]. There are numerous routes that can lead to the occurrence of PTCs. For example, in the mammalian immune system, in order to increase the repertoire of T-cell receptors through extensive DNA rearrangements often leads towards inclusion or exclusion of base pairs within a given gene sequence which manifests in a translational frameshift of the transcribed mRNA [Chang et al., 2007). Other modes of PTC introduction can arise through improper splicing—the chemical reaction that excises introns (intervening sequences) with the ligation of exonic sequences [Chang et al., 2007].

The basic principles of NMD

NMD is highly conserved existing from the simplest eukaryotes to the most complex metazoans (Losson and Lacroute, 1979; Perlick et al., 1996). There are three main factors that have been characterized to date that are essential in the execution of the proper NMD response. These are called upframeshift factors Upf1p, Upf2p, and Upf3p. Upf1p was discovered from studies conducted in the model yeast, *Saccharomyces cerevisiae* (Leeds et al., 1992). Furthermore, these studies also revealed that PTC-containing mRNAs have markedly increased half-lives in mutations of the Upf factors and this was due to the remarkable stability of PTC-containing mRNAs. The Upf factor, Upf1p, is a helicase (Leeds et al., 1992; Czaplinsli et al., 1998) and associates with the eukaryotic release factors (eRF) eRF1 and eRF3 (Czaplisnki et al., 1998). The other two NMD factors, Upf2p and Upf3p also associate with eRF1 and eRF3 (Wang et al., 2001). Furthermore, it has been shown that is a competition between RNA and eRF3 in binding to Upf1p (Czaplisnki et al., 1998). Such associations are important in the proper execution of the

NMD response. Although NMD is dispensable in lower eukaryotes such as yeast, it is required for viability in vertebrates. Studies have revealed that mice that are heterozygous for the Upf ortholog, Rent, are viable and normal but those that are homozygous are gestationally lethal (Medghalchi et al., 2001).

Though it is well known that Upf1p has helicase activity and is predominantly cytoplasmic [Lykke-Andersen et al., 2000], the precise biochemical role of Upf3p remains uncertain. Perhaps the only well-known facet about the activity and/or involvement of Upf3p is based on microscopy data which revealed that both Upf3p and Upf2p are nucleocytoplasmic shuttling proteins (Lykke-Anderson and Steitz, 2000). Interestingly, mammals have two copies of Upf3 annotated as *UPF3A* and *UPF3B* (Chang et al., 2007). However, it has been shown that UPF3A and UPF3B exert differing functions. UPF3A is less efficient at activating the NMD response than UPF3B (Kunz et al., 2006). Moreover, the study by Kuntz and colleagues has revealed that at the molecular level, the difference in UPF3A and UPF3B is within the C-terminal domains of the proteins [Kunz et al., 2006]. The C-terminus of UPF3B but not UPF3A is remarkably conserved across vertebrates [Kunz et al., 2006]. The *UPF3A* and *UPF3B* form a complex with the exon-junction complex factors Y14, Magoh, eIFAIII, and BTZ [Kunz et al., 2006]. Furthermore, extensive biochemical studies performed by Gehring and colleagues have shown that a critical, conserved arginine residue within the C-terminus of UPF3B is crucial for its function in eliciting NMD [Gehring et al., 2003]. Importantly, the study by Kunz and colleagues revealed that there are two distinct functional attributes of UPF3 proteins—the NMD response and translation activation which are independent of each other [Kunz et al., 2006].

UPF2 functions to bridge UPF1 and UPF3 [Chang et al., 2007] Furthermore, biochemical studies by Serin and colleagues have provided evidence that the C-terminus of UPF2 has the ability to interact with both UPF1 and UPF3 [Serin et al., 2001]. Studies aimed towards understanding the localization pattern of UPF2 have revealed that it occupies a peripheral niche outside of the nuclear membrane [Lykke-Anderson et al., 2000]. Furthermore, studies by Lejeune and colleagues have shown that UPF2 is found in purified nuclear extract [Lejeune et al., 2002]. However, an important question related to the precise mechanism of UPF2 recruitment is still unresolved and remains an active area of investigation.

Post-translational modifications of the NMD factors

The NMD factor UPF1 undergoes a cycle of phosphorylation and dephosphorylation by the Suppressor with Morphogenetic defect on Genitalia(SMG-1) phosphatidylinositol-3-kinase (PI3) (Grimson et al., 2004) and is required for the proper function of the UPF factors in the NMD response (Grimson et al., 2004). The SMG-1 kinase has specificity in phosphorylating serine and/or threonine residues [Yamashita et al., 2001].

Recently, it was reported that a stable protein complex in mammalian cells termed SURF (Smg1-Upf1-eRF1-eRF3) is present on the exon junction complex (EJC) (Kashima et al., 2006). The binding of this complex to the EJC results in UPF1 phosphorylation. This important finding provided connectivity between UPF factors, the EJC, and the SMG-1 kinase complex that performs the phosphorylation reaction [Kashima et al., 2006].

There have been four SMG factors that are involved in controlling the phosphorylation of UPF1: SMG1, SMG-5-SMG-6- and SMG-7 [Pulak and Anderson, 1993]. The SMG factors SMG-5;

SMG-6; and SMG-7 are important in regulating the dephosphorylation of UPF1/SMG2 and are localized mainly in the cytoplasm [Chiu et al., 2003]. It has also been shown that in addition to UPF1,UPF2 has also been found to be phosphorylated in human cells [Chiu et al., 2003]. However, although biochemical evidence suggests that UPF1 dephosphorylation is governed by complex formation between SMG5, SMG7, UPF1 and protein phosphatase 2A but not for dephosphorylation of UPF2.

These SMG factors are characterized by the presence of PIN domains, which have been implicated in possessing RNA degradation activity [Clissold and Ponting, 2000]. Furthermore, SMG factors are able to form efficient protein-protein complexes mediated via the presence of tetratricopeptide repeats (TPRs) which encode amphipathic α-helices [Das et al., 1998]. Although SMG5 and SMG7 have no phosphatase activity, their association with the N-terminal domain of UPF1 is necessary for subsequent UPF1 dephosphorylation by PP2A [Ohnishi et al., 2003]. Ohnishi and colleagues have offered insight into the physiological significance of UPF1 phosphorylation/dephosphorylation cycle mediated by SMG1 and the SMG5-SMG7-PP2A complex, respectively [Ohnishi et al., 2003]. Their studies suggest that a cycle of phosphorylation-dephosphorylaton is crucial for the "remodeling of NMD complexes" [Ohnishi et al., 2003].

The dephosphorylation of UPF1 is important in completing the non-sense mediated decay/mRNA surveillance cycle. Of particular importance are the complexes between SMG-5 and SMG-7, which function in the recognition of phosphoUPF1 and are part of a larger macromolecular assembly comprising protein phosphatase 2A [Anders et al., 2003; Ohnishi et al., 2003; Fukuhara et al., 2005]. Following the removal of these surveillance factors as a

function of phosphorylation-dephosphorylation, degradation can ensue from either the 5' direction following decapping [Muhlrad and Parker, 1994; Mitchell and Tollervey, 2003] or the 3' end following deadenylation [Chen and Shyu, 2003; Lejeune et al., 2003]. In *Saccharomyces cerevisiae*, the RNA decay factors localize in processing (P) bodies [Sheth and Parker, 2003; Sheth and Parker, 2006]. However, recent studies have shown that decay is initiated on polyribosomes and appears to be largely co-translational [Hu et al., 2009; Hu et al., 2010].

The mechanism of mRNA decay appears to be quite different in higher eukaryotes. In *Drosophila melanogaster*, an internal nick in the RNA serves as a prerequisite prior to the involvement of exonucleases responsible for the degradation of the message from either the 3'- or the 5'-end [Gatfield and Izzauralde, 2004]. This also appears to be the case in mammalian cells [Eberle et al., 2009] whereby SMG-6 generates an endonucleolytic nick in RNAs harboring nonsense mutations [Eberle et al., 2009].

The mechanism of NMD

In yeast, an important distance rule was developed to elucidate the basic mechanism of recognition of a PTC [Ruiz-Echevarria et al., 1998]. In these series of experiments, insertions of a downstream element (DSE) derived from the *PGK1* gene was incorporated at a given distance from the PTC-harboring *GCN4* transcript [Ruiz-Echevarria et al., 1998]. It was concluded that the NMD surveillance complex is not able to efficiently elicit a nonsense response if the DSE is inserted on the order of magnitude of greater than 200 base-pairs from the first PTC [Ruiz-Echevarria et al., 1998]. This suggests that there is an upper distance limit as to how far the surveillance complex is able to scan before initiating the NMD response in lower eukaryotes.

However, in higher eukaryotes, the mechanism of PTC recognition appears to be more complex. Earlier work has shed light and has also led to the development of a distance rule in metazoans. These studies have suggested that a transcript is deemed as a PTC-containing RNA if there is an occurrence of a PTC 50-55 nucleotides upstream of the most 3'exon-exon junction [reviewed in Nagy and Maquat, 1998].

An important breakthrough in understanding NMD was made when several papers were published reporting the presence of an important protein complex known as the exon junction complex [Le Hir et al., 2000]. This complex is precisely deposited (as mapped through an RNase H assay) ~22-24 nucleotides upstream of the exon-exon junction [Le Hir et al., 2000]. In terms of mRNA quality control, the function of the EJC has emerged as a molecular communication device [Chang et al., 2007]. Specifically, the EJC is able to transmit the location of a spliced intron relative to the position of the stop codon [Chang et al., 2007]. Recent evidence has shed additional light on the molecular interplay governing the initiation of NMD [Singh et al., 2008]. This study has suggested that there is an antagonistic relationship that exists with factors near the 3' UTR of an mRNA and the Upf proteins [Singh et al., 2008]. In particular, this report has shown that PABP is a key factor that opposes NMD and therefore inhibits the interaction of eRF3 and Upf1p [Singh et al., 2008]. Furthermore, in human cells, when PABP was positioned or tethered in the vicinity of a stop codon, it resulted in a diminished NMD response [Singh et al., 2008]. At least in the context of human cells, the process of NMD in thought to be residing predominantly in the cytoplasm [Singh et al., 2007]. A key result that supports this notion was that restricting Upf1 within the nucleus results in the severe impairment of the NMD response [Singh et al., 2007]. Recent studies have shed light on the importance of Upf1p in executing the

NMD response [Franks et al., 2010]. This report showed that the ATPase activity present within the helicase domain of Upf1p is necessary for the disassembly of factors deposited/associated with the RNA [Franks et al., 2010]. The lack of proper Upf1p helicase activity results in the accumulation of partially degraded intermediate forms of the RNA which associate with Upf factors and localize to processing bodies [Franks et al., 2010].

Components of the EJC

Studies have shown that there are four core proteins Y14, Magoh, eIF4AIII, and MLN51 that comprise the EJC [Le Hir et al., 2000]. Magoh and Y14 interact with each other as well as the conserved mRNA export factor, TAP [Kataoka et al., 2001]. Structural studies revealed that Y14 interacts with Magoh through its RNA binding domain [Lau et al., 2003]. The salient topological features of the Magoh crystal structure have shown that it has several antiparallel beta strands that pack against two alpha helices [Lau et al., 2003]. Furthermore, the binding/interaction of Magoh to Y14 blocks the RNA binding surface of Y14 [Lau et al., 2003]. The other core components of the EJC include the DexH/D-box family member of the RNA helicase family, eIF4AIII (the eukaryotic initiation factor AIII). Studies have shown that eIF4AIII helps other EJC components dock onto the EJC [Shibuya et al., 2004]. Moreover, it is known to shuttle in and out of the nucleus and associate with Magoh and Y14 [Shibuya et al., 2004]. In addition, the study conducted by Shibuya and colleagues determined that like the importance of the conserved NMD pathway helicase, UPF1, eIF4AIII is required for the progression of NMD [Shibuya et al., 2004]. Using a PTC-containing TCR-β RNA as a model, it was shown that depletion of eIF4AIII stabilized the TCR-β transcript [Shibuya et al., 2004]. The other core EJC factor, MLN51, also associates with eIF4AIII, Magoh, and Y14 [Ballut et al., 2005]. An N-terminal domain, the

SELOR sequence, has been shown to be important in binding RNA as well as associating with the other core EJC components [Ballut et al., 2005]. MLN51 also occupies a distinct spatial niche. The *in vivo* localization pattern suggests that it forms a ring of nuclear speckles [Ballut et al., 2005]. There are essential residues which reside in the N-terminal SELOR sequence that are critical for directing MLN51 into nuclear speckles [Ballut et al., 2005]. For example, an alanine scanning mutagenesis study has unraveled the importance of particular amino acids within this motif. An alanine substitution in place of a critical tryptophan residue within the SELOR sequence stretch completely abolishes the nuclear speckle pattern [Ballut et al., 2005]. Furthermore, there are downstream residues that were also found to be critical in directing MLN51 to a punctate nuclear speckle niche [Ballut et al., 2005].

In a study conducted by Reichert and colleagues, it was reported that there is a dynamic association of protein factors prior to splicing [Reichert et al., 2002]. For example, using biochemical methods, it was shown that the EJC factor Ref/Aly has the ability to associate with the spliceosome prior to the commencement of splicing [Reichert et al., 2002]. Furthermore, other factors namely "Y14, Magoh, RNPS1, UAP56, and SRm160 are found in the intermediate spliceosome" [Reichert et al., 2002]. The ligation of exons leads towards a dramatic shift in the protein composition resulting in the dissociation of RNP51, UAP56, and SRm160 [Reichert et al., 2002]. However, the main components comprising the core of the EJC are not subjected to a dynamic cycle of association-dissociation. In particular, it was discovered that the core factors Aly/REF, Magoh, and Y14 remain stably associated with the EJC indicating their static and long-lived association with the RNA [Reichert et al., 2002]. Studies have also shed light on the role of post-translational modifications in the destabilization and cycling of the EJC.

Specifically, a report by Hsu and colleagues focused on the role of phosphorylation and methylation of Y14 in regulating EJC dissociation [Hsu et al., 2005]. Phosphorylation within an arginine-serine-rich (RS-rich) region of the polypeptide was essential for the dissociation of Y14, which had occurred after mRNA surveillance [Hsu et al., 2005]. Furthermore, arginine methylation of Y14 was reportedly shown to be a phosphorylation antagonizer [Hsu et al., 2005]. These studies focused on the Y14 phosphorylation-methylation relationship is reminiscent of the role of cyclical phosphorylation and methylation that regulates the nucleo-cytoplasmic trafficking of the yeast RNA-binding protein, Npl3p [Gilbert et al., 2001].

The faux 3' UTR model

The basic principles governing the importance of the faux 3' UTR were carried out in yeast and the model was tested using a synthetic *PGK1* gene [Amrani et al., 2004]. One of the key findings from this study suggested that the NMD response is elicited as a result of an inherent failure by the ribosome to properly terminate translation near a 3' UTR [Amrani et al., 2004]. Second, the the lack of proper translation termination has immense ramifications on proper ribosome recycling [Amrani et al., 2004]. It is therefore suggested that the failure to terminate translation could therefore lead to the recruitment of Upf1p to the site of abnormal translation termination [Amrani et al., 2004]. Most importantly, this study has argued that at the mechanistic level, the NMD pathway in metazoans versus yeast is unlikely to be different [Amrani et al., 2004]. A much recent investigation into the faux UTR model has suggested that there could be distinct recruitment steps that allow for the commitment of Upf1p and Upf1p-associated factors to elicit the NMD response [Kervestin et al., 2012]. A recent landmark study in yeast revealed that NMD does not require the presence of a poly-A tail nor the poly-A tail binding protein, Pab1p [**Meaux**

et al., 2008]. The findings in this report have negated the long-standing distance hypothesis, which had stated that a critical determinant of eliciting the NMD response in yeast was determined in part by the nucleotide distance from the PTC to the beginning of the poly-A tail. Interestingly, the findings by Meaux and colleagues challenge the faux UTR model put forth by Amrani and others.

The involvement of NMD in regulating messenger RNA levels: A yeast perspective

Prior to our work on identifying new targets of the NMD pathway in yeast, there were numerous important studies that revealed a role for NMD in the regulation of the post-transcriptional aspects of gene expression. In particular, earlier genome-wide studies revealed that NMD may function in controlling the cellular abundance of hundreds of mRNAs [**Lelivelt and Culbertson, 1999; He and Jacobson, 2001; He et al., 2003; Guan et al., 2006**]. Genome-wide studies uncovered an unprecedented role for the NMD pathway in regulating the transcript levels for genes encoding components of the telomerase complex [**Dahlseid et al., 2003**]. Another important facet of this study was that it unraveled a role for NMD in controlling and balancing the levels of a particular group of transcripts without affecting their decay [**Dahlseid et al., 2003**]. A genome-wide study in yeast revealed a direct role for Upf1p in associating with its target RNAs [**Johansson et al., 2007**]. These findings expanded the repertoire and therefore have contributed immensely towards obtaining a more complete scenario of the precise role of Upf1p and the direct versus indirect target RNAs [**Johansson et al., 2007**]. Genome-wide studies on the NMD homolog Upf1p have also been performed in the fission yeast, *Schizosaccharomyces cerevisiae* [**Rodriguez-Gabriel et al., 2006**]. The *S. pombe* study showed that NMD may

function to regulate a large number of RNAs involved in the oxidative stress response [**Rodriguez-Gabriel et al., 2006**]. Much recent reports have revealed a role for NMD in regulating the *ASH1* mRNA [**Zheng et al., 2008**]. The *ASH1* mRNA is normally under a translationally repressive, NMD-insenstive mode as it is being transported out from the nucleus and into the cytoplasm via an actin network [Zheng et al., 2008]. However, translation repression is relieved and it becomes an NMD target [**Zheng et al., 2008**]. Another study has also highlighted the importance of NMD in the regulation of the *CPA1* gene [**Messenguy et al., 2002**]. These findings suggested that NMD acts on the 5'end of the *CPA1* gene and that there is a strong decay response in the presence of arginine [**Messenguy et al., 2002**]. A recent investigation has linked metal metabolism with NMD [**Johannson and Jacobson, 2010**].

The above studies highlight the importance of NMD in regulating the levels of normal and PTC-containing yeast mRNAs. However, other studies have shown how usage of alternate translation initiation sites (the so-called internal translation initiation sites) can cause frameshift mutations resulting in premature translation termination [**Welch and Jacobson, 1999**].

Taken together, the investigations on understanding the yeast NMD pathway and its substrates have deepened our understanding on the varied transcripts that are directly (as well as indirectly) subjected to NMD.

REFERENCES

Amrani N, Ganesan R, Kervestin S, Mangus DA, Ghosh S, Jacobson A. 2004. A faux 3'-UTR promotes aberrant termination and triggers nonsense-mediated mRNA decay. *Nature.* 432(7013):112-8.

Anders KR, Grimson A, Anderson P. 2003. SMG-5, required for C.elegans nonsense-mediated mRNA decay, associates with SMG-2 and protein phosphatase 2A. *EMBO J.* 22(3):641-50.

Ballut L, Marchadier B, Baguet A, Tomasetto C, Séraphin B, Le Hir H. 2005. The exon junction core complex is locked onto RNA by inhibition of eIF4AIII ATPase activity. *Nat Struct Mol Biol.* 12(10):861-9.

Chen CY, Shyu AB. 2003. Rapid deadenylation triggered by a nonsense codon precedes decay of the RNA body in a mammalian cytoplasmic nonsense-mediated decay pathway. *Mol Cell Biol.* 23(14):4805-13.

Chiu SY, Serin G, Ohara O, Maquat LE. 2003. Characterization of human Smg5/7a: a protein with similarities to Caenorhabditis elegans SMG5 and SMG7 that functions in the dephosphorylation of Upf1. *RNA.* 9(1):77-87.

Clissold PM, Ponting CP. 2000. PIN domains in nonsense-mediated mRNA decay and RNAi. *Curr Biol.* 10(24):R888-90.

Czaplinski K, Ruiz-Echevarria MJ, Paushkin SV, Han X, Weng Y, Perlick HA, Dietz HC, Ter-Avanesyan MD, Peltz SW. 1998. The surveillance complex interacts with the translation release factors to enhance termination and degrade aberrant mRNAs. *Genes Dev.* 12(11):1665-77.

Dahlseid JN, Lew-Smith J, Lelivelt MJ, Enomoto S, Ford A, Desruisseaux M, McClellan M, Lue N, Culbertson MR, Berman J. 2003. mRNAs encoding telomerase components and regulators are controlled by UPF genes in Saccharomyces cerevisiae. *Eukaryot Cell.* 2(1):134-42.

Das AK, Cohen PW, Barford D. 1998. The structure of the tetratricopeptide repeats of protein phosphatase 5: implications for TPR-mediated protein-protein interactions. *EMBO J.* 17(5):1192-9.

Eberle AB, Lykke-Andersen S, Mühlemann O, Jensen TH. 2009. SMG6 promotes endonucleolytic cleavage of nonsense mRNA in human cells. *Nat Struct Mol Biol.* 16(1):49-55.

Franks TM, Singh G, Lykke-Andersen J. 2010. Upf1 ATPase-dependent mRNP disassembly is required for completion of nonsense- mediated mRNA decay. *Cell.* 143(6):938-50.

Fukuhara N, Ebert J, Unterholzner L, Lindner D, Izaurralde E, Conti E. 2005. SMG7 is a 14-3-3-like adaptor in the nonsense-mediated mRNA decay pathway. *Mol. Cell* 17(4):537-47.

Gatfield D, Izaurralde E. 2004. Nonsense-mediated messenger RNA decay is initiated by endonucleolytic cleavage in Drosophila. *Nature.* 429(6991):575-8.

Gehring NH, Neu-Yilik G, Schell T, Hentze MW, Kulozik AE. 2003. Y14 and hUpf3b form an NMD-activating complex. *Mol Cell.* 11(4):939-49.

Gilbert W, Siebel CW, Guthrie C. 2001. Phosphorylation by Sky1p promotes Npl3p shuttling and mRNA dissociation. *RNA.* 7(2):302-13.

Grimson A, O'Connor S, Newman CL, Anderson P. 2004. SMG-1 is a phosphatidylinositol kinase-related protein kinase required for nonsense-mediated mRNA Decay in Caenorhabditis elegans. *Mol Cell Biol.* 24(17):7483-90.

Guan Q, Zheng W, Tang S, Liu X, Zinkel RA, Tsui KW, Yandell BS, Culbertson MR. 2006. Impact of nonsense-mediated mRNA decay on the global expression profile of budding yeast. *PLoS Genet.* 2(11):e203.

He F, Jacobson A. 2001. Upf1p, Nmd2p, and Upf3p regulate the decapping and exonucleolytic degradation of both nonsense-containing mRNAs and wild-type mRNAs. *Mol Cell Biol.* 21(5):1515-30.

He F, Li X, Spatrick P, Casillo R, Dong S, Jacobson A. 2003. Genome-wide analysis of mRNAs regulated by the nonsense-mediated and 5' to 3' mRNA decay pathways in yeast. *Mol Cell.* 12(6):1439-52.

Hsu IaW, Hsu M, Li C, Chuang TW, Lin RI, Tarn WY. 2005. Phosphorylation of Y14 modulates its interaction with proteins involved in mRNA metabolism and influences its methylation. *J Biol Chem.* 280(41):34507-12.

Hu W, Sweet TJ, Chamnongpol S, Baker KE, Coller J. 2009. Co-translational mRNA decay in *Saccharomyces cerevisiae*. *Nature.* 461(7261):225-9.

Hu W, Petzold C, Coller J, Baker KE. 2010. Nonsense-mediated mRNA decapping occurs on polyribosomes in *Saccharomyces cerevisiae*. *Nat Struct Mol Biol.* 17(2):244-7.

Johansson MJ, He F, Spatrick P, Li C, Jacobson A. 2007. Association of yeast Upf1p with direct substrates of the NMD pathway. *Proc Natl Acad Sci U S A.* 104(52):20872-7.

Johansson MJ, Jacobson A. 2010. Nonsense-mediated mRNA decay maintains translational fidelity by limiting magnesium uptake. *Genes Dev.* 24(14):1491-5.

Kataoka N, Diem MD, Kim VN, Yong J, Dreyfuss G. 2001. Magoh, a human homolog of Drosophila mago nashi protein, is a component of the splicing-dependent exon-exon junction complex. *EMBO J*. 20(22):6424-33.

Kervestin S, Li C, Buckingham R, Jacobson A. 2012. Testing the faux-UTR model for NMD: Analysis of Upf1p and Pab1p competition for binding to eRF3/Sup35p. *Biochimie.* [Epub ahead of print].

Kunz JB, Neu-Yilik G, Hentze MW, Kulozik AE, Gehring NH. 2006. Functions of hUpf3a and hUpf3b in nonsense-mediated mRNA decay and translation. *RNA.* 12(6):1015-22.

Kashima I, Yamashita A, Izumi N, Kataoka N, Morishita R, Hoshino S, Ohno M, Dreyfuss G, Ohno S. 2006. Binding of a novel SMG-1-Upf1-eRF1-eRF3 complex (SURF) to the exon junction complex triggers Upf1 phosphorylation and nonsense-mediated mRNA decay. *Genes Dev.* 20(3):355-67.

Lau CK, Diem MD, Dreyfuss G, Van Duyne GD. 2003. Structure of the Y14-Magoh core of the exon junction complex. *Curr Biol.* 13(11):933-41.

Leeds P, Wood JM, Lee BS, Culbertson MR. 1992. Gene products that promote mRNA turnover in Saccharomyces cerevisiae. *Mol Cell Biol.* 12(5):2165-77.

Le Hir H, Izaurralde E, Maquat LE, Moore MJ. 2000. The spliceosome deposits multiple proteins 20-24 nucleotides upstream of mRNA exon-exon junctions. *EMBO J*. 19(24):6860-9.

Lejeune F, Ishigaki Y, Li X, Maquat LE. 2002. The exon junction complex is detected on CBP80-bound but not eIF4E-bound mRNA in mammalian cells: dynamics of mRNP remodeling. *EMBO J.* 21(13):3536-45.

Lejeune F, Li X, Maquat LE. 2003. Nonsense-mediated mRNA decay in mammalian cells involves decapping, deadenylating, and exonucleolytic activities. *Mol. Cell* 12(3):675-87.

Lelivelt MJ, Culbertson MR. 1999. Yeast Upf proteins required for RNA surveillance affect global expression of the yeast transcriptome. *Mol Cell Biol.* 19(10):6710-9.

Losson R, Lacroute F. 1979. Interference of nonsense mutations with eukaryotic messenger RNA stability. *Proc Natl Acad Sci U S A*. 76(10):5134-7.

Lykke-Andersen J, Shu MD, Steitz JA. 2000. Human Upf proteins target an mRNA for nonsense-mediated decay when bound downstream of a termination codon. *Cell.* 103(7):1121-31.

Meaux S, van Hoof A, Baker KE. 2008. Nonsense-mediated mRNA decay in yeast does not require PAB1 or a poly(A) tail. *Mol Cell.* 29(1):134-40.

Medghalchi SM, Frischmeyer PA, Mendell JT, Kelly AG, Lawler AM, Dietz HC. 2001. Rent1, a trans-effector of nonsense-mediated mRNA decay, is essential for mammalian embryonic viability. *Hum Mol Genet.* 10(2):99-105.

Messenguy F, Vierendeels F, Piérard A, Delbecq P. 2002. Role of RNA surveillance proteins Upf1/CpaR, Upf2 and Upf3 in the translational regulation of yeast CPA1 gene. *Curr Genet.* 41(4):224-31.

Mitchell P, Tollervey D. 2003. An NMD pathway in yeast involving accelerated deadenylation and exosome-mediated 3'→5' degradation. *Mol Cell.* 11(5):1405-13.

Muhlrad D, Parker R. 1994. Premature translational termination triggers mRNA decapping. *Nature*. 370(6490):578-81.

Nagy E, Maquat LE. 1998. A rule for termination-codon position within intron-containing genes: when nonsense affects RNA abundance. *Trends Biochem Sci.* 23(6):198-9.

Ohnishi T, Yamashita A, Kashima I, Schell T, Anders KR, Grimson A, Hachiya T, Hentze MW, Anderson P, Ohno S. 2003. Phosphorylation of hUPF1 induces formation of mRNA surveillance complexes containing hSMG-5 and hSMG-7. *Mol Cell* 12(5):1187-200.

Perlick HA, Medghalchi SM, Spencer FA, Kendzior RJ Jr, Dietz HC. 1996. Mammalian orthologues of a yeast regulator of nonsense transcript stability. *Proc Natl Acad Sci U S A.* 93(20):10928-32.

Pulak R, Anderson P. 1993. mRNA surveillance by the Caenorhabditis elegans smg genes. *Genes Dev.* 7(10):1885-97.

Reichert VL, Le Hir H, Jurica MS, Moore MJ. 2002. 5' exon interactions within the human spliceosome establish a framework for exon junction complex structure and assembly. *Genes Dev*. 16(21):2778-91.

Rodríguez-Gabriel MA, Watt S, Bähler J, Russell P. 2006. Upf1, an RNA helicase required for nonsense-mediated mRNA decay, modulates the transcriptional response to oxidative stress in fission yeast. *Mol Cell Biol.* 26(17):6347-56.

Ruiz-Echevarría MJ, González CI, Peltz SW. 1998. Identifying the right stop: determining how the surveillance complex recognizes and degrades an aberrant mRNA. *EMBO J.* 17(2):575-89.

Serin G, Gersappe A, Black JD, Aronoff R, Maquat LE. 2001. Identification and characterization of human orthologues to Saccharomyces cerevisiae Upf2 protein and Upf3 protein (Caenorhabditis elegans SMG-4). *Mol Cell Biol.* 21(1):209-23.

Sheth U, Parker R. 2003. Decapping and decay of messenger RNA occur in cytoplasmic processing bodies. *Science.* 300(5620):805-8.

Sheth U, Parker R. 2006. Targeting of aberrant mRNAs to cytoplasmic processing bodies. *Cell.* 125(6):1095-109.

Shibuya T, Tange TØ, Sonenberg N, Moore MJ. 2004. eIF4AIII binds spliced mRNA in the exon junction complex and is essential for nonsense-mediated decay. *Nat Struct Mol Biol* 11(4):346-51.

Singh G, Jakob S, Kleedehn MG, Lykke-Andersen J. 2007. Communication with the exon-junction complex and activation of nonsense-mediated decay by human Upf proteins occur in the cytoplasm. *Mol Cell.* 27(5):780-92.

Singh G, Rebbapragada I, Lykke-Andersen J. 2008. A competition between stimulators and antagonists of Upf complex recruitment governs human nonsense-mediated mRNA decay. *PLoS Biol.* 6(4):e111.

Wang W, Czaplinski K, Rao Y, Peltz SW. 2001. The role of Upf proteins in modulating the translation read-through of nonsense-containing transcripts. *EMBO J.* 20(4):880-90.

Welch EM, Jacobson A. 1999. An internal open reading frame triggers nonsense-mediated decay of the yeast SPT10 mRNA. *EMBO J.* 18(21):6134-45.

Yamashita A, Ohnishi T, Kashima I, Taya Y, Ohno S. 2001. Human SMG-1, a novel phosphatidylinositol 3-kinase-related protein kinase, associates with components of the mRNA surveillance complex and is involved in the regulation of nonsense-mediated mRNA decay. *Genes Dev.* 15(17):2215-28.

Zheng W, Finkel JS, Landers SM, Long RM, Culbertson MR. 2008. Nonsense-mediated decay of ash1 nonsense transcripts in Saccharomyces cerevisiae. *Genetics.* 180(3):1391-405.

Molecular Cell
Article

Widespread Impact of Nonsense-Mediated mRNA Decay on the Yeast Intronome

Shakir Sayani,[1] Michael Janis,[1] Chrissie Young Lee,[1] Isabelle Toesca,[1] and Guillaume F. Chanfreau[1,*]
[1]Department of Chemistry and Biochemistry and the Molecular Biology Institute, University of California, Los Angeles, Los Angeles, CA 90095-1569, USA
*Correspondence: guillom@chem.ucla.edu
DOI 10.1016/j.molcel.2008.07.005

SUMMARY

Nonsense-mediated mRNA decay (NMD) eliminates transcripts carrying premature translation termination codons, but the role of NMD on yeast unspliced pre-mRNA degradation is controversial. Using tiling arrays, we show that many unspliced yeast pre-mRNAs accumulate in strains mutated for the NMD component Upf1p and the exonuclease Xrn1p. Intron identity and suboptimal splicing signals resulting in weak splicing were found to be important determinants in NMD targeting. In the absence of functional NMD, unspliced precursors accumulate in the cytoplasm, possibly in P-bodies. NMD can also complement RNase III-mediated nuclear degradation of unspliced *RPS22B* pre-mRNAs, degrades most unspliced precursors generated by a 5′ splice site mutation in *RPS10B*, and limits *RPS29B* unspliced precursors accumulation during amino acid starvation. These results show that NMD has a wider impact than previously thought on the degradation of yeast-unspliced transcripts and plays an important role in discarding precursors of regulated or suboptimally spliced transcripts.

INTRODUCTION

Nonsense-mediated mRNA decay (NMD) is an RNA surveillance pathway that eliminates transcripts carrying premature translation termination codons (PTCs; reviewed in Behm-Ansmant et al., 2007; Chang et al., 2007; Conti and Izaurralde, 2005; Lejeune and Maquat, 2005). This surveillance mechanism relies on the Upf proteins, which target PTC-containing transcripts for degradation (Chang et al., 2007; Conti and Izaurralde, 2005; Leeds et al., 1992; Lejeune and Maquat, 2005). The physiological functions of NMD have been analyzed in a variety of organisms. In mammalian cells, NMD prevents the accumulation of truncated proteins that would result from mutations found in patients affected by genetic diseases (Behm-Ansmant et al., 2007; Frischmeyer and Dietz, 1999). NMD also plays a role in regulating transcripts that have incorporated PTC-containing exons by alternative splicing (Green et al., 2003; Hillman et al., 2004; Hori and Watanabe, 2005; Lareau et al., 2007; Ni et al., 2007). In yeast and mammalian cells, NMD controls the expression of a large number of natural transcripts (Guan et al., 2006; He et al., 2003; Johansson et al., 2007; Lelivelt and Culbertson, 1999; Mendell et al., 2004). In *C. elegans*, *Arabidopsis*, and *Paramecium*, NMD contributes to the elimination of unproductively spliced mRNAs (Arciga-Reyes et al., 2006; Jaillon et al., 2008; Mitrovich and Anderson, 2000). NMD also controls the expression of *C. elegans* pseudogenes (Mitrovich and Anderson, 2005).

Due to the great likelihood of encountering intronic PTCs, it seems logical that NMD would target unspliced pre-mRNAs for degradation in all eukaryotes. However, the impact of NMD on unspliced pre-mRNA degradation in the model yeast *S. cerevisiae* has been controversial. Unspliced forms of three pre-mRNAs were found to accumulate in the *upf1Δ* mutant (He et al., 1993; Li et al., 1995). However, the analysis of the splicing and expression of intron-containing transcripts using splicing microarrays in the *xrn1Δ*, *upf1Δ*, or *upf3Δ* mutants failed to reveal widespread accumulation of unspliced pre-mRNAs (Burckin et al., 2005; Clark et al., 2002; Pleiss et al., 2007). In addition, several studies have pointed to nuclear or cytoplasmic degradation pathways for yeast unspliced pre-mRNAs that are independent of NMD. Unspliced transcripts generated by a mutation of the Prp2p splicing factor are not stabilized by NMD mutations (Bousquet-Antonelli et al., 2000), but their accumulation is increased by inactivation of the nuclear exosome, suggesting nuclear decay. Inactivation of the nuclear exosome component Rrp6p also increases the accumulation of unspliced transcripts of genes for which the spliceosome is not associated with the sites of transcription (Moore et al., 2006). In support of the hypothesis of a nuclear retention and degradation system is the finding that depletion of the nuclear pore-associated Mlp1p protein increases the leakage of unspliced pre-mRNAs of an inefficiently spliced reporter transcript (Galy et al., 2004). Specialized nuclear degradation systems for unspliced pre-mRNAs have also been described that rely on the nuclear RNase III Rnt1p (Danin-Kreiselman et al., 2003). In contrast to these findings, which suggest nuclear degradation of several yeast unspliced pre-mRNAs, the decay of actin intron-based reporter transcripts containing splicing signals mutations depends on Xrn1p, the cytoplasmic 5′ → 3′ exonuclease, but is not affected by Upf1p absence (Hilleren and Parker, 2003). The decay of several cytoplasmic unspliced meiotic transcripts is also independent of Upf1p (Scherrer and Spingola, 2006).

Interestingly, these observations were made on different transcripts, suggesting transcript-specific degradation pathways. These observations led us to revisit the global impact of NMD on yeast intron-containing transcripts (hereby called the

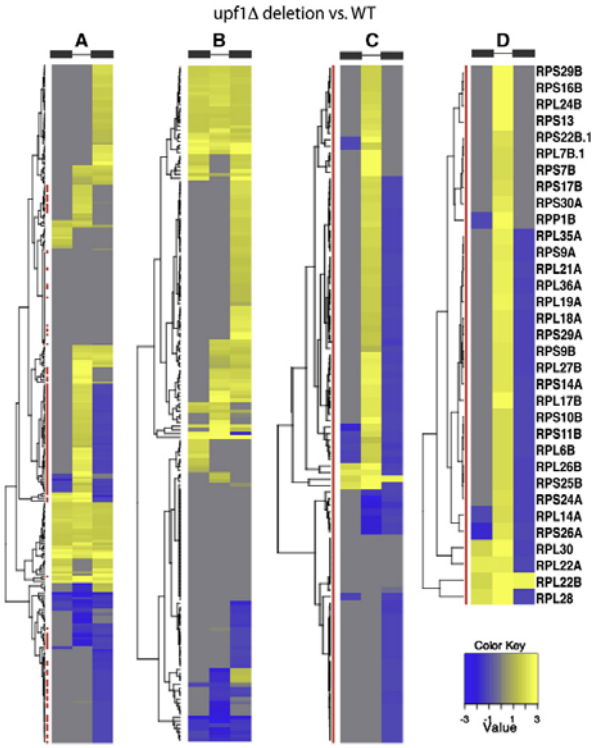

Figure 1. Tiling Array Analysis of Exons and Intron Signals in the *upf1Δ* Strain Relative to Wild-Type

(A) Dendrograms of all ICGs.

(B) Dendrogram of non-RPGs.

(C) Dendrogram of RPGs.

(D) Dendrogram of RPGs that show an increase of intronic signal. Exons are represented by boxes, and introns are represented by a line. Yellow represents increase, and blue represents decrease. For genes exhibiting two introns, the first intron is indicated by .1.

intronome). In this study, using tiling array analysis of strains lacking Xrn1p or Upf1p, we show that NMD eliminates a large number of unspliced pre-mRNAs, many of which are not spliced with high efficiency, due in part to suboptimal splicing signals. Taken together with previous studies, these results show that the mechanisms of degradation of unspliced pre-mRNAs are multiple and sometimes complementary, underscoring the importance of various surveillance pathways for unprocessed species.

RESULTS

Tiling Microarray Analysis of the *S. cerevisiae* Intronome in *upf1Δ* and *xrn1Δ* Deletion Strains

To investigate the role of NMD in intron-containing transcripts expression and unspliced pre-mRNA degradation, we monitored the accumulation of intron-containing genes (ICGs) using Affymetrix *S. cerevisiae* tiling arrays in the *upf1Δ* and *xrn1Δ* deletion strains. Upf1p is one of the main components of the yeast NMD machinery (Leeds et al., 1991), and Xrn1p is the major 5′→ 3′ exonuclease that degrades transcripts through the NMD pathway (He and Jacobson, 2001). Although Xrn1p also plays a role in constitutive mRNA degradation, we expected bona fide NMD targets to present similar profiles in *upf1Δ* or *xrn1Δ* mutant strains, as shown in previous expression microarray studies (He et al., 2003). We chose to use tiling arrays, since these have been previously used to efficiently detect intronic RNAs (Juneau et al., 2007; Zhang et al., 2007) and also because previously described custom splicing arrays did not reveal widespread effects of NMD mutants on unspliced precursor accumulation (Burckin et al., 2005; Clark et al., 2002; Pleiss et al., 2007). Four independent cultures were used for wild-type, *xrn1Δ*, and *upf1Δ* mutants, and probes prepared from the corresponding RNAs were hybridized to Affymetrix tiling arrays. We monitored the expression of probe sets corresponding to intronic and exonic regions of 278 intron-containing genes (ICGs) and corresponding to 287 intronic features, since nine ICGs contain two introns. Following bioinformatics analysis (described in the Supplemental Data available online), classification of transcripts according to phenotypic classes was confirmed by visual inspection of the tiling array profiles (see examples in the Supplemental Data).

Figure 1 shows the clustering of exon1, intron, and exon 2 signals in the *upf1Δ* mutant strain compared to wild-type for all ICGs. This clustering revealed that a subpopulation of ICGs shows an increase of intronic signal in the *upf1Δ* strain compared to the wild-type, without major change of signal in exonic sequences (Figure 1A). Strikingly, most of these ICGs corresponded to ribosomal protein genes (RPGs) as represented by red bars on the left side of the dendrogram (Figure 1). Analysis of the intron-containing RPGs subpopulation (Figure 1C) showed that 31% of RPG introns (33 introns) had a more than 2-fold increase of intronic signal in the *upf1Δ* mutant compared to wild-type. Compared to the number of ICGs showing a more than 2-fold increase of intronic levels in the non-RPGs population (19), there is a significant enrichment for RPGs (p value $< 1.6 \times 10^{-5}$). The subpopulation of RPGs for which elevated (>2-fold) levels of intronic signals were observed upon Upf1p inactivation (hereby called NMD sensitive) is shown in detail in Figure 1D. Most of these did not exhibit any change or only a slight decrease in exonic signal. One exception was *RPL22B*, for which an increase in exonic signal was detected in *upf1Δ* (Figure 1D; Figure S1). This effect could be explained by the fact that the amount of unspliced *RPL22B* that accumulates in *upf1Δ* is so high that it exceeds that of spliced *RPL22B* in wild-type (see below, Figure 7). When non-RP ICGs were clustered separately (Figure 1B), the main cluster was a family of ICGs for which a signal increase in *upf1Δ* occurred throughout exonic and intronic regions. Many of these ICGs correspond to subtelomeric genes

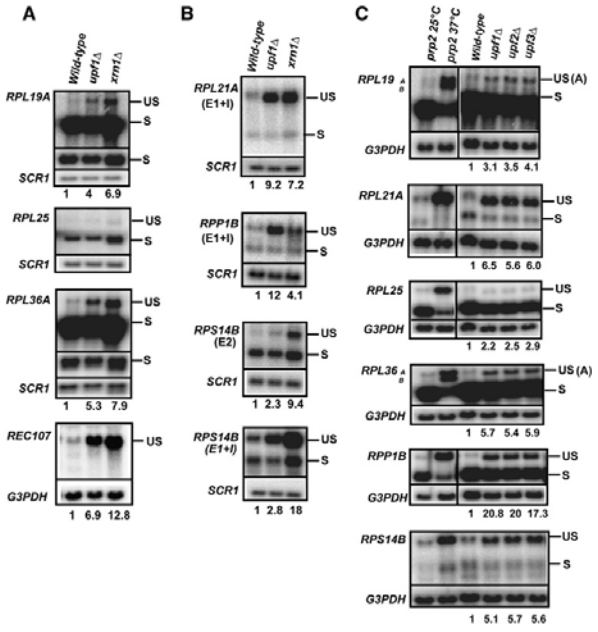

Figure 2. Northern Blot Analysis of ICGs in Wild-Type and NMD Mutant Strains

(A and B) Detection of unspliced ICGs in wild-type, *upf1Δ*, and *xrn1Δ* strains. Shown are the signals obtained by hybridization of northern blots with the indicated probes, which covered exon1 (E1), intron (I), and exon2 (E2) unless indicated otherwise. US, Unspliced pre-mRNA; S, Spliced mRNA. Numbers indicate the fold increase accumulation of unspliced relative to wild-type. *SCR1* or *G3PDH* were used as loading controls.

(C) Detection of unspliced RPGs in wild-type, *upf1Δ*, *upf2Δ*, and *upf3Δ* strains. The *prp2*-ts strain was used as a positive control for the detection and migration of unspliced precursors.

encoding helicase-like proteins. The overall signal increase in these regions for the *upf1Δ* mutant was also observed in neighboring regions outside of these genes; therefore, this phenotype might have been the result of a decrease of subtelomeric silencing. Because it is unclear whether or not these genes are actually functional, we did not analyze this subset of genes further.

We also analyzed intronic and exonic signals in the *xrn1Δ* strain relative to the wild-type strain (Figure S2). The increase of intronic signal observed in the *upf1Δ* strain for many RPGs was also observed in *xrn1Δ* (Figure S2). To visualize the differences between ICGs expression in the *xrn1Δ* and *upf1Δ* strains, we compared the array profiles of ICGs between these two strains. Several ICGs exhibited an increase in exonic signals in *xrn1Δ* compared to *upf1Δ* (Figure S3) without change in intronic signal (top of the dendrogram, Figure S3), which suggested increased spliced mRNA levels. This increase could be attributed to the role of Xrn1p in general mRNA degradation (Parker and Song, 2004). We also found transcripts for which intronic signals were higher in *xrn1Δ* compared to *upf1Δ*, suggesting that some unspliced precursors accumulate to higher levels when the exonuclease component is disrupted. Quantification of intronic and exonic signals is provided in Table S3. Some genes also showed a stronger accumulation of both intronic and exonic signals in the *xrn1Δ* strain compared to the *upf1Δ* strain, consistent with a stronger accumulation of unspliced and spliced species in the *xrn1Δ* strain compared to *upf1Δ*. Both RPGs and non-RPGs were found among those, including the *YRA1* transcript, which exhibited a strong increase of intronic and exonic signals in the *xrn1Δ* strain compared to wild-type, but not in the *upf1Δ* strain (Figure S3). These findings are consistent with previous studies, which involved Xrn1p, but not Upf1p, in the degradation of *YRA1* unspliced mRNAs (Dong et al., 2007; Preker and Guthrie, 2006). However, the overall clustering patterns were very similar in the strain lacking Xrn1p compared to the strain lacking Upf1p, strengthening the argument that transcripts for which intronic signal accumulation is observed are targeted by NMD.

Effects Detected on Tiling Arrays Can Be Reproduced by Northern Blot Analysis

Tiling arrays analysis showed an accumulation of intronic signal for many RPG transcripts in the *upf1Δ* and *xrn1Δ* mutants. While this accumulation was consistent with an increase of unspliced pre-mRNAs in these mutants (with the level of unspliced largely smaller than those of spliced mRNAs), we could not formally exclude that the observed intronic signal was the result of a lack of degradation of the excised introns. We therefore validated the microarray results by analyzing a set of candidates by northern blot. Figure 2 shows the northern blot analysis of several ICGs in the *upf1Δ* and *xrn1Δ* deletion strains. To further test if unspliced pre-mRNA accumulation occurs generally in NMD mutants, we also analyzed unspliced transcripts accumulation in mutants lacking Upf2p and Upf3p (Figure 2C). As a positive control, we used a strain carrying a thermosensitive mutation in the splicing factor Prp2p to detect the presence of unspliced pre-mRNAs. These experiments showed that whenever we detected an increase in intronic signal by tiling arrays, we were also able to detect unspliced pre-mRNAs by northern blot analysis (Figure 2). This effect was observed mostly for RPGs, but also for the *REC107* meiotic transcript (Figure 2A). We also analyzed *RPL25* by northern blot, which did not show any intronic signal accumulation in the *upf1Δ* and *xrn1Δ* strains on tiling arrays. We were unable to detect an increase of unspliced *RPL25* precursors in these mutants, while these precursors were readily detectable in the *prp2-1* splicing mutant. Interestingly, the quantitative differences between strains on the tiling arrays could be reproduced by northern blot. For example, the *RPL21A* intronic signal relative to wild-type was similar for the *upf1Δ* and *xrn1Δ* mutant strains as judged by tiling arrays (Figure S5A) or by northern blot (Figure 3B). The *RPP1B* transcript exhibited higher intronic signal in *upf1Δ* than in *xrn1Δ* on the tiling arrays (Figure S5B), which was confirmed by northern blot (Figure 2B). Reciprocally,

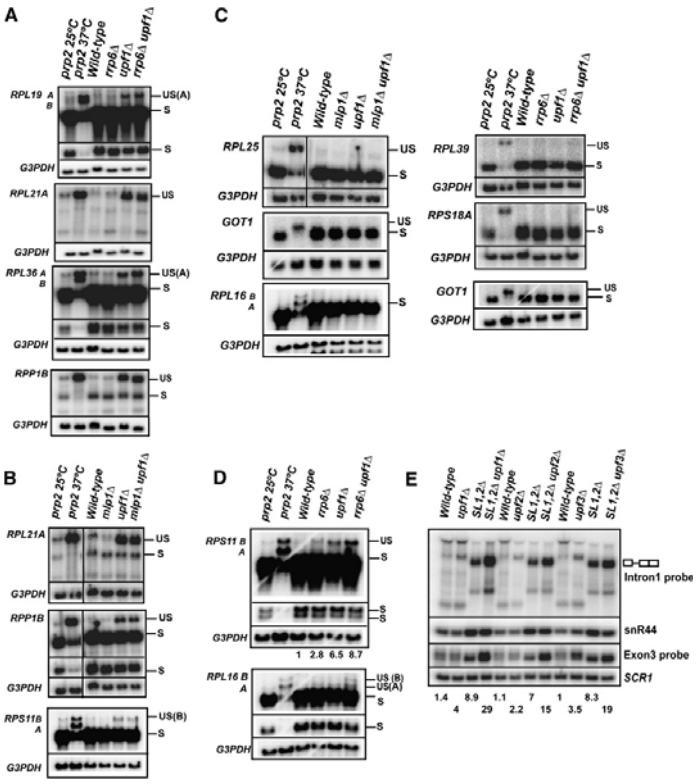

Figure 3. Effects of NMD Mutations Combined with Inactivation of Rrp6p, Mlp1p, or of Rnt1p Stem-Loops on the Accumulation of Unspliced Pre-mRNAs

(A) Expression of RPGs and detection of unspliced RPGs in wild-type, *upf1Δ* and *rrp6Δ*, and *upf1Δrrp6Δ* strains for NMD-sensitive transcripts. For some transcripts, different exposures are shown to properly visualize mRNAs. Legends are the same as in Figure 2.

(B) Expression of RPGs and detection of unspliced RPGs in wild-type, *upf1Δ* and *mlp1Δ*, and *upf1Δ mlp1Δ* strains for NMD-sensitive transcripts. Legends are the same as in Figure 2.

(C) Expression of RPGs and lack of detection of unspliced RPGs in wild-type, *upf1Δ*, *mlp1Δ*, *rrp6Δ*, *upf1Δ mlp1Δ*, and *upf1Δrrp6Δ* strains for NMD-insensitive transcripts. Legends are the same as in Figure 2.

(D) Inactivation of NMD and of Rrp6 shows synergistic effects on the accumulation of two unspliced pre-mRNAs. Legends are the same as in (A).

(E) Analysis of *RPS22B* in strains carrying a deletion of the Rnt1p-target stem-loops (SL1,2Δ) and/or carrying mutations of NMD components. Shown are the signals obtained by hybridization of the same membrane with the indicated probes.

RPS14B exhibited stronger intronic signal in *xrn1Δ* than in *upf1Δ* on the arrays (Figure S5B), which was also detected by northern blot (Figure 2B). In addition, elevated exonic *RPS14B* signal was detected in the *xrn1Δ* strain on the arrays (Figure S5C), which was confirmed by higher levels of spliced mRNAs on the northern blot (Figure 2B). Therefore, the relative differences detected by the tiling arrays can be used with confidence to predict relative differences in gene expression between strains. However, numbers extrapolated from the tiling array analysis were generally lower than the quantifications of the northern analysis (compare numbers in Figure 2 and Table S3), suggesting that the tiling array analysis underestimates the quantitative effects of NMD. Finally, the observation that unspliced precursors accumulate to similar levels in the *upf1Δ*, *upf2Δ*, and *upf3Δ* strains (Figure 3C) emphasizes the fact that these unspliced precursors are NMD targets.

Effects of the Combined Inactivation of NMD and of the Nuclear Exosome Component Rrp6p or of the Nuclear Retention Protein Mlp1p on the Accumulation of Unspliced Transcripts

To test whether additional nuclear degradation or retention systems contributed to the degradation of unspliced NMD targets, we combined the *upf1Δ* deletion with a deletion of either *RRP6* or *MLP1*. Rrp6p is a component of the nuclear exosome, and some unspliced pre-mRNAs have been shown to accumulate in *rrp6* mutants (Bousquet-Antonelli et al., 2000; Moore et al., 2006). The accumulation of unspliced pre-mRNAs was first analyzed for the NMD-sensitive RPGs *RPL19A*, *RPL21A*, *RPL36A*, and *RPP1B* (Figure 3A). The inactivation of Rrp6p did not result in an increase of these unspliced pre-mRNAs, nor did it exacerbate the accumulation of unspliced pre-mRNAs when combined with the *upf1Δ* deletion (Figure 3A). This result suggests that these pre-mRNAs are not subjected to nuclear surveillance but that their principal mode of degradation relies on NMD.

Mlp1p is required for nuclear retention of an inefficiently spliced *RP51B*-based pre-mRNA reporter transcript (Galy et al., 2004). We analyzed the accumulation of the NMD-sensitive pre-mRNAs *RPL21A*, *RPP1B*, and *RPS11B* in *upf1Δ*, *mlp1Δ*, and *upf1Δ m1p1Δ* strains (Figure 3B). Mlp1p depletion in the *upf1Δ* strain did not exacerbate the accumulation of these unspliced pre-mRNAs (Figure 3B), suggesting that the Mlp1p-mediated nuclear retention system is not active on these pre-mRNAs. We conclude that these transcripts are not retained in the nucleus and that they can escape to the cytoplasm where they are targeted by NMD (see below, Figure 6).

We also investigated whether Rrp6p or Mlp1p depletion, alone or in combination with Upf1p depletion, could result in the accumulation of unspliced pre-mRNAs for NMD-insensitive ICGs. Northern blot analysis of *RPS18A*, *RPL39*, and *GOT1*, which are unaffected by the *upf1Δ* or *xrn1Δ* mutations, did not reveal

any accumulation of unspliced pre-mRNA in the *rrp6Δ* or *rrp6Δ upf1Δ* mutants (Figure 3C), indicating that these transcripts either do not produce significant levels of unspliced pre-mRNAs or that their degradation relies on other pathways. Similarly, *MLP1* deletion in combination with the *UPF1* deletion did not result in accumulation of unspliced *RPL25*, *RPL16A/B*, or *GOT1* mRNAs (Figure 3C), suggesting that these transcripts are probably not retained in the nucleus, which would have explained their insensitivity to NMD.

Finally, *RPS11B* and *RPL16A* were the only transcripts for which inactivation of both Rrp6p and of Upf1p resulted in a minor increase in unspliced transcripts compared to the single mutants (Figure 3D). These results show that in some particular cases, the nuclear exosome can functionally complement NMD in the degradation of unspliced transcripts.

NMD Complements Rnt1p-Mediated Degradation of Unspliced *RPS22B* Species

RPS22B contains two introns, the second of which contains the box H/ACA snoRNA snR44. We previously showed that Rnt1p, a nuclear double-stranded RNA endonuclease, cleaves a stem-loop structure in the first intron, triggering degradation of the unspliced or partially spliced precursors containing intron 1 (Danin-Kreiselman et al., 2003). Since *RPS22B* was found among NMD targets (Figure 1), we tested whether NMD could complement Rnt1p-mediated degradation for this transcript by combining the *upf1Δ* deletion with a deletion of both stem-loops in the first intron of *RPS22B* (*ΔSL1+2*, see Danin-Kreiselman et al., 2003). We then monitored the accumulation of unspliced *RPS22B* species in these mutants (Figure 3E). While the deletion of the stem-loops or of *UPF1* resulted in only a modest increase of unspliced pre-mRNAs, the double mutant showed a dramatic increase of partially spliced pre-mRNAs that retain intron 1 (Figure 3E). An increase in partially spliced *RPS22B* transcripts that retain intron 1 was also observed when the stem-loop deletion was combined with Upf2p or Upf3p inactivation (Figure 3E). These results show that the NMD pathway complements Rnt1p-mediated degradation in preventing the accumulation of unspliced *RPS22B* species. We also found that the amount of *RPS22B*-spliced mRNAs were increased in the *upf1Δ*, *ΔSL1+2* double mutant, compared to wild-type or to the corresponding single mutants. This result was also observed when Upf2p or Upf3p were inactivated in addition to the stem-loop deletion (Figure 3D). In contrast, the amount of *snR44* was not increased in any of the double mutants (Figure 3D, *snR44* probe). This result shows that both Rnt1p-mediated degradation, and more surprisingly, the NMD pathway, compete with splicing. These two degradation pathways thereby titrate a significant fraction of precursors away from the splicing pathway, rendering precursor degradation rate limiting for the production of spliced *RPS22B* mRNAs.

Intron Identity Is a Key Determinant for Targeting of Unspliced Pre-mRNAs to NMD

We next investigated the determinants of NMD targeting for unspliced transcripts. Experiments described in the Supplemental Data showed that UTR sequences, promoter identity, or chromatin environment were not likely to be major determinants for

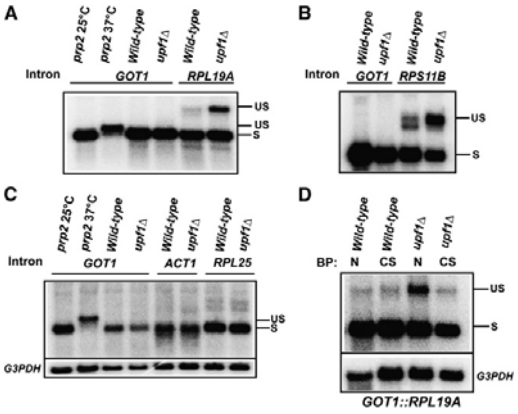

Figure 4. NMD Targeting Is Influenced by Intron Identity and Suboptimal Splicing Signals

(A) Detection of spliced and unspliced *GOT1* transcripts (*GOT1* riboprobe) in wild-type, *prp2-ts*, *upf1Δ*, in strains where the natural *GOT1* intron was replaced by that of *RPL19A*, and in the same strain where Upf1p was inactivated.

(B) Similar to (A), except that the *GOT1* intron was replaced by that of *RPS11B*.

(C) Similar to (A), except that the *GOT1* intron was replaced by that of actin (*ACT1*) or *RPL25*.

(D) Legends are the same as in (A). Strains indicated as N contain the natural *RPL19A* branchpoint (BP) UAACUAAC; strains indicated as CS contain the consensus sequence UACUAAC.

NMD targeting. Therefore, we focused our investigations on the role of intronic elements using an intron replacement strategy. We replaced the small intron (80 nt) of the *GOT1* gene, which is NMD insensitive, with those of *RPL19A* or *RPS11B*, which are NMD sensitive. The lack of sensitivity of *GOT1* to NMD is not due to the lack of PTCs, as these were found in unspliced *GOT1*. Intron replacement was performed by homologous recombination at the *GOT1* chromosomal locus using the *delitto perfetto* technique (Storici et al., 2001), followed by *UPF1* knockout. When the *GOT1* intron was replaced with that of *RPL19A*, unspliced chimeric *GOT1-RPL19A* precursors were found to accumulate, and this accumulation was strongly exacerbated by Upf1p inactivation (Figure 4A). The same result was observed when the *GOT1* intron was replaced by that of *RPS11B* (Figure 4B). A doublet of bands was observed for unspliced chimeric *GOT1-RPS11B* precursors, which might indicate, in addition to the bona fide unspliced transcripts, a cryptic splice site or cryptic transcription initiation event triggered by the insertion of the *RPS11B* intron into the *GOT1* gene. To rule out that modifying *GOT1* intronic structure perturbs its splicing efficiency, we replaced the *GOT1* intron with those of *ACT1* or *RPL25*, which are NMD-insensitive. In contrast to the result observed with *RPL19A* or *RPS11B*, we did not detect unspliced precursor accumulation when the *GOT1* intron was replaced with *ACT1* or *RPL25*, even in the absence of Upf1p (Figure 4C). This was not due to the lack of PTCs, as many could be found in these chimeric precursors (data not shown). Finally, the intron sizes of *RPL19A* (506 nt), *RPS11B* (511 nt), *ACT1* (305 nt), or *RPL25* (414 nt) are comparable, ruling out a size-specific effect.

This experiment unambiguously shows that intron identity is a major determinant of NMD targeting and that substituting the intron of an NMD-insensitive transcript (*GOT1*) with an intron of an NMD-sensitive one (*RPL19A* or *RPS11B*) is sufficient to target this chimeric-unspliced transcript to NMD.

Introns With Suboptimal Splicing Signals Are Enriched among NMD Targets, and the Accumulation of Unspliced *RPL19A* in the *upf1Δ* Mutant Can Be Prevented by Changing Its Suboptimal Branchpoint to the Consensus Sequence

The previous experiments showed that intron identity is a major determinant of NMD targeting. This effect was not likely due to PTC position the within the intron (which would mimic the *faux* UTR model; Amrani et al., 2004), as transcripts with different intron sizes, 3′ exon sizes, and PTC positioning are found in NMD-sensitive and NMD-insensitive clusters (data not shown). Thus, we investigated whether NMD-sensitive ICGs are enriched for introns containing suboptimal splicing signals. When we analyzed the proportion of introns containing suboptimal splicing signals (i.e., those that contain either a 5′ splice site that differs from the canonical GUAUGU and/or a branchpoint that deviates from the canonical UACUAAC), we found that they comprise 46% of NMD-sensitive introns (45/98) compared to 35% for NMD-insensitive introns (67/189). This significant ($p < 0.05$) enrichment for suboptimal splicing signals in NMD-sensitive introns suggested that unspliced precursors might accumulate in NMD mutants because of their intrinsically inefficient splicing. To test the hypothesis of a contribution of suboptimal splicing signals to NMD targeting, we mutated the branchpoint of the *RPL19A* intron that was previously transposed in *GOT1*. The suboptimal UAACUAAC sequence was changed to the consensus UACUAAC by *delitto perfetto*, followed by Upf1p inactivation. Although this mutation had no effect on *GOT1* expression in the context of active NMD (Figure 4D, lanes 1and 2), it was sufficient to prevent unspliced *GOT1* pre-mRNAs accumulation when Upf1p was inactivated (Figure 4D). This experiment demonstrates that NMD targeting resides, at least for *RPL19A* and for a fraction of NMD-sensitive ICGs, in their suboptimal splicing signals that drive production of unspliced precursors.

Unspliced *RPS10B* Transcripts Resulting from a 5′ Splice Site Mutation Are Stabilized by NMD Inactivation

Unspliced precursors resulting from splice site or branchpoint mutations of *ACT1* or *RP51* are typically detectable without NMD perturbation (Chanfreau et al., 1994; Hilleren and Parker, 2003; Vijayraghavan et al., 1986). However, the previous results suggested that NMD might be involved in degrading unspliced transcripts generated by splice site mutations. We tested this hypothesis by introducing a mutation in the 5′ splice site (SS) of *RPS10B*. This gene was chosen because inactivation of Upf1p resulted in increased *RPS10B* intronic signal by tiling arrays (Figure S4). The 5′SS was mutated from GUAUGU to GCAUAU at the *RPS10B* chromosomal locus by *delitto perfetto*. As expected, this mutation resulted in a strong decrease of spliced *RPS10B* (Figure 5A). While this mutation is expected to completely block *RPS10B* splicing, the residual spliced mRNA detected might be due to crosshybridization of the riboprobe with the *RPS10A* paralogue. More importantly, and in contrast to results observed with *ACT1*- or *RP51*-based reporters (Chanfreau et al., 1994; Hilleren and Parker, 2003; Vijayraghavan et al., 1986), unspliced precursors did not accumulate to high levels in this 5′SS mutant strain. However, when this 5′SS mutation was combined with deletion of *UPF1*, *UPF2*, or *UPF3*, all double mutants showed a dramatic stabilization of unspliced *RPS10B* pre-mRNAs (Figure 5A). This result shows that NMD targets unspliced mutant transcripts of the *RPS10B* gene for degradation and that these unspliced species do not accumulate to high levels unless NMD is inactivated. We also tested whether inactivation of the nuclear exosome component Rrp6p would exacerbate *RPS10B* precursor accumulation in the *RPS10B* 5′SS mutant. Strikingly, Rrp6p inactivation in this mutant resulted only in a slight increase of unspliced precursors (Figure 5B), indicating that these transcripts are, in majority, targeted by NMD and that the nuclear exosome only plays a modest role in their degradation. When the same 5′SS mutation was introduced into the *ACT1* intron transposed into the *GOT1* gene (see Figure 4), unspliced precursors

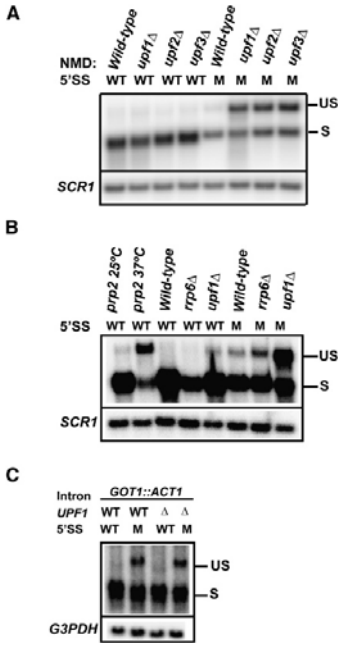

Figure 5. NMD Inactivation Exacerbates Accumulation of Unspliced Precursors Generated by a 5′ Splice Site Mutation of *RPS10B*

(A) Detection of *RPS10B* transcripts in strains carrying a wild-type *RPS10B* gene or with a 5′ splice site (5′SS) mutation (M) in *RPS10B*, alone, or in combination with deletion of *UPF1*, *UPF2*, or *UPF3*. Legends are the same as in Figure 2.

(B) Legends are the same as in (A), with the effects of the inactivation of Rrp6p.

(C) Legends are the same as in (A), except that the 5′SS mutation was introduced in the *ACT1* intron that was transposed in the *GOT1* gene (see Figure 4B).

levels were not exacerbated by NMD inactivation (Figure 5C). This result is consistent with previous results showing that unspliced *ACT1* precursors are immune to NMD (Hilleren and Parker, 2003) and confirms that different precursor transcripts obey different modes of degradation as the *ACT1* precursor and several other unspliced transcripts resulting from a *prp2* mutation are discarded through degradation pathways other than NMD (Bousquet-Antonelli et al., 2000; Hilleren and Parker, 2003).

Unspliced *RPS10B* Precursors Are Degraded by NMD in the Cytoplasm and May Be Targeted to P-Bodies

A yeast NMD reporter substrate was previously shown to be targeted to cytosolic P-bodies (Sheth and Parker, 2006). If unspliced precursors are NMD targets, we expect that they should accumulate in P-bodies in the absence of functional NMD. In addition, we would expect them to accumulate in diffuse cytoplasmic signal in the absence of Upf1p, which is required for P-body formation and substrate targeting (Sheth and Parker, 2006). To test this hypothesis, we investigated the localization of unspliced *RPS10B* precursors using fluorescence in situ hybridization. In the context of functional NMD, unspliced *RPS10B* transcripts that accumulate naturally are detected exclusively in the nucleus (Figure 6A), adjacent to or overlapping the DAPI staining (80% of cells, n = 60), possibly because unspliced transcripts are degraded quickly once they reach the cytoplasm. Strikingly, in strains lacking NMD components Upf1p or Upf2p, unspliced *RPS10B* was found mostly in the cytoplasm (Figure 6A; *upf1Δ*, 95.2% of cells, n = 63; *upf2Δ*, 72.3% of cells, n = 36). In *upf2Δ* cells, this cytoplasmic signal was concentrated in multiple foci that we suspect to be P-bodies (Figure 6A). In contrast to unspliced *RPS10B* pre-mRNAs, the nuclear localization of the control U14 snoRNA transcripts was unaffected in NMD mutants (Figure 6B). These results are consistent with previous studies describing the localization of a reporter NMD substrate in P-bodies in the absence of Upf2p (Sheth and Parker, 2006). We could not formally demonstrate that those are P-bodies, but given their cytoplasmic localization and previous demonstration that yeast NMD substrates are targeted to P-bodies (Sheth and Parker, 2006), this makes this conclusion very likely.

NMD Limits the Accumulation of Unspliced Precursors during Amino Acid Starvation

Unspliced precursors of many RPGs accumulate during amino acid starvation (Pleiss et al., 2007). These results have been interpreted as a selective inhibition of splicing of these RPGs during this stress. We noticed a large overlap of NMD targets detected in this study and of RPGs affected by amino acid starvation (Figure 7A). Furthermore, it has been shown that amino acid starvation can inhibit NMD (Mendell et al., 2004). Therefore, an accumulation of unspliced RPGs in amino acid starvation could be interpreted by a possible inactivation of NMD and by the inhibition of the degradation of some of these unspliced precursors in these conditions. We therefore investigated whether NMD inactivation would be epistatic to the unspliced precursor accumulation phenotype observed during amino acid starvation. Wild-type and *upf1Δ* strains were shifted to a medium containing 50 mM aminotriazole (3AT) to induce amino acid starvation. The level of unspliced *RPS29B* and *RPL22B*, which was found to be both NMD sensitive and affected by amino acid starvation, was then assessed by northern blot. In wild-type cells, unspliced precursors of *RPS29B* and *RPL22B* were detected transiently after 10 min in 3AT medium, after which their levels reverted to close to normal levels (Figure 7). We observed the same increase of unspliced *RPS29B* precursors in the *upf1Δ* strain, showing that this increase was not likely due to NMD inhibition since NMD is defective in this mutant. The accumulation of unspliced transcripts was, however, higher in the *upf1Δ* strain than in wild-type, indicating that NMD is used to limit the accumulation of unspliced *RPS29B* precursors generated during amino acid starvation. We could not detect an increase of unspliced precursors for *RPL22B* in the *upf1Δ* strain, possibly because the very high levels of unspliced precursors observed before the shift could mask the small increase of unspliced transcripts observed in the wild-type (1.8-fold). As a negative control, *RPL25*, which is not an NMD target and was not found to be affected by amino acids starvation, did not exhibit unspliced transcripts accumulation during this treatment (Figure 7). In conclusion, the results observed with *RPS29B* show that NMD is used to limit the amount of some unspliced transcripts resulting from splicing inhibition during amino acid starvation.

DISCUSSION

In this study, we revisited the effect of the inactivation of the Upf1p and Xrn1p components of the NMD system on unspliced pre-mRNA accumulation in yeast. We show, using tiling arrays, that a significant fraction of the yeast intronome population is affected by NMD inactivation, as 31% of RPGs and 33% of all introns show an accumulation of unspliced precursors when Upf1p is inactivated. The phenotypes observed in the *upf1Δ* or *xrn1Δ* strains are most of the time similar (Figure S2). Some exceptions were found, including *YRA1*, which has been shown to rely on a sequence-specific degradation system to degrade its inefficiently spliced precursors (Dong et al., 2007; Preker and Guthrie, 2006). Previous splicing microarray analysis of the *upf1Δ*, *xrn1Δ*, and *upf3Δ* mutants failed to reveal a widespread effect of NMD mutations on unspliced precursor accumulation (Burckin et al., 2005; Clark et al., 2002; Pleiss et al., 2007) and in particular on RPGs (Pleiss et al., 2007). While these results may seem contradictory to those presented here, it should be noted that these studies were focused on detecting the effects of splicing mutations or inhibition during stress. Since the accumulation of unspliced precursors is usually higher in splicing mutants than in NMD mutants (Figure 2), it is possible that these previous studies did not consider the increase of unspliced precursors observed in NMD mutants significant. Another possibility to explain this apparent discrepancy may be that using tiling arrays, which cover a large fraction of the intronic sequences, increased the detection of smaller effects, leading to a higher sensitivity. Regardless of these differences, our results, combined with studies showing intronic detection by tiling arrays in the debranching enzyme mutant (Juneau et al., 2007; Zhang et al., 2007), demonstrate that these arrays are efficient to detect changes in ICG transcripts accumulation, as differences predicted by tiling array profiles were confirmed by northern blot analysis (Figure 2B).

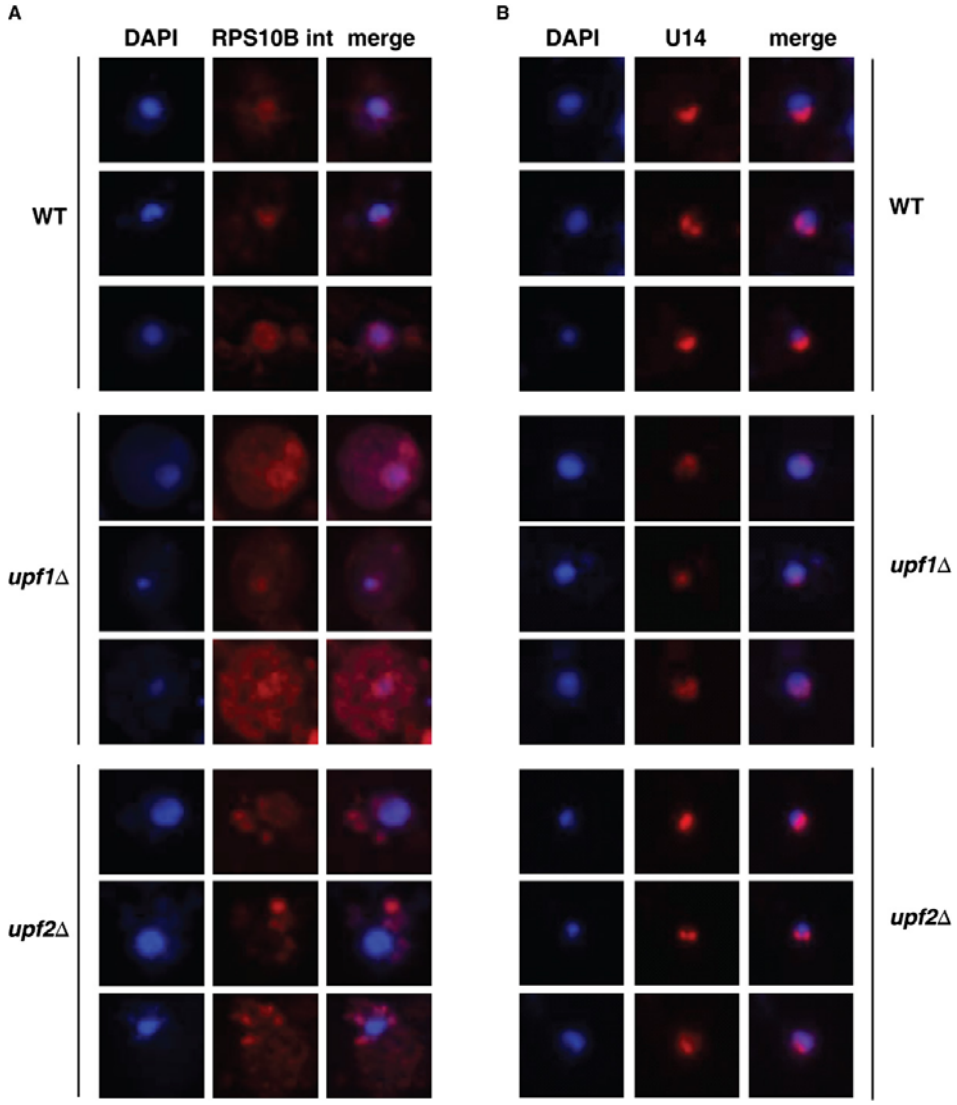

Figure 6. Localization of Unspliced *RPS10B* Precursors by Fluoresecent In Situ Hybridization
(A) Shown are the DAPI staining (blue) for nuclear DNA, intron *RPS10B* FISH (red), and merged images for the wild-type, *upf1Δ*, and *upf2Δ* strains.
(B) U14 snoRNA FISH (red) is shown as a control in the same strains.

What Are The Determinants of NMD Targeting for Unspliced Yeast Pre-mRNAs?

In the case of transcripts for which we did not detect any unspliced pre-mRNAs accumulation in *upf1Δ* or *xrn1Δ* strains, we do not know whether this reflects very efficient splicing or whether some precursors escape splicing but are degraded by alternative degradation pathways. In the first hypothesis, these transcripts might represent a subpopulation with a high level of cotranscriptional splicing (Moore et al., 2006; Tardiff et al., 2006), minimizing the production of unspliced pre-mRNAs. However, many ICGs, which do not show cotranscriptional spliceosome recruitment, do not show any unspliced precursor

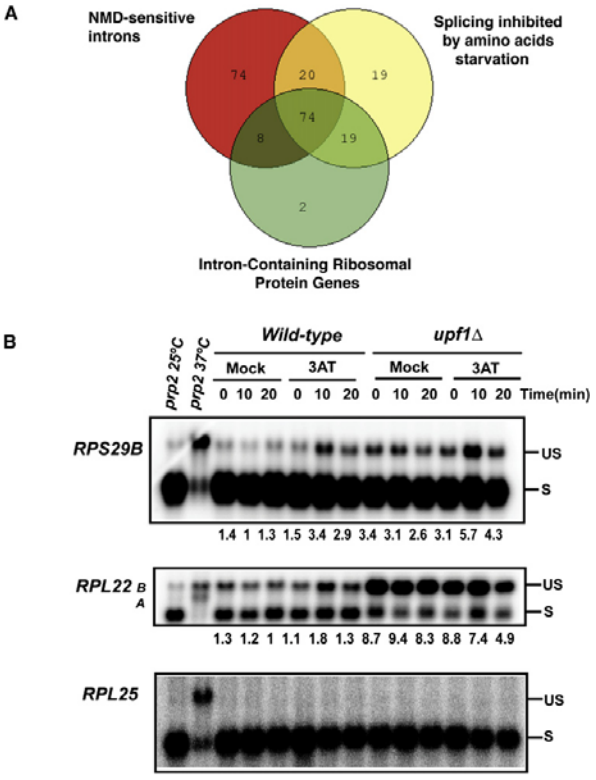

Figure 7. Detection of Unspliced Precursors in Wild-Type and *upf1Δ* Strains during Amino Acid Starvation

(A) Venn diagram of the overlap between Intron-containing RPGs, ICGs affected by Upf1p inactivation, and ICGs for which splicing is inhibited by amino acids starvation (Pleiss et al., 2007).

(B) Indicated strains were shifted for 10 or 20 min in a medium containing 50 mM 3AT or untreated (mock) and probed for the indicated RPGs. Relative amount of unspliced precursors in the different conditions was standardized to the mock value showing the lowest amount of unspliced precursors.

accumulation in NMD mutants either (data not shown). Results from Moore et al. (2006) are consistent with the hypothesis that these transcripts are retained in the nucleus by Mlp1p and degraded by the nuclear exosome. Therefore, these results would be inconsistent with the idea that a lack of cotranscriptional splicing favors NMD targeting. Instead, we prefer the idea that unspliced precursors that accumulate in *upf1Δ* or *xrn1Δ* strains correspond to inefficiently spliced transcripts, not because of a lack of cotranscriptional splicing but because of intronic features. In favor of this hypothesis is the observation that introns containing suboptimal splicing signals are enriched in NMD targets and that restoring the suboptimal branchpoint of the *RPL19A* intron back to the canonical sequence is sufficient to prevent unspliced precursors accumulation in the *upf1Δ* strain (Figure 4D). This strongly suggests that NMD targeting is determined by intronic features, which ultimately drives splicing efficiency. The suboptimal splicing of the other fraction of NMD-sensitive transcripts that present canonical splice site signals could result from competing secondary structures (Goguel et al., 1993) or *trans*-acting effects. This model cannot completely explain why certain precursors resulting from splicing mutations, including the historical *ACT1* model, are immune to NMD (Figure 5C). These transcripts are degraded by other degradation systems, such as the nuclear exosome for some meiotic pre-mRNAs (Moore et al., 2006) or by Xrn1p in the cytoplasm (Hilleren and Parker, 2003; Scherrer and Spingola, 2006). The determinants of this differential targeting remain to be investigated.

Significance of NMD-Dependent Degradation of Unspliced Pre-mRNAs

The involvement of NMD in the degradation of a large number of unspliced transcript is not unprecedented and seems to be conserved throughout eukaryotic evolution. In *C. elegans*, NMD degrades inefficiently spliced ribosomal protein precursor transcripts (Mitrovich and Anderson, 2000), and in *Paramecia*, NMD also limits the accumulation of unspliced precursors (Jaillon et al., 2008). Therefore, this phylogenetic conservation probably reflects an important role for NMD in the degradation of unspliced precursors of suboptimally spliced transcripts. This function is important for cell survival as the deletion of the NMD component Upf1p is synthetic lethal with the inactivation of the splicing/nuclear retention factor BBP/ScSF1 (Rutz and Seraphin, 2000). This suggests that NMD might be required to prevent the cellular toxicity generated by high amounts of unspliced cytoplasmic transcripts.

Ribosomal protein genes are highly and tightly regulated at many levels in yeast, including splicing (Warner, 1999; Zhao et al., 2003). The large number of RPGs identified here as NMD targets suggests that NMD might be involved in preventing the accumulation of unspliced RPG transcripts generated during regulated splicing throughout various physiological conditions. To illustrate this point, we found that NMD limits the levels of unspliced *RPS29B* precursors generated by splicing inhibition during amino acid starvation (Pleiss et al., 2007). Thus, NMD plays a role in limiting accumulation of unspliced precursors during a known physiological stress, and it could play a similar role under other conditions that have yet to be determined, such as other stresses or life stages that result in modulations of splicing efficiency.

EXPERIMENTAL PROCEDURES

Strains and Media

The list of yeast strains used in this study is provided in the Supplemental Data. Strains used for tiling array profiling were grown in synthetic complete medium. All other strains were grown in YPD. Cells were harvested during log phase (OD_{600}, 0.4 to 0.8). Amino acid starvation experiments were performed as described (Pleiss et al., 2007). Strains were constructed via one-step PCR

product-based gene disruption (Longtine et al., 1998) or by *delitto perfetto* (Storici et al., 2001).

Microarray Analysis

Four biological replicates of wild-type, *upf1Δ*, and *xrn1Δ* from the BY4741 background were grown independently and analyzed by Affymetrix yeast tiling microarray analysis. Probes preparation, hybridization, and tiling array scanning were performed according to the manufacturer's instructions. Methods used for bioinformatics analysis of the tiling arrays are described in the Supplemental Data.

Northern Blots and Fluorescent In Situ Hybridization

Northern blots were hybridized with radioactive probes in Church buffer (250 mM sodium phosphate, pH 7.2; 1% bovine serum albumin; 7% sodium dodecyl sulfate; and 1 mM EDTA) at 67°C–70°C overnight and washed twice at room temperature with 2× SSPE with 0.1% SDS for 20 min, then at room temperature in 0.1× SSPE, 0.1% SDS. A last wash with prewarmed 0.1× SSPE buffer with 0.1% SDS was performed at 67°C for 5 min. All probes were antisense riboprobes with the exception of the *G3PDH* and *SCR1* probes, generated by random priming from PCR products. Riboprobes were synthesized using Ambion T3 MaxiScript kits (Supplemental Experimental Procedures) from PCR templates in which a T3 RNA polymerase promoter had been incorporated through the reverse primer. Blots were imaged using a Molecular Dynamics Phosphorimager Scanner or a compatible Bio-Rad scanner system. FISH with the RPS10B intronic probe was performed as described in Supplemental Experimental Procedures. FISH with the U14 probe was performed as described (Henras et al., 2004).

ACCESSION NUMBERS

Microarray data are accessible in the GEO database (accession number GSE11621).

SUPPLEMENTAL DATA

The Supplemental Data include Supplemental Experimental Procedures, three tables, and seven figures and can be found with this article online at http://www.molecule.org/cgi/content/full/31/3/360/DC1/.

ACKNOWLEDGMENTS

We thank the UCLA Microarray Core Facility for help with microarray hybridization and scanning; Lauren May for constructing the strain carrying a double mutation in Rrp6 and the 5′ splice site of *RPS10B*; J. Gober for use of his fluorescence microscope; J. Pleiss and C. Guthrie for communication of results prior to publication; and D.L. Black, C. Coffinier, and D. Egecioglu for critical reading of the manuscript. This work was supported by NIH grant GM61518 to G.F.C. and NSF grant DGE-9987641 to M.J.

Received: December 12, 2007
Revised: April 26, 2008
Accepted: July 8, 2008
Published: August 7, 2008

REFERENCES

Amrani, N., Ganesan, R., Kervestin, S., Mangus, D.A., Ghosh, S., and Jacobson, A. (2004). A faux 3′-UTR promotes aberrant termination and triggers nonsense-mediated mRNA decay. Nature *432*, 112–118.

Arciga-Reyes, L., Wootton, L., Kieffer, M., and Davies, B. (2006). UPF1 is required for nonsense-mediated mRNA decay (NMD) and RNAi in Arabidopsis. Plant J. *47*, 480–489.

Behm-Ansmant, I., Kashima, I., Rehwinkel, J., Sauliere, J., Wittkopp, N., and Izaurralde, E. (2007). mRNA quality control: an ancient machinery recognizes and degrades mRNAs with nonsense codons. FEBS Lett. *581*, 2845–2853.

Bousquet-Antonelli, C., Presutti, C., and Tollervey, D. (2000). Identification of a regulated pathway for nuclear pre-mRNA turnover. Cell *102*, 765–775.

Burckin, T., Nagel, R., Mandel-Gutfreund, Y., Shiue, L., Clark, T.A., Chong, J.L., Chang, T.H., Squazzo, S., Hartzog, G., and Ares, M., Jr. (2005). Exploring functional relationships between components of the gene expression machinery. Nat. Struct. Mol. Biol. *12*, 175–182.

Chanfreau, G., Legrain, P., Dujon, B., and Jacquier, A. (1994). Interaction between the first and last nucleotides of pre-mRNA introns is a determinant of 3′ splice site selection in S. cerevisiae. Nucleic Acids Res. *22*, 1981–1987.

Chang, Y.F., Imam, J.S., and Wilkinson, M.F. (2007). The nonsense-mediated decay RNA surveillance pathway. Annu. Rev. Biochem. *76*, 51–74.

Clark, T.A., Sugnet, C.W., and Ares, M., Jr. (2002). Genomewide analysis of mRNA processing in yeast using splicing-specific microarrays. Science *296*, 907–910.

Conti, E., and Izaurralde, E. (2005). Nonsense-mediated mRNA decay: molecular insights and mechanistic variations across species. Curr. Opin. Cell Biol. *17*, 316–325.

Danin-Kreiselman, M., Lee, C.Y., and Chanfreau, G. (2003). RNAse III-mediated degradation of unspliced pre-mRNAs and lariat introns. Mol. Cell *11*, 1279–1289.

Dong, S., Li, C., Zenklusen, D., Singer, R.H., Jacobson, A., and He, F. (2007). YRA1 autoregulation requires nuclear export and cytoplasmic Edc3p-mediated degradation of its pre-mRNA. Mol. Cell *25*, 559–573.

Frischmeyer, P.A., and Dietz, H.C. (1999). Nonsense-mediated mRNA decay in health and disease. Hum. Mol. Genet. *8*, 1893–1900.

Galy, V., Gadal, O., Fromont-Racine, M., Romano, A., Jacquier, A., and Nehrbass, U. (2004). Nuclear retention of unspliced mRNAs in yeast is mediated by perinuclear Mlp1. Cell *116*, 63–73.

Goguel, V., Wang, Y., and Rosbash, M. (1993). Short artificial hairpins sequester splicing signals and inhibit yeast pre-mRNA splicing. Mol. Cell. Biol. *13*, 6841–6848.

Green, R.E., Lewis, B.P., Hillman, R.T., Blanchette, M., Lareau, L.F., Garnett, A.T., Rio, D.C., and Brenner, S.E. (2003). Widespread predicted nonsense-mediated mRNA decay of alternatively-spliced transcripts of human normal and disease genes. Bioinformatics *19* (*Suppl 1*), i118–i121.

Guan, Q., Zheng, W., Tang, S., Liu, X., Zinkel, R.A., Tsui, K.W., Yandell, B.S., and Culbertson, M.R. (2006). Impact of nonsense-mediated mRNA decay on the global expression profile of budding yeast. PLoS Genet *2*, e203. 10.1371/journal.pgen.0020203.

He, F., and Jacobson, A. (2001). Upf1p, Nmd2p, and Upf3p regulate the decapping and exonucleolytic degradation of both nonsense-containing mRNAs and wild-type mRNAs. Mol. Cell. Biol. *21*, 1515–1530.

He, F., Peltz, S.W., Donahue, J.L., Rosbash, M., and Jacobson, A. (1993). Stabilization and ribosome association of unspliced pre-mRNAs in a yeast upf1-mutant. Proc. Natl. Acad. Sci. USA *90*, 7034–7038.

He, F., Li, X., Spatrick, P., Casillo, R., Dong, S., and Jacobson, A. (2003). Genome-wide analysis of mRNAs regulated by the nonsense-mediated and 5′ to 3′ mRNA decay pathways in yeast. Mol. Cell *12*, 1439–1452.

Henras, A.K., Bertrand, E., and Chanfreau, G. (2004). A cotranscriptional model for 3′-end processing of the Saccharomyces cerevisiae pre-ribosomal RNA precursor. RNA *10*, 1572–1585.

Hilleren, P.J., and Parker, R. (2003). Cytoplasmic degradation of splice-defective pre-mRNAs and intermediates. Mol. Cell *12*, 1453–1465.

Hillman, R.T., Green, R.E., and Brenner, S.E. (2004). An unappreciated role for RNA surveillance. Genome Biol. *5*, R8.

Hori, K., and Watanabe, Y. (2005). UPF3 suppresses aberrant spliced mRNA in Arabidopsis. Plant J. *43*, 530–540.

Jaillon, O., Bouhouche, K., Gout, J.F., Aury, J.M., Noel, B., Saudemont, B., Nowacki, M., Serrano, V., Porcel, B.M., Segurens, B., et al. (2008). Translational control of intron splicing in eukaryotes. Nature *451*, 359–362.

Johansson, M.J., He, F., Spatrick, P., Li, C., and Jacobson, A. (2007). Association of yeast Upf1p with direct substrates of the NMD pathway. Proc. Natl. Acad. Sci. USA *104*, 20872–20877.

Juneau, K., Palm, C., Miranda, M., and Davis, R.W. (2007). High-density yeast-tiling array reveals previously undiscovered introns and extensive regulation of meiotic splicing. Proc. Natl. Acad. Sci. USA *104*, 1522–1527.

Lareau, L.F., Inada, M., Green, R.E., Wengrod, J.C., and Brenner, S.E. (2007). Unproductive splicing of SR genes associated with highly conserved and ultraconserved DNA elements. Nature *446*, 926–929.

Leeds, P., Peltz, S.W., Jacobson, A., and Culbertson, M.R. (1991). The product of the yeast UPF1 gene is required for rapid turnover of mRNAs containing a premature translational termination codon. Genes Dev. *5*, 2303–2314.

Leeds, P., Wood, J.M., Lee, B.S., and Culbertson, M.R. (1992). Gene products that promote mRNA turnover in Saccharomyces cerevisiae. Mol. Cell. Biol. *12*, 2165–2177.

Lejeune, F., and Maquat, L.E. (2005). Mechanistic links between nonsense-mediated mRNA decay and pre-mRNA splicing in mammalian cells. Curr. Opin. Cell Biol. *17*, 309–315.

Lelivelt, M.J., and Culbertson, M.R. (1999). Yeast Upf proteins required for RNA surveillance affect global expression of the yeast transcriptome. Mol. Cell. Biol. *19*, 6710–6719.

Li, Z., Paulovich, A.G., and Woolford, J.L., Jr. (1995). Feedback inhibition of the yeast ribosomal protein gene CRY2 is mediated by the nucleotide sequence and secondary structure of CRY2 pre-mRNA. Mol. Cell. Biol. *15*, 6454–6464.

Longtine, M.S., McKenzie, A., III, Demarini, D.J., Shah, N.G., Wach, A., Brachat, A., Philippsen, P., and Pringle, J.R. (1998). Additional modules for versatile and economical PCR-based gene deletion and modification in Saccharomyces cerevisiae. Yeast *14*, 953–961.

Mendell, J.T., Sharifi, N.A., Meyers, J.L., Martinez-Murillo, F., and Dietz, H.C. (2004). Nonsense surveillance regulates expression of diverse classes of mammalian transcripts and mutes genomic noise. Nat. Genet. *36*, 1073–1078.

Mitrovich, Q.M., and Anderson, P. (2000). Unproductively spliced ribosomal protein mRNAs are natural targets of mRNA surveillance in C. elegans. Genes Dev. *14*, 2173–2184.

Mitrovich, Q.M., and Anderson, P. (2005). mRNA surveillance of expressed pseudogenes in C. elegans. Curr. Biol. *15*, 963–967.

Moore, M.J., Schwartzfarb, E.M., Silver, P.A., and Yu, M.C. (2006). Differential recruitment of the splicing machinery during transcription predicts genome-wide patterns of mRNA splicing. Mol. Cell *24*, 903–915.

Ni, J.Z., Grate, L., Donohue, J.P., Preston, C., Nobida, N., O'Brien, G., Shiue, L., Clark, T.A., Blume, J.E., and Ares, M., Jr. (2007). Ultraconserved elements are associated with homeostatic control of splicing regulators by alternative splicing and nonsense-mediated decay. Genes Dev. *21*, 708–718.

Parker, R., and Song, H. (2004). The enzymes and control of eukaryotic mRNA turnover. Nat. Struct. Mol. Biol. *11*, 121–127.

Pleiss, J.A., Whitworth, G.B., Bergkessel, M., and Guthrie, C. (2007). Rapid, transcript-specific changes in splicing in response to environmental stress. Mol. Cell *27*, 928–937.

Preker, P.J., and Guthrie, C. (2006). Autoregulation of the mRNA export factor Yra1p requires inefficient splicing of its pre-mRNA. RNA *12*, 994–1006.

Rutz, B., and Seraphin, B. (2000). A dual role for BBP/ScSF1 in nuclear pre-mRNA retention and splicing. EMBO J. *19*, 1873–1886.

Scherrer, F.W., Jr., and Spingola, M. (2006). A subset of Mer1p-dependent introns requires Bud13p for splicing activation and nuclear retention. RNA *12*, 1361–1372.

Sheth, U., and Parker, R. (2006). Targeting of aberrant mRNAs to cytoplasmic processing bodies. Cell *125*, 1095–1109.

Storici, F., Lewis, L.K., and Resnick, M.A. (2001). In vivo site-directed mutagenesis using oligonucleotides. Nat. Biotechnol. *19*, 773–776.

Tardiff, D.F., Lacadie, S.A., and Rosbash, M. (2006). A genome-wide analysis indicates that yeast pre-mRNA splicing is predominantly posttranscriptional. Mol. Cell *24*, 917–929.

Vijayraghavan, U., Parker, R., Tamm, J., Iimura, Y., Rossi, J., Abelson, J., and Guthrie, C. (1986). Mutations in conserved intron sequences affect multiple steps in the yeast splicing pathway, particularly assembly of the spliceosome. EMBO J. *5*, 1683–1695.

Warner, J.R. (1999). The economics of ribosome biosynthesis in yeast. Trends Biochem. Sci. *24*, 437–440.

Zhang, Z., Hesselberth, J.R., and Fields, S. (2007). Genome-wide identification of spliced introns using a tiling microarray. Genome Res. *17*, 503–509.

Zhao, Y., Sohn, J.H., and Warner, J.R. (2003). Autoregulation in the biosynthesis of ribosomes. Mol. Cell. Biol. *23*, 699–707.

Chapter 3—Nuclear quality control of RNA degradation

The diverse functions of the nuclear exosome

The yeast nuclear exosome is a multisubunit degradosome with specificity of degrading RNA molecules from the 3'→5' direction (**Mitchell et al., 1997**). Biochemical analysis has shown approximately eleven constituents of which ten are exoribonucleases (and nine of these have human homologs) (**Allmang et al., 1999**). Mutations in exosome components cause the accumulation of many extended/unprocessed forms of non-coding RNAs (**van Hoof et al., 2000**). In particular, exosome mutants displayed a large accumulation of the 3'-extended form of the U4 snoRNA (**van Hoof et al., 2000**). The 3'-end processing of the 5.8s rRNA, snRNAs, and snoRNAs depended specifically on Rrp6p and Mtr4p (**van Hoof et al., 2000**). However, the turnover of these unprocessed required Ski2p, which is a component of the cytoplasmic exosome (**van Hoof et al., 2000**). This study revealed the distinct nature of processing and degradation that is carried out by the nuclear and cytoplasmic exosome complexes.

The exosome components also function in quality-control of transcription. For example, RNA polymerase II (RNA pol II) dependent transcripts that fail to acquire a poly-A tail are retained at the site of transcription and are rapidly degraded (**Hilleren et al., 2001**). This site-of-transcription retention mechanism requires Rrp6p (**Hilleren et al., 2001**). Another exosome component, Rrp47, is a cofactor that functions during non-coding, stable RNA maturation (**Mitchell et al., 2003**). Other facets of the nuclear exosome extend beyond processing and degradation of non-coding RNAs. For example, the levels of the NAB2 transcript which encodes a poly-A binding protein is controlled by the exosome factor, Rrp6p (**Roth et al., 2005**). Intergenically-transcribed polII transcripts as well as hypermodified tRNAs are degraded by a mechanism that involves the poly-A polymerases Trf4p and Trf5p (comprising the TRAMP

complex) as well as nuclear exosome mediated turnover of these unstable transcripts (**Wyers et al., 2005; Vanacova et al., 2005**). This mechanism of polyadenylation dependent, nuclear exosome-mediated turnover appears to be ancient since there is a parallel, active poly-A dependent degradation system in bacterial species (**Wyers et al., 2005**). In addition to contributing to the turnover of unstable, intergenically transcribed RNAs, the exosome factor, Rrp6p also functions in degrading normal transcripts. The extant of nuclear degradation is dependent upon the extent to which these transcripts are retained in the nucleus (**Kuai et al., 2005**). Trf4p and Trf5p were further characterized to be exclusively RNA-poly-A polymerases with no evidence for DNA polymerization (**Haracska et al., 2005**). Recent evidence has linked the involvement of Trf4p and Trf5p to processes beyond the degradation of cryptically transcribed transcripts. For example, studies in the fission yeast, *Schizosaccharomyces pombe* (*S. pombe*) have shown that the TRAMP complex components Trf4p and Trf5p have an active function in the suppression of heterochromatic gene expression by enforcing the recruitment of the exosome (**Buhler et al., 2007**). Other studies have suggested that Trf5p is recruited co-transcriptionally to enforce surveillance in nucleolar loci (**Wery et al., 2009**). Other reports have illuminated distinct roles for Trf4p and Trf5p (**San Paolo et al., 2009**). A genome-wide study aimed at globally assessing the effects of *TRF4* or *TRF5* deletion on the post-transcriptional regulation of gene expression revealed that these factors participate in the turnover of spliced introns as well as a class of antisense transcripts generated from loci encoding for genes involved in phosphate metabolism (**San Paolo et al., 2009**). Surprisingly, a phenotypic consequence of TRF4 disruption in yeast causes severe telomere shortening which is indicative of putative role of Trf4p in the regulation of telomere length and perhaps even exerting the integrity of telomeres (**San Paolo et al., 2009**). Future studies would need to be done in order to investigate the

molecular mechanism through which Trf4p aids in the stability of telomeres. Studies in metazoans have suggested that the organization of the TRAMP complex degradosome is distinct from lower eukaryotes (**Lubas et al., 2011**). Biochemical studies of the Air1p and Air2p factors of the yeast TRAMP complex has elucidated the importance of the cysteine residues in the zinc knuckle motifs in mediating the intercomplex association with Trf4p as well as a role in the degradation of Crytpic Unstable Transcripts (CUTs) (**Fasken et al., 2011**). An IWRXY motif located within Air2p was shown to be essential for its stable association with Trf4p (**Fasken et al., 2011**). Much recent work has defined zinc-knuckles 2-4 as being critical for RNA binding and specifically knuckle four being important for TRAMP activity (**Holub et al., 2012**).

Genome-wide studies aimed towards obtaining a global snapshot of the impact of poly-A dependent degradation have revealed several key features (**Wang et al., 2008**). For example, in yeast, the major transcripts that are degraded through this adenylation-dependent turnover arise from loci encoding transcripts that encode meiotic factors, messagess originating from or near heterochromatic loci, and transcripts near the sub-telomeric loci (**Wang et al., 2008**). Interestingly, meiotic transcript regulation and turnover under vegetative conditions is strikingly diverse. An investigation into the regulatory circuitry ensuring regulation of a fission yeast gene encoding for a meiotic cyclin, *CRS1*, suggests that it requires an additional factor, Mmi1p, which has been shown to be essential for the subsequent degradation of the *CRS1* transcript by the exosome (**McPheeters et al., 2009**).

Studies aimed at precisely understanding the specific roles of each of the exosome factors has revealed independent functions for the Rrp6p factor (**Callahan and Butler, 2008**). In this report, it was shown that depletion of perturbation of Rrp6p causes accumulation of Rrp6p-dependent

substrates which were distinct from those of Dis3p. This investigation further revealed that there is a synergistic accumulation of Dis3p and Rrp6p-dependent targets (core exosome targets) but there was no further hyperaccumulation of Rrp6p-specific targets (**Callahan and Butler, 2008**). The importance of Rrp6p and Dis3p was further highlighted in a study aimed towards elucidating the importance of the THO complex. In this investigation, RNAs transcribed in THO mutant strains were retained at the site of transcription and were subsequently degraded due to malfunctions in proper mRNP assembly (**Assenholt et al., 2008**). This quality control mechanism was also elicited by the exosome 3'→5'—exonuclease, Dis3p (**Assenholt et al., 2008**).

Retention and Export: Opposing forces

Prior to the export of an mRNA, there needs to be proper association with a distinct set pf export factors that function to govern its integrity during the passage from the nucleus to the cytoplasm. One key conserved export factor is Mex67p (nomenclature in *Saccharomyces cerevisiae*), which was discovered through a genetic interaction with Nup85p (**Segref et al., 1997**). A thermosensitive mutation in Mex67p (the allelic *mex67-5*) caused an increase in polyadenylated [p(A)] RNA, which identified Mex67p as a key factor involved in regulating the export of RNA molecules from the nucleus. It was further shown that it has a broad specificity in regulating the export of a diverse group of RNA pol II transcripts (**Hurt et al., 2000**). Other studies have shown that hyperadenylated RNA species persist upon malfunction of Mex67p as well as a slew of other factors required for proper RNA export (**Hilleren and Parker, 2001**). Genome-wide studies aimed at obtaining a quantitative snapshot of the precise number of RNA molecules

trafficked by Mex67p revealed a value comprising close to 1200 mRNAs (**Hieronymus and Silver, 2003**).

The movement of the Mex67p-Mtr2p heterodimeric protein complex requires association of Mtr2p with several nuclear pore components (**Strasser et al., 2000**). These nucleoporins often contain repetitive motifs comprising GLFG, FXFG, and FG (**Strasser et al., 2000**). Other studies have shown that the GLFG type nucleoporins Nup116 and Nup100p facilitate the binding of Mex67p and Kap95p (**Strawn et al., 2001**). Experiments in mammalian cells have shown that the C-terminal of TAP is essential for targeting it to the nuclear rim and association with components of the nuclear pore complex (**Bachi et al., 2000**).

TAP, the human homolog was discovered as a factor that was essential in binding to retroviral constitutive transport elements (RCTE or CTE) (**Gruter et al., 1998**). Further analyses revealed that TAP, like Mex67p, predominantly occupies an intranuclear niche (**Katahira et al., 1999**) and a leucine rich repeat motif located within an N-terminal domain of TAP is essential for binding to the target RNA (**Braun et al., 1999**). P15, a human homolog of the yeast Mtr2p factor also associates with TAP and co-expression of TAP and p15 restores a synthetic lethal Mtr2p-Mex67p mutation, which provides further proof of the existence of homologous factors in human cells and vice versa (**Katahira et al., 1999**). In vivo, Mex67p interacts with Mtr2p, which in turn associates with Nup85 in facilitating the export of RNAs (**Santos-Rosa et al., 1998**).

REFERENCES

Allmang C, Petfalski E, Podtelejnikov A, Mann M, Tollervey D, Mitchell P. 1999. The yeast exosome and human PM-Scl are related complexes of 3'→5' exonucleases. *Genes Dev.* 13(16): 2148-58.

Assenholt J, Mouaikel J, Andersen KR, Brodersen DE, Libri D, Jensen TH. 2008. Exonucleolysis is required for nuclear mRNA quality control in yeast THO mutants. *RNA*. 14(11):2305-13.

Bachi A, Braun IC, Rodrigues JP, Panté N, Ribbeck K, von Kobbe C, Kutay U, Wilm M, Görlich D, Carmo-Fonseca M, Izaurralde E. 2000. The C-terminal domain of TAP interacts with the nuclear pore complex and promotes export of specific CTE-bearing RNA substrates. *RNA*. 6(1):136-58.

Braun IC, Rohrbach E, Schmitt C, Izaurralde E. 1999. TAP binds to the constitutive transport element (CTE) through a novel RNA-binding motif that is sufficient to promote CTE-dependent RNA export from the nucleus. *EMBO J.* 18(7):1953-65.

Bühler M, Haas W, Gygi SP, Moazed D. 2007. RNAi-dependent and -independent RNA turnover mechanisms contribute to heterochromatic gene silencing. *Cell.* 129(4):707-21.

Callahan KP, Butler JS. 2008. Evidence for core exosome independent function of the nuclear exoribonuclease Rrp6p. *Nucleic Acids Res.* 36(21):6645-55.

Fasken MB, Leung SW, Banerjee A, Kodani MO, Chavez R, Bowman EA, Purohit MK, Rubinson ME, Rubinson EH, Corbett AH. 2012. Air1 zinc knuckles 4 and 5 and a conserved IWRXY motif are critical for the function and integrity of the Trf4/5-Air1/2-Mtr4 polyadenylation (TRAMP) RNA quality control complex. *J Biol Chem.* 286(43):37429-45.

Grüter P, Tabernero C, von Kobbe C, Schmitt C, Saavedra C, Bachi A, Wilm M, Felber BK, Izaurralde E. 1998. TAP, the human homolog of Mex67p, mediates CTE-dependent RNA export from the nucleus. *Mol Cell.* 1(5):649-59.

Haracska L, Johnson RE, Prakash L, Prakash S. 2005Trf4 and Trf5 proteins of Saccharomyces cerevisiae exhibit poly(A) RNA polymerase activity but no DNA polymerase activity. . *Mol Cell Biol.* 25(22):10183-9.

Hieronymus H, Silver PA. 2003. Genome-wide analysis of RNA-protein interactions illustrates specificity of the mRNA export machinery. *Nat Genet.* 33(2):155-61.

Hilleren P, McCarthy T, Rosbash M, Parker R, Jensen TH. 2001. Quality control of mRNA 3'-end processing is linked to the nuclear exosome. *Nature.* 413(6855):538-42.

Holub P, Lalakova J, Cerna H, Pasulka J, Sarazova M, Hrazdilova K, Arce MS, Hobor F, Stefl R, Vanacova S. 2012. Air2p is critical for the assembly and RNA-binding of the TRAMP complex and the KOW domain of Mtr4p is crucial for exosome activation. *Nucleic Acids Res.* Epub ahead of print.

Hurt E, Strässer K, Segref A, Bailer S, Schlaich N, Presutti C, Tollervey D, Jansen R. 2000. Mex67p mediates nuclear export of a variety of RNA polymerase II transcripts. *J Biol Chem.* 275(12):8361-8.

Kuai L, Das B, Sherman F. 2005. A nuclear degradation pathway controls the abundance of normal mRNAs in Saccharomyces cerevisiae. *Proc Natl Acad Sci U S A.* 102(39):13962-7.

Lubas M, Christensen MS, Kristiansen MS, Domanski M, Falkenby LG, Lykke-Andersen S, Andersen JS, Dziembowski A, Jensen TH. 2011. Interaction profiling identifies the human nuclear exosome targeting complex. *Mol Cell.* 43(4):624-37.

McPheeters DS, Cremona N, Sunder S, Chen HM, Averbeck N, Leatherwood J, Wise JA. . 2009. A complex gene regulatory mechanism that operates at the nexus of multiple RNA processing decisions. *Nat Struct Mol Biol.* 16(3):255-64.

Mitchell P, Petfalski E, Shevchenko A, Mann M, Tollervey D. 1997. The exosome: a conserved eukaryotic RNA processing complex containing multiple 3'-->5' exoribonucleases. *Cell*. 91(4): 457-66.

Mitchell P, Petfalski E, Houalla R, Podtelejnikov A, Mann M, Tollervey D. 2003. Rrp47p is an exosome-associated protein required for the 3' processing of stable RNAs. *Mol Cell Biol.* 23(19):6982-92.

Roth KM, Wolf MK, Rossi M, Butler JS. 2005. The nuclear exosome contributes to autogenous control of NAB2 mRNA levels. *Mol Cell Biol*. 25(5):1577-85.

San Paolo S, Vanacova S, Schenk L, Scherrer T, Blank D, Keller W, Gerber AP. 2009. Distinct roles of non-canonical poly(A) polymerases in RNA metabolism. *PLoS Genet.* 5(7):e1000555.

Santos-Rosa H, Moreno H, Simos G, Segref A, Fahrenkrog B, Panté N, Hurt E. 1998. Nuclear mRNA export requires complex formation between Mex67p and Mtr2p at the nuclear pores. *Mol Cell Biol.* 18(11):6826-38.

Segref A, Sharma K, Doye V, Hellwig A, Huber J, Lührmann R, Hurt E. 1997. Mex67p, a novel factor for nuclear mRNA export, binds to both poly(A)+ RNA and nuclear pores. *EMBO J.* 16(11):3256-71.

Strässer K, Bassler J, Hurt E. 2000. Binding of the Mex67p/Mtr2p heterodimer to FXFG, GLFG, and FG repeat nucleoporins is essential for nuclear mRNA export. *J Cell Biol.* 150(4):695-706.

Strawn LA, Shen T, Wente SR. 2001. The GLFG regions of Nup116p and Nup100p serve as binding sites for both Kap95p and Mex67p at the nuclear pore complex. *J Biol Chem.* 276(9):6445-52.

van Hoof A, Lennertz P, Parker R. 2000. Yeast exosome mutants accumulate 3'-extended polyadenylated forms of U4 small nuclear RNA and small nucleolar RNAs. *Mol Cell Biol.* 20(2):441-52.

Vanácová S, Wolf J, Martin G, Blank D, Dettwiler S, Friedlein A, Langen H, Keith G, Keller W. 2005. A new yeast poly(A) polymerase complex involved in RNA quality control. *PLoS Biol.*3(6):e189.

Wang SW, Stevenson AL, Kearsey SE, Watt S, Bähler J. 2008. Global role for polyadenylation-assisted nuclear RNA degradation in posttranscriptional gene silencing. *Mol Cell Biol.* 28(2):656-65.

Wery M, Ruidant S, Schillewaert S, Leporé N, Lafontaine DL. 2009. The nuclear poly(A) polymerase and Exosome cofactor Trf5 is recruited cotranscriptionally to nucleolar surveillance. *RNA*. 15(3):406-19.

Wyers F, Rougemaille M, Badis G, Rousselle JC, Dufour ME, Boulay J, Régnault B, Devaux F, Namane A, Séraphin B, Libri D, Jacquier A. 2005. Cryptic pol II transcripts are degraded by a nuclear quality control pathway involving a new poly(A) polymerase. *Cell*. 121(5):725-37.

Chapter 3A—Functional redundancy between nuclear and cytoplasmic RNA degradation pathways limits the accumulation of unspliced transcripts

Shakir Sayani[1] and Guillaume F. Chanfreau[1]*

[1]From the Department of Chemistry and Biochemistry and the Molecular Biology Institute, University of California, Los Angeles, Los Angeles, CA 90095

*To whom correspondence should be addressed: guillom@chem.ucla.edu

ABSTRACT

The nuclear Exosome and the Nonsense-mediated mRNA decay pathway (NMD) have been implicated in the degradation of distinct unspliced transcripts in *S.cerevisiae*. In this study, we show that these two systems can cooperate to limit the accumulation of unspliced mRNAs. Using steady-state and decay analyses, we show that while specific unspliced transcripts rely solely on NMD or on the nuclear exosome for their degradation, some unspliced RNAs are degraded efficiently only when both the nuclear exosome and NMD are inactivated. The specificity in the pre-mRNAs degradation pathways can be manipulated by changing the rate of export or retention of these mRNAs. For instance, reducing nuclear export of pre-mRNAs mostly degraded by NMD results in a higher fraction of unspliced transcripts degraded by the nuclear exosome. Reciprocally, inactivating the Mlp retention factors result in a higher fraction of unspliced transcripts degraded by NMD for transcripts that are normally most targeted by the nuclear exosome. The mode of degradation of unspliced pre-mRNAs is not determined by intron or promoter identity. Overall, these results demonstrate that a functional redundancy exist between nuclear and cytoplasmic degradation pathways for unspliced pre-mRNAs. Our results suggest that these RNA degradation pathways are mostly non-specific and that the degradation routes are mainly determined by the efficiency of their nuclear export rates.

Introduction

Eukaryotic organisms have developed compartmentalized degradation systems to ensure the timely turnover of numerous classes of RNA molecules (reviewed in (Houseley et al., 2006; Chang et al., 2007). The major pathways that function during RNA degradation are the nuclear exosome (Mitchell et al., 1997), which is stimulated by the activity of the TRAMP complex (LaCava et al., 2005; Wyers et al., 2005) and the deadenylation and decapping of mRNAs and degradation by the cytoplasmic exonuclease, Xrn1p (reviewed in (Tucker & Parker, 2000)). After initial removal of the poly-A tail, turnover can also be promoted by the cytoplasmic 3'→5'—exosome (Tucker & Parker, 2000). Recent studies have shown that the promoter identity can influence the decay route of RNA molecules (Bregman et al., 2011).

Degradation of unspliced (intron-retained) mRNAs is a major quality control mechanism that prevents the translation of unprocessed or partially processed transcripts that would result in the production of truncated proteins due to the likelihood of encountering a stop codon (PTC) in the intronic sequences. Because of the prevalence of PTC in the intronic sequences, many unspliced RNAs are targeted by nonsense-mediated decay in a variety of species (He et al., 1993; Mitrovich & Anderson, 2000; Jaillon et al., 2008; Sayani et al., 2008). However, the degradation of unspliced RNAs is not limited to the NMD system. Previous studies have shown the involvement of nuclear degradation systems, involving multiple components, such as the nuclear exosome (Bousquet-Antonelli et al., 2000; Moore et al., 2006), the RNase III endonuclease Rnt1p (Danin-Kreiselman et al., 2003), and the nuclear poly(A)-binding protein (Lemieux et al., 2011) in the degradation of unspliced pre-mRNAs. A role for retention factors that could putatively function in the nuclear sequestration of unspliced transcripts was previously

implicated (Galy et al., 2004), which would increase the likelihood of nuclear degradation. However, this report did not reveal any physiological targets as it was based on studies with reporter transcripts (Galy et al., 2004). In addition to these nuclear degradation pathways, unspliced pre-mRNAs can also be degraded in the cytoplasm in a pathway that is dependent on the 5'-3' exonuclease Xrn1p but independent from NMD (Hilleren & Parker, 2003; Dong et al., 2007). In the case of transcripts degraded by the cytoplasmic RNA turnover machinery, the importance of proper nuclear export for efficient pre-mRNA degradation was demonstrated by showing the involvement of Mex67p for the export and subsequent Edc3p-dependent degradation of the *YRA1* pre-mRNA (Dong et al., 2007). All these studies suggest that the degradation routes for unspliced pre-mRNAs are relatively specific, as most unspliced pre-mRNAs accumulate mostly in the absence of either nuclear or cytoplasmic degradation pathways.

In this study, through steady state as well as decay rate analysis of unspliced transcripts, we reveal that certain unspliced precursors are degraded in a cooperative manner requiring both the nuclear exosome and non-sense mediated decay. We also show that the nuclear exosome can provide a larger role in the degradation of unspliced transcripts when these transcripts are sequestered in the nucleus upon inhibition of RNA export. We show that the perinuclear factors, Mlp1p and Mlp2p can have a role in the retention of an endogenous unspliced transcript that appears to be predominantly degraded by the nuclear exosome. Replacement of the native promoter sequences with GAL did not lead to changes in the accumulation profile of the unspliced transcript nor did it redirect the native degradation route for the turnover of unspliced transcripts. Lastly, we show that intron identity is not a determinant of the degradation route for

unspliced RNAs. Overall, these results show that the degradation pathways for unspliced pre-mRNAs are largely non-specific and are mostly determined by their nuclear export efficiency.

RESULTS

Higher accumulation of specific unspliced transcripts in strains lacking the nuclear exosome component Rrp6p and NMD factors

Our previous work revealed that the nonsense mediated decay (NMD) pathway targets and degrades a large number of unspliced transcripts in *S.cerevisiae*(Sayani et al., 2008). Accumulation of unspliced pre-mRNAs was mostly observed for transcripts exhibiting suboptimal splicing signals. However, we noticed that numerous transcripts that showed suboptimal splicing sequences (splice sites or branchpoints) did not reveal any major accumulation of unspliced transcripts in strains lacking NMD factors (Sayani et al., 2008). Two hypotheses could explain this phenomenon. First, it is possible that these intron-containing genes are efficiently spliced, despite their suboptimal splicing signals, and therefore do not accumulate unspliced precursors to detectable levels. On the other hand, we reasoned that some of these intron-containing genes might produce unspliced transcripts, but that their turnover could be dependent upon more than one degradation pathway. The nuclear exosome has been implicated in degrading some unspliced transcripts (Bousquet-Antonelli et al., 2000; Moore et al., 2006), suggesting that it might cooperate with NMD to degrade some of these transcripts. To test this hypothesis, we constructed yeast strains that lacked the nuclear exosome component Rrp6p, as well as the NMD factors Upf1p or Upf2p. Using intronic riboprobes, we investigated the accumulation of unspliced transcripts in *wild-type*, *rrp6Δ*, *upf1Δ*, *upf2Δ*, *rrp6Δ upf1Δ*, or *rrp6Δ*

upf2Δ for the intron-containing genes *MND1*, *RPS11A*, *RPL16A*, *SNC1*, *COF1*, *RPL22A*, *RPL18B*, *RPS17B*, and *RPL22B* (Fig.1). The use of these intronic riboprobes allowed the specific detection of unspliced pre-mRNAs without interference of signal from the mature mRNAs, which typically accumulate at much higher levels. In addition, the use of these intronic riboprobes allowed us to detect specific isoforms of ribosomal protein pre-mRNAs, as opposed to both isoforms in the case of highly similar duplicated genes. We did not observe any strong accumulation of unspliced precursors in the *wild-type*, *rrp6Δ*, *upf1Δ*, or *upf2Δ* single mutant strains for *MND1*, *SNC1*, *RPS11A*, *RPL16A* and *COF1*. However, we detected a stronger accumulation of unspliced transcripts in the *rrp6Δ upf1Δ* and *rrp6Δ upf2Δ* double mutant strains for these genes (Fig.1A). In the case of *RPL22A*, unspliced transcripts were not detected in the *wild-type* or *rrp6*Δ strains. However, an increase in the levels of unspliced precursors was observed in the *upf1*Δ strain and this accumulation was exacerbated in the *rrp6*Δ *upf1*Δ strain (Fig.1B). These observations suggested that the NMD and the nuclear exosome can cooperate to promote the turnover of unspliced species of these transcripts. In contrast, we did not detect high levels of unspliced precursors in *wild-type* or in the *upf1*Δ strains for the *RPL18B* transcript (Fig.1B). However, high levels of unspliced transcript were present in the *rrp6*Δ strain, and these levels further increased in the *rrp6*Δ *upf1*Δ strain; (Fig.1B). This result suggests that while the major degradation pathways of unspliced *RPL18B* species occur through the nuclear exosome, NMD can also participate in the degradation of these unspliced species when the nuclear exosome is inactivated. Unspliced transcripts that were found to accumulate to higher levels in yeast strains lacking both Rrp6p and NMD components hereby referred to as as RNMD (Rrp6p and Nonsense Mediated Decay)-sensitive transcripts.

The greater accumulation of unspliced species in strains lacking both degradation pathways was observed only in specific genes. For instance, unspliced precursors of *RPS17B* could be detected in *upf1Δ* or *upf2*Δ strains, but the extent of accumulation in the *rrp6Δ upf1Δ* or *rrp6Δ upf2Δ* double mutants was similar to single mutants (Fig.1B). Similarly, very high levels of unspliced precursors were detected in the *upf1*Δ strain for *RPL22B*, but these levels were not increased in the double-mutant *rrp6*Δ *upf1*Δ (Fig.1B). Based on the steady state analysis of the levels of unspliced transcripts, these results suggest that some unspliced precursor transcripts are degraded through a complex turnover route potentially involving two pathways, while others seem to be targeted mostly through a single mode of degradation.

Analysis of the rate of turnover of unspliced transcripts in NMD and *rrp6*-deficient strains

The previous observations based on steady-state analysis suggested that two pathways might cooperate to limit the accumulation of unspliced transcripts. However, we could not rule out that indirect splicing defects might result in the differential accumulation of unspliced precursors in these double mutants. In order to demonstrate that the effects observed above are directly linked to RNA turnover, we analyzed the rates of decay of some of these unspliced precursors in *wild-type*, *rrp6Δ*, *upf1Δ*, and *rrp6Δupf1Δ* strains. To this end, we used a conditional galactose promoter that allowed us to control the expression of some of these intron-containing genes as a function of the carbon source. We inserted the galactose promoter approximately fifty base-pairs upstream of the translation start site of five intron-containing genes: *RPP1B*, *RPS11A*, *RPL16A*, *RPS17B* and *RPL22B*, and then derived yeast strains that lacked either Rrp6p, Upf1p, or both

components. Each strain was grown in galactose-containing medium until logarithmic growth phase (OD_{600nm} = ~0.4-0.8) and then switched to glucose-containing medium. The kinetics of turnover of unspliced RNAs were then assessed after this switch to glucose-containing medium. As shown in Figure 2A, all five intron-containing genes (*RPP1B*, *RPS11A*, *RPL16A*, *RPS17B*, and *RPL22B*) exhibited a rapid turnover of the unspliced transcripts in *wild-type* as well as in cells lacking the nuclear exosome component, Rrp6p, such that unspliced transcripts were undetectable after approximately three minutes. A similar pattern was observed for *RPP1B*, *RPS11A*, and *RPL16A* in *upf1Δ* strains. Strikingly, the turnover of the unspliced precursors of *RPP1B*, *RPS11A* and *RPL16A* exhibited a considerable delay in the *rrp6Δ upf1Δ* strain compared to the single mutant strains, which was in excellent agreement with the steady-state accumulation profiles observed in Fig.1. This result directly demonstrates that the nuclear exosome and NMD can be functionally redundant to promote the turnover of unspliced precursors for these transcripts. By contrast, the decay of *RPS17B* and *RPL22B* unspliced precursors exhibited a considerable lag in turnover in the *upf1Δ* single mutant, and the decay rate of *RPS17B* and *RPL22B* was very similar in the *upf1Δ* and the *rrp6Δ upf1Δ* strains (Fig.2A), further showing that NMD is the major turnover route for unspliced *RPS17B* and *RPL22B* transcripts. We also analyzed the steady-state level of some of these unspliced transcripts when expressed from the *GAL* promoter in galactose medium, and showed that the differences observed between strains when these genes are expressed from their endogenous promoters can be reproduced when these intron-containing genes are expressed from the *GAL* promoter (Fig.2B). This observation suggests that replacement of the promoter of these genes by the *GAL* promoter does not perturb the degradation pathway for these unspliced species. Taken together, the results obtained from

the steady-state and turnover studies show that unspliced pre-mRNAs species of *RPS11A*, *RPL16A* and *RPP1B* are being degraded in a synergistic manner, which involves the action of two turnover systems. However, *RPS17B* and *RPL22B* unspliced transcripts are targeted and degraded predominantly by the action of the NMD pathway.

Transposition of a RNMD-sensitive intron is not sufficient to provide sensitivity to both degradation systems

In order to investigate the determinants of sensitivity of an unspliced transcript to a specific degradation pathway, we undertook an intron-replacement strategy similar to the one we had utilized in a previous study (Sayani et al., 2008). We chose the *GOT1* locus, which is an intron-containing gene with a small intron that does not lead to the production of unspliced transcripts (Sayani et al., 2008). We replaced the native *GOT1* intron and replaced it with a transposed NMD-sensitive intron (*RPS17B*) or an RNMD-sensitive intron (*RPL16A*) and then derived *rrp6*Δ, *upf1*Δ, or *rrp6*Δ *upf1*Δ strains. Transposition of the NMD-sensitive *RPS17B* intron did not lead to appreciable chimeric unspliced transcripts in the *wild-type* or *rrp6*Δ strains (Fig.3). However, a large accumulation of unspliced precursor was detected in the *upf1*Δ and similar levels in the *rrp6*Δ*upf1*Δ strain. This suggested and consistent with our previous studies (Sayani et al., 2008) that inclusion of an NMD-sensitive intron into a NMD-insensitive locus leads to the effective production of chimeric unspliced transcripts that can be targeted and degraded by the NMD pathway. Next, we analyzed unspliced transcript accumulation for the transposed *RPL16A* intron in *wild-type*, *rrp6*Δ, *upf1*Δ, or *rrp6*Δ *upf1*Δ strains. Consistent with the pattern of *RPL16A*

unspliced transcript accumulation at its normal locus (Fig.1A), we did not observe high levels of chimeric unspliced transcripts *in trans* in the *wild-type* or *rrp6*Δ strains (Fig.3). Surprisingly, however, chimeric unspliced *RPL16Ai::GOT1* transcripts were observed in the *upf1*Δ strain and the accumulation was not increased in the *rrp6*Δ *upf1*Δ double mutant strain. This result shows that the transposition of an RNMD-sensitive intron into an RNMD-insensitive locus does not lead to an RNMD-dependent mode of degradation of chimeric unspliced *RPL16Ai::GOT1* transcripts, suggesting that the determinant of the degradation route for unspliced pre-mRNAs are contained within regions of the pre-mRNA other than the intronic sequence.

The RNA export factor, Mex67p, modulates the turnover fate of unspliced transcripts

The previous results showed that two independent systems exist to degrade unspliced transcripts, one in the cytoplasm and one in the nucleus. In some cases, these two degradation systems can cooperate to degrade specific unspliced transcripts (Fig.1 and 2). These observations suggested that the mode of degradation of unspliced transcripts might be directly influenced by their rate of export. Specifically, we predicted that the turnover of an unspliced transcript which is predominantly dependent on NMD might rely on the nuclear exosome for turnover if the rate of nuclear export of this unspliced pre-mRNA is perturbed. In order to test this hypothesis, we utilized a yeast strain that carried a deletion of the essential RNA export factor Mex67p at the genomic locus and containing a plasmid expressing either a wild-type version or an allelic version expressing a thermosensitive point mutant (Segref et al., 1997). We then derived strains that lacked the exosome component, Rrp6p, or the NMD factor, Upf1p, and analyzed the

accumulation of unspliced transcripts in these strains upon inactivation of mRNA export in the *mex67-5* thermosensitive strain. We used two NMD-sensitive intron-containing genes (*RPS17B* or *GAL::RPS17B* and *RPL22B*) and one intron-containing gene whose unspliced transcript is degraded predominantly by the nuclear exosome (*RPL18B*) as candidates to investigate the potential cytoplasmic-to-nuclear shift in unspliced transcript turnover upon the induction of an export defect after the shift to the non-permissive temperature of 37°C. As expected, we did not observe a significant accumulation of unspliced transcripts for the strains grown at the permissive temperature of 25°C expressing *MEX67* in a wild-type or an *RRP6*-null background for both *RPS17B* and *RPL22B*, but unspliced precursors were observed for the *RPL18B* transcript in the *rrp6*Δ strain (Fig.4A). On the other hand, unspliced transcripts were detected for *RPS17B* and *RPL22B* in the *MEX67 upf1Δ* strain. A similar pattern of unspliced transcript accumulation was observed for strains expressing *mex67-5* in the *wild-type*, *rrp6Δ*, or *upf1Δ* background at the permissive temperature (Fig.4A). When the cells were shifted to non-permissive temperature (37°C), a general increase in unspliced transcripts was detected in the *MEX67, MEX67 rrp6Δ* and the *MEX67 upf1Δ* strains for both *RPS17B* and *RPL22B* but not for *RPL18B* (Fig.4A). This might be the result of a mild heat-shock resulting in a partial inhibition of splicing. In the case of *RPL22B*, most unspliced precursors are degraded by NMD during a shift to 37°C, as these species were found to accumulate much more dramatically in the *MEX67 upf1Δ* background. Strikingly, upon inhibition of mRNA export in the *mex67-5* strain shifted to 37°C, a large fraction of unspliced transcripts are now degraded by the exosome as shown by the reduction of unspliced transcripts observed in the *upf1Δ* background and the increase of unspliced transcripts in the *rrp6Δ* strain. This increase is apparent for *RPL22B* but is even more pronounced for

RPS17B as shown by the dramatic accumulation of unspliced RNAs in the *mex67-5 rrp6Δ* strain (Fig.4A). In the case of *RPL18B*, we did not detect any further increase of unspliced RNAs in that strain in these conditions (Fig.4A), showing that the increase of unspliced precursors observed upon inhibition of export in the *rrp6Δ* background for *RPS17B* and *RPL22B* is specific to these species. This shift in the degradation pathway of unspliced precursors from NMD to the nuclear exosome upon inhibition of nuclear export could also be detected when the *RPS17B* mRNA was expressed from a galactose promoter (Fig.4B). Thus, this shift in the degradation pathway from NMD to the nuclear exosome upon inhibition of mRNA export does not depend on the promoter from which these transcripts are being generated. Taken together, these results indicate that upon inhibition of RNA export in the *mex67-5* strain at the non-permissive temperature of 37°C, a large fraction of unspliced transcripts normally degraded by NMD are now retained in the nucleus and targeted for turnover by the nuclear exosome. These results also demonstrate that the export of several unspliced pre-mRNAs from the nucleus is dependent on the mRNA export factor, Mex67p, as shown previously for the *YRA1* pre-mRNA (Dong et al., 2007).

Mlp proteins function to retain the nuclear-degraded *RPL18B* unspliced transcript

It was previously reported that the nuclear factor Mlp1p functions in the retention of unspliced RNAs (Galy et al., 2004). However, these studies were based on the utilization of reporter constructs that contained a small, synthetic inefficiently spliced intron. We reasoned that Mlp1p might function in regulating the retention of unspliced RNAs that are predominantly degraded by the nuclear exosome. We hypothesized that in the absence of the potential retention-exerting activity of Mlp1p, these unspliced transcripts would be present at a higher concentration in the

cytoplasm, which would then be targeted and degraded by the activity of the non-sense mediated decay pathway. In order to investigate this hypothesis, we chose *RPL18B* as a model intron-containing gene, which accumulates high levels of unspliced transcripts upon inactivation of the nuclear exosome (Fig.1 and 4). We created and utilized yeast strains deleted for the genes encoding the similar (but not identical) retention factors Mlp1p (*mlp1Δ*) and Mlp2p (*mlp2Δ*), and also generated combinatorial double-delete mutants of *MLP1* and *UPF1* (*mlpΔ1upf1Δ*), *MLP2* and *UPF1* (*mlp2Δ upf1Δ*) and a triple-delete mutant comprising of deletions in *MLP1*, *MLP2*, and *UPF1* (*mlp1Δ mlp2Δ upf1Δ*). As expected and shown in Figure 5A, the single-mutants *mlp1Δ*, *mlp2Δ*, or *upf1Δ* did not display high levels of *RPL18B* unspliced transcript compared to the wild-type strain. However, large amounts of unspliced transcript were detected in the *rrp6Δ* strain. Strikingly, we observed higher amount of unspliced precursors in the *mlp1Δupf1Δ* double-mutant compared to the *upf1Δ* or *mlp1Δ* single-deletion strains. This observation was further supported by an increased unspliced transcript accumulation in the *mlp2Δupf1Δ* double-mutant and in the *mlp1Δmlp2Δupf1Δ* triple mutant. We further expanded our investigation and tested other intron-containing genes that exhibited an RNMD behavior (*RPL16A*, *RPL22A*) or an NMD-specific unspliced accumulation profile (*RPL22B*). As shown in Figure 5B, we did not observe any appreciable accumulation of unspliced precursor in *wild-type*, *mlp1Δ*, or *mlp2Δ* strains for *RPL16A*, *RPL22A*, and *RPL22B*. As expected, a strong accumulation of unspliced transcripts was detected in the *upf1Δ* strain. However, we did not observe an exacerbation in the accumulation of *RPL16A*, *RPL22A*, and *RPL22B* unspliced precursors for the *mlp1Δupf1Δ*, *mlp2Δupf1Δ*, or *mlp1Δmlp2Δupf1Δ* double or triple mutants. We conclude that the Mlp proteins can function in the retention of unspliced RNAs in the case of the *RPL18B* transcripts, but that

their role might be limited to a few transcripts exhibiting a primarily nuclear mode of degradation.

DISCUSSION

In this study, we have investigated the role of functionally redundant degradation pathways in unspliced RNAs turnover and have implicated a novel, dual-targeting strategy for certain intron-containing genes that is dependent on the activity of the nuclear exosome component, Rrp6p, and the NMD pathway. In particular, we found seven intron-containing genes that exhibit such a synergistic mode of degradation. This bipartite strategy reveals that the turnover of certain unspliced transcripts is more complex than previously thought and is controlled by the exosome action in the nucleus as well as NMD targeting in the cytoplasm. Because the nuclear exosome component that we have inactivated, Rrp6p is not essential for the function of the nuclear exosome, it is possible that other transcripts also rely on this dual mode of degradation but that they are not dependent on Rrp6p. One hypothesis that would explain the presence of a combinatorial strategy would be that particular sequences within the RNMD-transcripts render them amenable for turnover by two systems. Intronic sequences have been shown to be essential in autoregulation of intron-containing RNA transcripts as well as their degradation (Barta & Iggo, 1995); (Preker & Guthrie, 2006); (Dong et al., 2007; Sayani et al., 2008). Therefore, based on these findings, we had reasoned that the cooperative mode of degradation exhibited by certain unspliced transcripts could lay within their intronic sequences. The results obtained in our intron transposition experiment showed that a transposed intron of an RNMD gene, *RPL16Ai*, does not confer RNMD-sensitivity in *trans*. Furthermore, transposition of an NMD-sensitive intron, *RPS17Bi*, did lead to high levels of chimeric *GOT1::RPS17B* transcripts that were largely

degraded by NMD, but the levels of chimeric unspliced were not further exacerbated in *rrp6Δ upf1Δ* indicating that the NMD pathway was the major route for chimeric unspliced precursor turnover. Thus, although the intron identity is important for NMD-sensitive introns in conferring inefficient splicing in *cis* and *trans* (this study and (Sayani et al., 2008)), the intronic sequence alone does not render a specific unspliced RNA sensitive to degradation by both the nuclear exosome and NMD (Fig3).

Our results support a model suggesting that the balance between nuclear and cytoplasmic degradation of unspliced transcripts is dependent on the rate of export of these precursors from the nucleus into the cytoplasm. A kinetic delay in the rate of RNA export could potentially result in a higher fraction of unspliced transcripts in the nucleus and thus be targeted for turnover by the nuclear exosome. This model is supported by earlier studies showing that unspliced species generated in a prp2-ts mutant are mostly degraded by the nuclear exosome (Bousquet-Antonelli et al., 2000). The importance of this nuclear degradation pathway explains the observation that defects in Prp2p function have been shown to result in nuclear retention of unspliced species (Gencheva et al., 2010). We found that upon normal RNA export, unspliced transcripts of several transcripts are effectively targeted and degraded by the action of the NMD pathway (this study and (Sayani et al., 2008)). However, upon malfunction of RNA export, a large proportion of unspliced precursors are potentially still harbored within the nucleus and are now degraded by the action of the nuclear exosome. Such shifts in the turnover pathways of unspliced transcripts reveal the dynamic nature of RNA turnover that is modulated and/or controlled by the activity of the conserved RNA export factor, Mex67p. It would be of interest to determine whether in addition to unspliced transcripts, Mex67p has a role in the export of other short-lived RNAs. In

order to investigate the involvement of putative factors that functions in opposition to RNA export (and Mex67p), we found a physiologically-relevant target for the peripheral nuclear retention factors, Mlp1p and Mlp2p. We show that these factors are active in retaining a nuclear-degraded unspliced transcript (*RPL18B*) but that they do not seem to act on unspliced transcripts that are degraded by the combinatorial action of the nuclear exosome and NMD (*RPL16A* and *RPL22A*) or solely through NMD (*RPL22B*). These results show that unspliced transcripts that are degraded through either through NMD alone or a synergistic action of the nuclear exosome and NMD are not under an active retention control by the Mlp factors Mlp1p and/or Mlp2p. It is likely that *RPL18B* is not the only transcript that is directly retained by the Mlp factors. Future (genome-wide) studies should reveal the global extent of Mlp1p and/or Mlp2p retention functions for unspliced RNAs and other endogenous transcripts.

Contrary to recent studies (Bregman et al., 2011), our data show that replacement of upstream promoter sequences as well as regulatory elements does not lead to a change in the post-transcriptional degradation fate of an unspliced transcript. For example, replacement of the native promoter with a galactose-inducible (*GAL*) one for the intron-containing *RPS11A* did not lead to a change in the levels of the unspliced transcript. The *RPS11A* unspliced precursor transcribed from the native or the galactose-inducible promoters was degraded in a cooperative manner requiring the involvement of the nuclear exosome and NMD. Similarly, replacement of the *RPS17B* promoter sequence with the GAL promoter did not lead to changes in unspliced transcript accumulation nor in the switch in the decay pathway of the NMD-sensitive *RPS17b* gene. We obtained similar results that were consistent with the native as well as with the GAL promoter for *RPP1B*, *RPL22B*, and *RPL16A* (data not shown). Thus, it appears that the promoter

identity does not play a major function in determining the degradation route of specific unspliced pre-mRNAs.

Taken together, these results show that the degradation of unspliced transcripts is largely generic and likely rule out the possibility of particular sequences in making a transcript directly susceptible to the enzymatic activity of a specific nuclear or cytoplasmic degradation system. Instead, sensitivity of different transcripts to different degradation systems might be the result of the equilibrium between the rates of export or nuclear retention. While export or retention efficiency might depend on specific signals within the unspliced transcripts, it is unlikely that these sequences make the transcript intrinsically prone to the action of the exosome or NMD. Instead, subcellular localization seems to be the major determinant in deciding on the degradation route for these species. This dual mechanism of RNA quality control has far reaching implications beyond the surveillance and degradation of unspliced transcripts in yeast. A number of non-coding RNAs are known to be under an active RNA surveillance circuit that involves the surveillance of unspliced species. Studies on the Air non-coding (nc) RNA showed that it is an atypical RNA pol II transcript that undergoes splicing and export. However, the unspliced transcript is mostly sequestered in the nucleus (Seidl et al., 2006). Although this study did not directly reveal a role for the nuclear exosome in the degradation of nuclear-retained Air ncRNA, the observation that it is highly unstable strongly suggests that the nuclear exosome might be involved. A complex involvement of NMD and the nuclear exosome has also been implicated in the regulation of the Xist ncRNA in mammalian cells (Ciaudo et al., 2006). Thus, it appears that modulation of export rate and synergistic involvement of nuclear and cytoplasmic

degradation activities is not limited to unspliced transcripts degradation but can also affect other classes of transcripts, making it a general strategy to regulate RNA expression and turnover.

MATERIALS AND METHODS

Yeast strains utilized in this study

Strain	Genotype	Source
ySSC001	BY4741 or BY4742	Open Biosystems
ySSC002	*rrp6*Δ*::KAN*	Open Biosystems
ySSC003	*upf1*Δ*::KAN*	Open Biosystems
ySSC004	*upf2*Δ*::KAN*	Open Biosystems
ySSC004	*rrp6*Δ*::KAN upf1*Δ*::HIS*	Sayani et al., 2008
ySSC005	*rrp6*Δ*::HIS upf2*Δ*::TRP*	This study
ySSC006	*KAN-GAL::RPP1B*	This study
ySSC007	same as ySSC006 but with *rrp6::HIS*	This study
ySSC008	same as ySSC006 but with *upf1::HIS*	This study
ySSC009	same as ySSC006 but with rrp6::HIS upf1::HYGR	This study
ySSC010	*KAN-GAL::RPS11A*	This study
ySSC011	same as ySSC010 but with *rrp6::HIS*	This study
ySSC012	same as ySSC010 but with *upf1::HIS*	This study
ySSC013	same as ySSC010 but with *rrp6::HIS upf1::HYGR*	This study
ySSC014	*KAN-GAL::RPL16A*	This study
ySSC015	same as ySSC014 but with *rrp6*Δ	This study
ySSC016	same as ySSC014 but with *upf1*Δ	This study
ySSC017	same as ySSC014 but with *rrp6*Δ *upf1*Δ	This study
ySSC018	*KAN-GAL::RPS17B*	This study
ySSC019	same as ySSC018 but with *rrp6*Δ	This study

ySSC020	same as ySSC018 but with *upf1*Δ	This study
ySSC021	same as ySSC018 but with *rrp6*Δ *upf1*Δ	This study
ySSC022	*KAN-GAL::RPL22B*	This study
ySSC023	same as ySSC022 but with *rrp6*Δ	This study
ySSC024	same as ySSC022 but with *upf1*Δ	This study
ySSC025	same as ySSC022 but with *rrp6*Δ *upf1*Δ	This study
ySSC026	p*MEX67*, *mex67*Δ	Segref et al., 1997
ySSC027	p*mex67-5*, *mex67*Δ	Segref et al., 1997
ySSC028	same as ySSC026 but with *rrp6*Δ	This study
ySSC029	same as ySSC026 but with *upf1*Δ	This study
ySSC030	same as ySSC027 but with *rrp6*Δ	This study
ySSC031	same as ySSC027 but with upf1Δ	This study
ySSC032	same as ySSC027 but with *KAN-GAL::RPS17B*	This study
ySSC033	same as ySSC032 but with *rrp6*Δ	This study
ySSC034	same as ySSC032 but with *upf1*Δ	This study
ySSC035	*mlp1*Δ	Open Biosystems
ySSC036	*mlp2*Δ	Open Biosystems
ySSC037	*mlp1*Δ *upf1*Δ	Sayani et al., 2008
ySSC038	*mlp1*Δ *mlp2*Δ	This study
ySSC039	*mlp2*Δ *upf1*Δ	This study
ySSC040	*mlp1*Δ *mlp2*Δ *upf1*Δ	This study
ySSC041	*GOT1* gene with a transposed *RPL16A* intron	This study
ySSC042	same as ySSC041 but with *rrp6*Δ	This study

ySSC043	same as ySSC041 but with *upf1*Δ	This study
ySSC044	same as ySSC041 but with *rrp6*Δ *upf1*Δ	This study
ySSC045	*GOT1* gene with a transposed *RPS17B* intron	This study
ySSC046	same as ySSC045 but with *rrp6*Δ	This study
ySSC047	same as ySSC045 but with *upf1*Δ	This study
ySSC048	same as ySSC045 but with *rrp6*Δ *upf1*Δ	This study

Generation of yeast strains

Yeast strains were constructed using a one-step PCR strategy using standard yeast molecular genetics protocols. All strains were genotyped through the purification of clonal genomic DNA and using primers flanking the cassette region upstream and downstream of the ORF of interest.

Growth of yeast cultures

All yeast cultures were grown in either YPD or YPGal medium to an OD_{600} of ~0.3-0.8. Typically, 50mL culture volumes were harvested (with the exception of the decay time-point aliquots, which were approximately 25mL) and harvested cells were utilized for total RNA extraction.

RNA extraction and quantitation

Total RNA was extracted by resuspending cells (from either an ~50mL or ~25 mL culture volume) in ~400µL of RNA buffer (50mM Tris-HCl, pH 7.4; 100 mM NaCl; 10mM EDTA) and vortexed with glass beads for 2 minutes at room temperature followed by an incubation on ice for an equal amount of time. This was followed by the addition of ~100µL of 10% SDS. ~500µL

of RNA-based phenol-chloroform was added and vortexed for ~1 minute and incubated at 65°C for six minutes followed by a re-vortexing step for one minute. The tubes were spun at 13,200 rpm for five minutes and the supernatant layer was transferred to a new tube followed by two additional phenol-chloroform extraction steps as above (1 minute vortexing followed by centrifugation but without the 65°C step). After the final phenol-chloroform extraction, ~1mL of 95% ethanol was added with 200µL 3.2 M sodium acetate, pH5.2 and total RNA was precipitated at -20°C overnight. Tubes were spun at 13,200 rpm for 20 minutes at room temperature and resultant supernatant was discarded and 200 µL of 70% ethanol was added to wash the pelleted total RNA sample. After a brief centrifugation step at 13,200 rpm, the 70% ethanol was discarded and the total RNA pellets were resuspended in sterile water and vortexed until the pellets were completely resuspended. RNA quantitation was carried out in duplicate at λ=260nm (normally, RNAs were diluted 1:1000 or 1:500). ~10µg of RNA was utilized and combined with denaturing buffer (formamide and formaldehyde) and incubated at 65°C for ~15 minutes followed by addition of 2µL of loading dye (EDTA, glycerol, bromophenol blue, xylene cyanol).

Synthesis of probes

With the exception of the *SCR1* probe (which was generated through random priming), all probes were antisense, intronic riboprobes that spanned the intronic region of each of the target intron-containing genes that were studied. Riboprobe generation encompassed utilization of an amplified intron containing the T3 RNA Polymerase promoter at the 3'end. Briefly, 3µL of product was utilized as a template with 1 µL each of rATP, rCTP, and rGTP, and 2-3 µL of α-

32-P-UTP; 4 µL of 5x Promega transcription buffer, 2 µL of 100mM DTT and 1 µL of T3 RNA polymerase (Promega). The *in vitro* transcription reaction was incubated at 37°C for one hour followed by the addition of 1 µL of DNase (to degrade template DNA) and further incubated at 37°C for 15 minutes. The probe was then added to Church hybridization buffer.

Northern blotting

~10µg of total RNA (quantitated in duplicate at λ=260nm) were loaded onto 1.2 % denaturing agarose gels (7.5% formaldehyde, 1X MOPS buffer) and gels were transferred through capillary action onto positively charged nylon membrane (purchased from GE Healthcare/Life Sciences, catalog number RPN 303B) overnight. The blots were crosslinked with a Stratagene UV-crosslinker. Northern blots were hybridized overnight at ~65-70°C with desired probes in Church buffer (0.5M sodium phopshate, pH7.2; 7% SDS; and 1% BSA). After hybridization, blots were washed twice between 65- 70°C with 2x SSPE, 0.1%SDS buffer; and once with 0.1xSSPE, 0.1% SDS buffer. Blots were exposed at least overnight (or longer if needed) and scanned with a BioRad scanner.

Decay experiments

The galactose promoter was amplified from a plasmid obtained from Mark Longtine (Longtine et al., 1998). It was inserted approximately 50 base-pairs upstream of the translation start site. Strains expressing a desired intron-containing ribosomal protein gene under the control of the galactose promoter were grown overnight in a large culture (~200mL) in YPGalactose medium between 25-30°C. When cells were in logarithmic phase (typically OD600nm of ~0.3-0.8), an

aliquot (~25mL) of the cells were removed and added to a 50mL falcon tube containing 95% ethanol that was cooled at -80°C and spun down at 3000rpm for 1.5 minutes. The liquid was decanted and the tubes containing the spun cells were stored at -20°C until they were ready for further use. The first timepoint (t=0 minutes) was treated as the steady-state. The remainder of the culture grown in YPGal was spun down, decanted and immediately resuspended in YPD medium to induce transcriptional repression and subsequently four additional timepoints were collected (exactly as described above) at three, six, ten, and fifteen minutes post-transcriptional shutoff.

ACKNOWLEDGMENTS

This work was supported by a National Institutes of Health Grant to GFC (5R01GM061518-11). We would like to thank Kevin Roy for advice and help with the construction of yeast strains, sharing reagents, and unpublished data; Dr. Cesar Fernandez for advice and sharing reagents.

FIGURE LEGENDS

Figure1. Northern blot analysis of intron-containing genes

Northern blot steady-state analysis of unspliced transcripts in various single and double RNA degradation mutants. Blots were probed with an intronic (*i*) riboprobe and either *SCR1* or *GAPDH* was utilized as a loading control. Both the *SCR1* and the *GAPDH* probes were generated via random priming and these genes were used as loading controls.

Figure 2. Decay analysis of unspliced transcripts.

Each of the intron-containing ribosomal protein gene was placed under the control of the conditional galactose promoter approximately 50 base pairs upstream of the translation start site leading to the creation of five conditionally expressed ribosomal protein genes: *GAL::RPP1B*, *GAL::RPS11A*, *GAL::RPL16A*, *GAL::RPS17B*, *GAL::RPS22B*. Each of the knockouts (*rrp6*Δ, *upf1*Δ, *rrp6*Δ *upf1*Δ) was derived from a single isogenic wild-type strain. Each of the timepoints are indicated in minutes. *SCR1* was utilized as a loading control.

Figure 3. Transposition of a RNMD-sensitive intron is not sufficient to provide sensitivity to both degradation systems. The native *GOT1* intron was replaced by the *RPL16A* or the *RPS17B* intron and the *wild-type*, *rrp6*Δ, *upf1*Δ, or *rrp6*Δ *upf1*Δ strains were derived. A *GOT1* exon 2 antisense RNA probe was used to assay for the spliced and chimeric unspliced transcripts. *SCR1* or *GAPDH* was used as a loading control.

Figure 4. RNA export inhibition can result in a higher fraction of unspliced transcripts targeted by the nuclear exosome. *RPL22B* and *RPS17B*(or *GAL::RPS17B*) are NMD targets and *RPL18B* is predominantly degraded by the nuclear exosome. Cells were grown at the permissive temperature of 25°C until they reached logarithmic phase and were shifted to the non-permissive temperature of 37°C for approximately three hours. Northern blot analysis was performed with an intron-spanning antisense RNA probe to detect the accumulation of each of the unspliced transcripts. *SCR1* was used as a loading control.

Figure 5. Mlp1p and/or Mlp2p function in retaining the nuclear-degraded unspliced *RPL18B* transcripts but not unspliced precursors that are cooperatively degraded by exosome/NMD or NMD. Northern analysis was performed on the *RPL18B* unspliced transcript (

predominantly degraded by the nuclear exosome); or *RPL22A* and *RPL16A* (cooperatively degraded by exosome and NMD); or *RPL22B* (predominantly degraded by NMD). *SCR1* was used as a loading control.

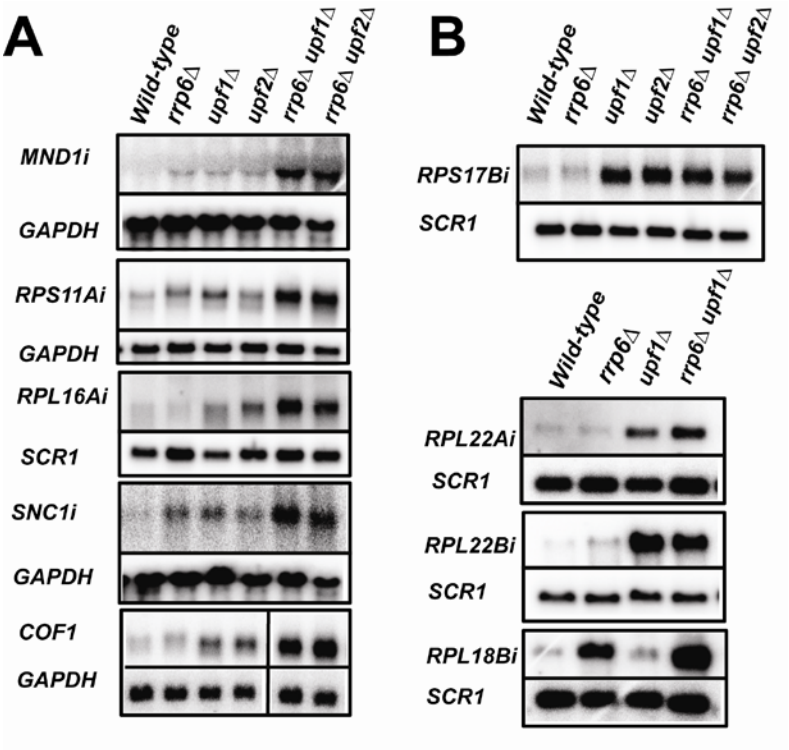

Figure1. Northern blot analysis of intron-containing genes

Northern blot steady-state analysis of unspliced transcripts in various single and double RNA degradation mutants. Blots were probed with an intronic (*i*) riboprobe and either *SCR1* or *GAPDH* was utilized as a loading control. Both the *SCR1* and the *GAPDH* probes were generated via random priming and these genes were used as loading controls.

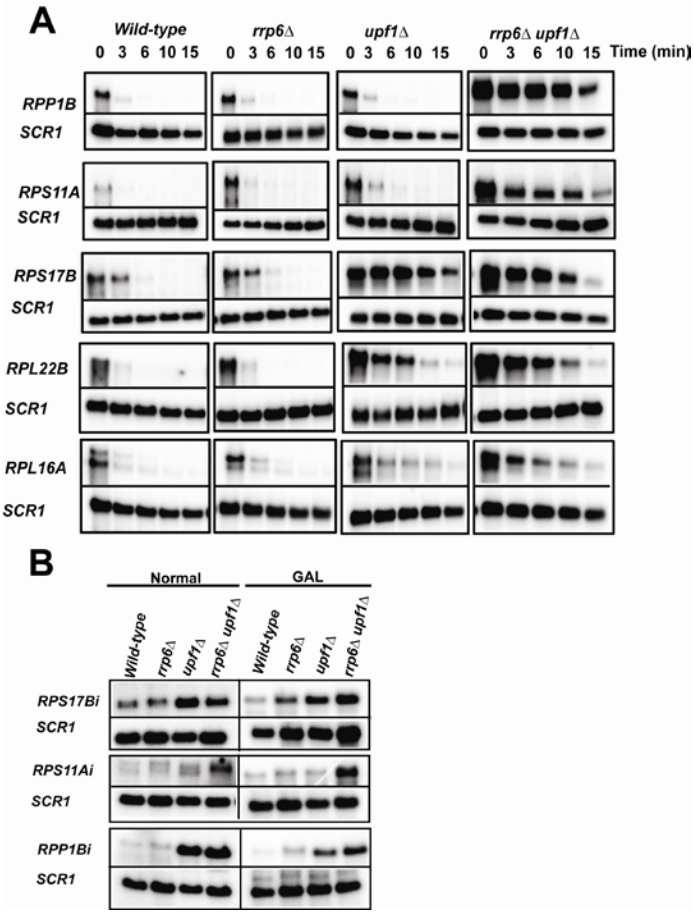

Figure 2. Decay analysis of unspliced transcripts.

Each of the intron-containing ribosomal protein gene was placed under the control of the conditional galactose promoter approximately 50 base pairs upstream of the translation start site leading to the creation of five conditionally expressed ribosomal protein genes: *GAL::RPP1B*, *GAL::RPS11A*, *GAL::RPL16A*, *GAL::RPS17B*, *GAL::RPS22B*. Each of the knockouts (*rrp6*Δ, *upf1*Δ, *rrp6*Δ *upf1*Δ) was derived from a single isogenic wild-type strain. Each of the timepoints are indicated in minutes. *SCR1* was utilized as a loading control.

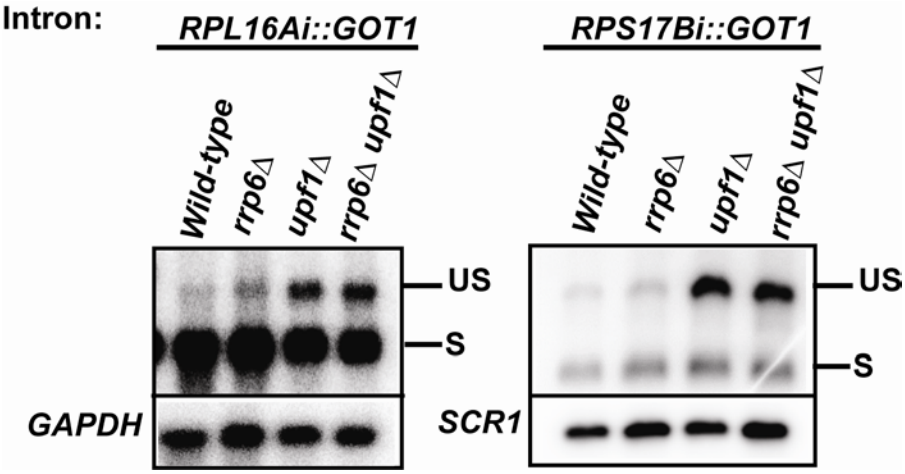

Figure 3. Transposition of a RNMD-sensitive intron is not sufficient to provide sensitivity to both degradation systems. The native *GOT1* intron was replaced by the *RPL16A* or the *RPS17B* intron and the *wild-type*, *rrp6*Δ, *upf1*Δ, or *rrp6*Δ *upf1*Δ strains were derived. A *GOT1* exon 2 antisense RNA probe was used to assay for the spliced and chimeric unspliced transcripts. *SCR1* or *GAPDH* was used as a loading control.

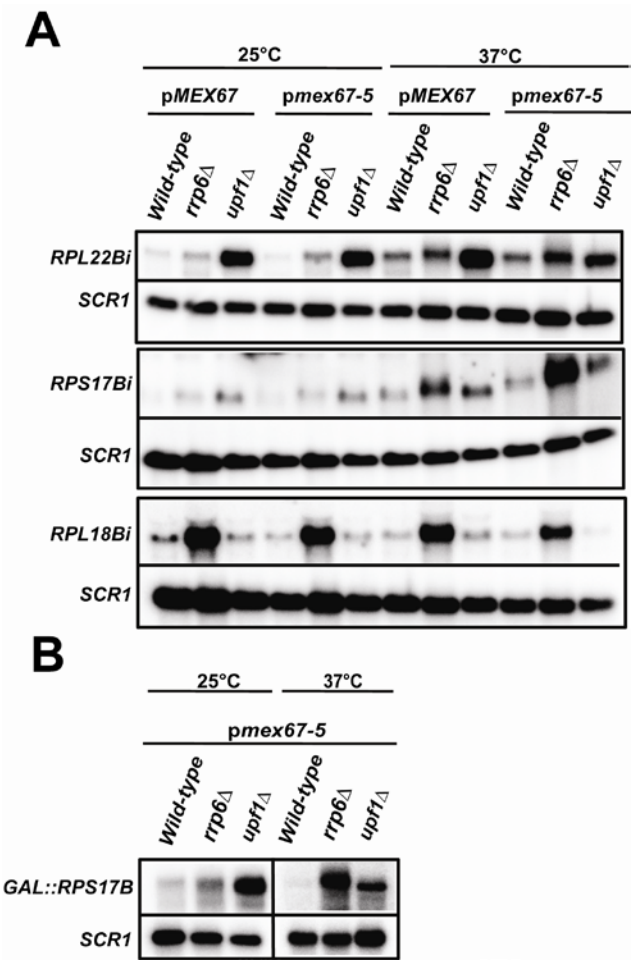

Figure 4. RNA export inhibition can result in a higher fraction of unspliced transcripts targeted by the nuclear exosome. *RPL22B* and *RPS17B*(or *GAL::RPS17B*) are NMD targets and *RPL18B* is predominantly degraded by the nuclear exosome. Cells were grown at the permissive temperature of 25°C until they reached logarithmic phase and were shifted to the non-permissive temperature of 37°C for approximately three hours. Northern blot analysis was performed with an intron-spanning antisense RNA probe to detect the accumulation of each of the unspliced transcripts. *SCR1* was used as a loading control.

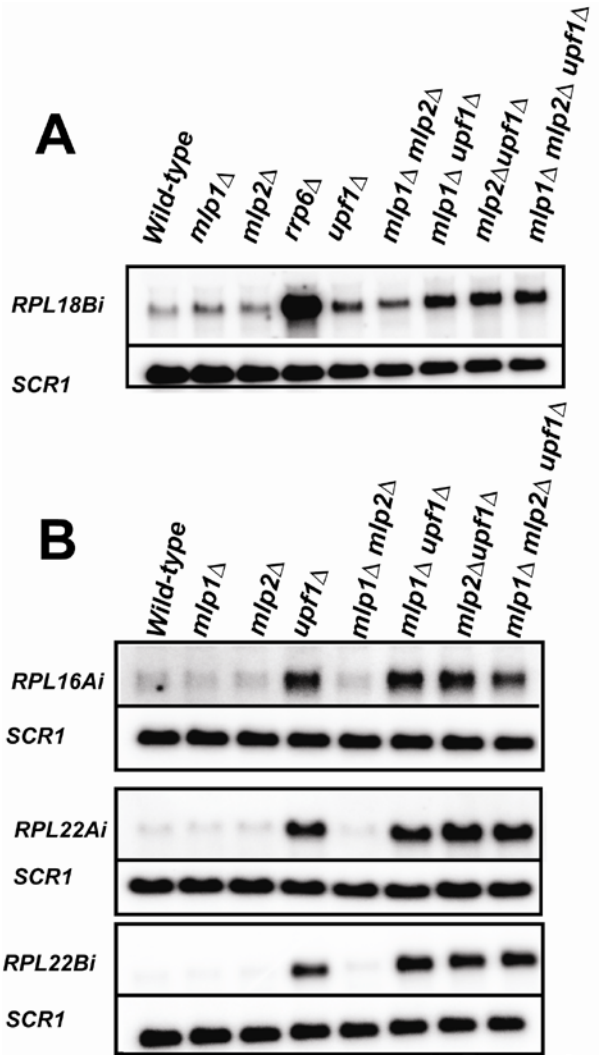

Figure 5. Mlp1p and/or Mlp2p function in retaining the nuclear-degraded unspliced *RPL18B* transcripts but not unspliced precursors that are cooperatively degraded by exosome/NMD or NMD. Northern analysis was performed on the *RPL18B* unspliced transcript (predominantly degraded by the nuclear exosome); or *RPL22A* and *RPL16A* (cooperatively degraded by exosome and NMD); or *RPL22B* (predominantly degraded by NMD). *SCR1* was used as a loading control.

REFERENCES

Barta I, Iggo R. 1995. Autoregulation of expression of the yeast Dbp2p 'DEAD-box' protein is mediated by sequences in the conserved DBP2 intron. *EMBO J 14*:3800-3808.

Bousquet-Antonelli C, Presutti C, Tollervey D. 2000. Identification of a regulated pathway for nuclear pre-mRNA turnover. *Cell 102*:765-775.

Bregman A, Avraham-Kelbert M, Barkai O, Duek L, Guterman A, Choder M. 2011. Promoter elements regulate cytoplasmic mRNA decay. *Cell 147*:1473-1483.

Chang YF, Imam JS, Wilkinson MF. 2007. The Nonsense-Mediated Decay RNA Surveillance Pathway. *Annu Rev Biochem 76*:51-74.

Ciaudo C, Bourdet A, Cohen-Tannoudji M, Dietz HC, Rougeulle C, Avner P. 2006. Nuclear mRNA degradation pathway(s) are implicated in Xist regulation and X chromosome inactivation. *PLoS Genet 2*:e94.

Danin-Kreiselman M, Lee CY, Chanfreau G. 2003. RNAse III-mediated degradation of unspliced pre-mRNAs and lariat introns. *Mol Cell 11*:1279-1289.

Dong S, Li C, Zenklusen D, Singer RH, Jacobson A, He F. 2007. YRA1 autoregulation requires nuclear export and cytoplasmic Edc3p-mediated degradation of its pre-mRNA. *Mol Cell 25*:559-573.

Galy V, Gadal O, Fromont-Racine M, Romano A, Jacquier A, Nehrbass U. 2004. Nuclear retention of unspliced mRNAs in yeast is mediated by perinuclear Mlp1. *Cell 116*:63-73.

Gencheva M, Lin TY, Wu X, Yang L, Richard C, Jones M, Lin SB, Lin RJ. 2010. Nuclear retention of unspliced pre-mRNAs by mutant DHX16/hPRP2, a spliceosomal DEAH-box protein. *J Biol Chem 285*:35624-35632.

He F, Peltz SW, Donahue JL, Rosbash M, Jacobson A. 1993. Stabilization and ribosome association of unspliced pre-mRNAs in a yeast upf1- mutant. *Proc Natl Acad Sci U S A 90*:7034-7038.

Hilleren PJ, Parker R. 2003. Cytoplasmic degradation of splice-defective pre-mRNAs and intermediates. *Mol Cell 12*:1453-1465.

Houseley J, LaCava J, Tollervey D. 2006. RNA-quality control by the exosome. *Nat Rev Mol Cell Biol 7*:529-539.

Jaillon O, Bouhouche K, Gout JF, Aury JM, Noel B, Saudemont B, Nowacki M, Serrano V, Porcel BM, Segurens B, Le Mouel A, Lepere G, Schachter V, Betermier M, Cohen J, Wincker P, Sperling L, Duret L, Meyer E. 2008. Translational control of intron splicing in eukaryotes. *Nature 451*:359-362.

LaCava J, Houseley J, Saveanu C, Petfalski E, Thompson E, Jacquier A, Tollervey D. 2005. RNA degradation by the exosome is promoted by a nuclear polyadenylation complex. *Cell 121*:713-724.

Lemieux C, Marguerat S, Lafontaine J, Barbezier N, Bahler J, Bachand F. 2011. A Pre-mRNA degradation pathway that selectively targets intron-containing genes requires the nuclear poly(A)-binding protein. *Mol Cell 44*:108-119.

Mitchell P, Petfalski E, Shevchenko A, Mann M, Tollervey D. 1997. The exosome: a conserved eukaryotic RNA processing complex containing multiple 3'-->5' exoribonucleases. *Cell 91*:457-466.

Mitrovich QM, Anderson P. 2000. Unproductively spliced ribosomal protein mRNAs are natural targets of mRNA surveillance in C. elegans. *Genes Dev 14*:2173-2184.

Moore MJ, Schwartzfarb EM, Silver PA, Yu MC. 2006. Differential recruitment of the splicing machinery during transcription predicts genome-wide patterns of mRNA splicing. *Mol Cell 24*:903-915.

Preker PJ, Guthrie C. 2006. Autoregulation of the mRNA export factor Yra1p requires inefficient splicing of its pre-mRNA. *RNA 12*:994-1006.

Sayani S, Janis M, Lee CY, Toesca I, Chanfreau GF. 2008. Widespread impact of nonsense-mediated mRNA decay on the yeast intronome. *Mol Cell 31*:360-370.

Segref A, Sharma K, Doye V, Hellwig A, Huber J, Luhrmann R, Hurt E. 1997. Mex67p, a novel factor for nuclear mRNA export, binds to both poly(A)+ RNA and nuclear pores. *EMBO J 16*:3256-3271.

Tucker M, Parker R. 2000. Mechanisms and control of mRNA decapping in Saccharomyces cerevisiae. *Annu Rev Biochem 69*:571-595.

Wyers F, Rougemaille M, Badis G, Rousselle JC, Dufour ME, Boulay J, Regnault B, Devaux F, Namane A, Seraphin B, Libri D, Jacquier A. 2005. Cryptic pol II transcripts are degraded by a nuclear quality control pathway involving a new poly(A) polymerase. *Cell 121*:725-737.